NTNU – Trondheim
Norwegian University of
Science and Technology

Degradation of Amines

Maren Teresa Johansen

Chemical Engineering and Biotechnology
Submission date: June 2013
Supervisor: Anne Fiksdahl, IKJ
Co-supervisor: Hallvard Svendsen, IKP
Hanna Knuutila, IKP

Norwegian University of Science and Technology
Department of Chemistry

Acknowledgements

This work has been performed at the Department of Chemistry at the Norwegian University of Science and Technology (NTNU). Some of the analyses have also been done in collaboration with the SINTEF Biotechnology group.

I would like to thank my supervisor, Anne Fiksdahl, for giving me the opportunity to do this thesis, and Hallvard F. Svendsen for guidance and advice at the Department of Chemical Engineering. I would also like to thank my co-supervisor Hanna Knuutila for following the process, and offering help in all practical aspects of the work. Solrun Vevelstad has been very helpful by giving guidance in the experimental work and for sharing knowledge through scientific discussions.

The support I've had from my friends and family has been highly motivational, and given me strength to both have a social life and a life in the lab.

Abstract

In view of the rising amounts of greenhouse gases in the atmosphere, preventing CO_2 emissions has become increasingly important. The combustion of fossil fuels for energy production and transportation is a large contributor to the problem.

One of the ways to reduce the amounts of CO_2 being released from combustion is carbon capture and storage (CCS). Post-combustion is the capturing method which has been deemed the easiest to apply to existing power plants in a short period of time. Absorption of CO_2 by MEA is the most common method used in post-combustion carbon capture, but there are still many aspects of the process that are not fully understood. Understanding the absorption mechanisms will make it easier to make more economical and environmentally friendly choices in the future.

In this thesis the oxidative degradation of monoethanolamine (MEA) has been studied using an open batch setup. The stability of MEA has been studied under different temperatures and concentrations of oxygen in the gas stream. These experiments give a matrix of experiments performed at 55, 65 and 75 °C, with oxygen concentrations of 6, 21, 50 and 98% in the gas stream. To monitor how well the experimental results could be trusted, the water balance was maintained throughout the experiments, and the pH was measured in the flasks capturing volatile degradation compounds.

To get a detailed picture of the degradation, the weight percent of nitrogen and the CO_2 concentration has been found in the end samples, and the alkalinity and MEA concentration was found for all the samples.

11 known degradation compounds have been monitored for the different experiments, and the conditions these compounds are formed at have been compared with the suggested reaction mechanisms. 4 of the products were analyzed as anions using Ion chromatography (IC), and 7 secondary reaction products were analyzed as part of a degradation mix in LC-MS.

The dependency of these compounds to temperature and oxygen conditions has been discussed. The primary degradation compounds seems to show a more direct correlation to oxygen flow or temperature, while the secondary degradation reaction shows a bigger variation of temperature and oxygen dependency relative to the conditions of the experiments.

Various analytical methods for determination of the known compounds were used to determine the concentration of the degradation compounds in the experiments. The accuracy of these methods was investigated, and the results investigated for both LC-MS, GC-MS and IC-EC, showed large variations.

Mixing experiments were performed to investigate the unknown mechanism of *N*-(2-hydroxyethyl) glycine.

Sammendrag

I lys av den økende mengden klimagasser i atmosfæren, har fangst av CO_2 blitt stadig viktigere. Forbrenning av fossilt brennstoff for å mette klodens økende energibehov bidrar til at store mengder CO_2 slippes ut i atmosfæren.

En av måtene for å redusere mengden CO_2 som blir frigjort fra forbrenning er karbonfangst og lagring (CCS). "Post-combustion" fangst av CO_2 er det alternativet som er enklest å ta i bruk for eksisterende kraftverk. Absorpsjon av monoetanolamin (MEA) er den vanligste metoden som brukes i post-combustion fangst, men det er fortsatt mange aspekter av prosessen som ikke er forstått fullt ut. Å øke forståelsen av absorpsjonsmekanismene vil gjøre det lettere å lage mer økonomiske og miljøvennlige valg i fremtiden.

I denne avhandlingen har den oksidative nedbrytning av monoetanolamin (MEA) blitt studert under et åpent batch system. Stabiliteten av MEA er undersøkt under forskjellige temperaturer og konsentrasjoner av oksygen i gass-strømmen. Disse eksperimentene gir en matrise av eksperimenter utført ved 55, 65 og 75 ° C, med oksygenkonsentrasjoner på 6, 21, 50 og 98% i gass-strømmen. For å overvåke gyldigheten av de eksperimentelle resultatene ble vannbalansen holdt, og pH ble målt i gassbolbleflaskene brukt til å fange flyktige degraderingsprodukter.

For å få et detaljert bilde av degraderingen, har vektprosenten av nitrogen og CO2-konsentrasjonen blitt funnet i sluttprøvene, og alkalitet og MEA-konsentrasjonen ble funnet for alle prøvene.

11 kjente degraderingsprodukter ble vurdert i de ulike forsøkene, og betingelsene for dannelse av disse produktene har blitt sammenlignet med de foreslåtte reaksjonsmekanismene. 4 av produktene ble analysert som anioner ved hjelp av ionekromatografi (IC), og 7 sekundære reaksjonsprodukter ble analysert som en del av en degraderingsproduktblanding i LC-MS.

Avhengigheten av disse forbindelsene til temperatur og oksygenkonsentrasjon i gassstrømmen har blitt diskutert. De primære degraderingsproduktene synes å vise en mer direkte sammenheng til oksygenstrøm og/ eller temperatur, mens de sekundære degraderingsreaksjonene viser en større variasjon av temperatur- og oksygenavhengighet i forhold til betingelsene for forsøkene.

Forskjellige analysemetoder for bestemmelse av forbindelsene ble brukt til å bestemme konsentrasjonene av degraderingsproduktene i eksperimentene, og det ble funnet usikkerheter i både LC-MS, GC-MS og IC-EC.

Blandingseksperimenter ble utført for å undersøke den ukjente mekanisme av N-(2-hydroksyetyl) glycin.

Symbols and Abbreviations

M	Molar mass
NL	Mass of gas equal to the mass of 1 liter
V_{max}	Maximum variation in the difference between two results
CCS	Carbon capture and Storage
CAS	Chemical Abstracts Service
CI	Chemical ionization
EI	Electron impact ionization
FID	Flame ionization detector
GC	Gas chromatography
GC-MS	Gas chromatography-mass spectrometry
GHG	Greenhouse gases
GLC	Gas-liquid chromatography
GSC	Gas-solid chromatography
HSS	Heat-stable salts
IC	Ion chromatography
IC-EC	Ion chromatography-electrochemical detection
LC	Liquid chromatography
LC-MS	Liquid chromatography-mass spectrometry
$M^{(n+1)+}$	Oxidized metal cation
m/z	Mass to charge ratio
MS	Mass spectrometry
MFC	Mass Flow Controller
NIST	National Institute of Standard
NPD	Nitrogen-phosphorous detector
PLOT	Porous layer open tubular
PPM	Parts per million (mg/kg)
SIM	Selective ion mode
TCD	Thermal conductivity detector
WCOT	Wall coated open tubular
wt%	Weight percentage
α	Loading of solution (mol CO_2 per mol amine)
α	Carbon in α-position
β	Carbon in β-position
Ω	Electrical resistence
BHEOX	*N, N'*-bis(2-hydroxyethyl) oxalamide
ClO_2	chlorine dioxide
CO_2	carbon dioxide
DEA	diethanolamine
Fe^{3+}	ferric ion

H_2	hydrogen
H_2O	water
H_2SO_4	sulphuric acid
HEA	*N*-(2-hydroxyethyl) acetamine
HEF	*N*-(2-hydroxyethyl) formamine
HEI	*N*-(2-hydroxyethyl) imidazole
HEGly	*N*-(2-hydroxyethyl) glycine
HEPO	4-(2-hydroxyethyl) piperazin-2-one
HEEDA	*N*-(2-hydroxyethyl) ethylenediamine
Na_2SO_4	sodium sulphate
MEA	monoethanolamine
NH_3	ammonia
O_2	oxygen
O_2%	Volume fraction of oxygen in gas flow into reactor
OZD	2-oxazolidinone

Table of Contents

1. Introduction

The global temperature is rising, and human emissions of greenhouse gases (GHG) are one of the main contributers [1]. This can have a large effect on the environment, and as of 2009 over 100 countries have agreed to try to keep the rise in temperature below 2 °C relative to pre-industrial temperatures [2, 3]. CO_2 is the largest contributor to the increase of greenhouse gases, and the concentration of CO_2 has been increasing in the atmosphere, as can be seen by the Keeling curve, Figure 1.1 [4].

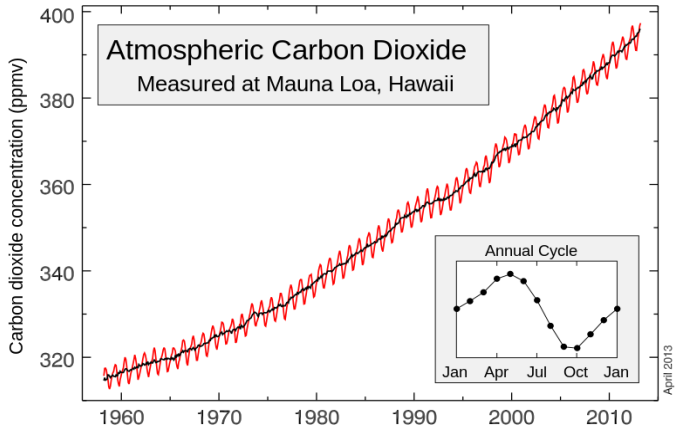

Figure 1.1: The concentration of CO_2 in the atmosphere, measured at Mauna Lua in Hawaii[5].

One of the methods that can be used to minimize the release of CO_2 to the atmosphere is carbon capture and storage (CCS) [6]. CCS uses a range of technologies to capture CO_2 emitted from preparation or combustion of fossil fuels, and from certain industrial processes [7]. These technologies are separated in three major capture systems: Oxy-fuel, post-combustion and pre-combustion capture, Figure 1.2 [8]. In addition chemical looping combustion processes (CLC) can be used to separate CO_2 directly from the combustion chamber as a separate stream [9].

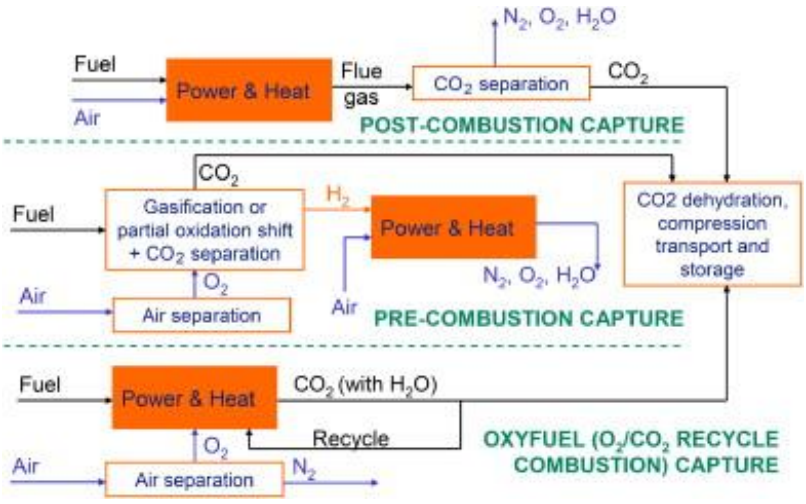

Figure 1.2: The three main CO_2 capture technologies [10].

Introduction

Oxyfuel combustion uses pure oxygen for combustion giving a flue gas consisting of H_2O and CO_2, where CO_2 can separated easily. Pre-combustion systems process the fuel into CO_2 and H_2, where H_2 is used as the energy source for combustion. Post-combustion systems uses technologies such as absorption, adsorption and membranes to separate or remove the CO_2 from the flue gas after combustion [11].

Post-combustion carbon capture is the only technique than can efficiently be employed on exiting power plants, and absorption is the most effective method for large-scale plants[12]. The process involves absorption of CO_2 by a suitable solvent, and the CO_2 is subsequently regenerated by heating the solution in a desorption column, Figure 1.3. Rao and Rubin showed that an amine based absorption systems are suitable for capturing CO_2 in combustion based power plants[13].

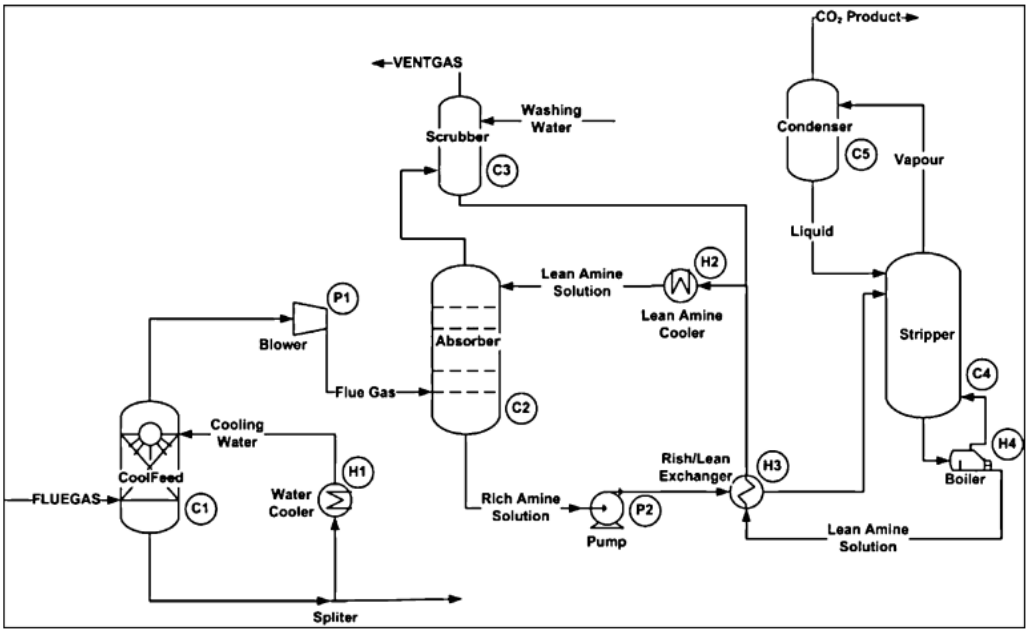

Figure ***1.3: Flow sheet for amine-based CO_2 capture and removal[14].***

The most common absorption solvents are amines. The reactions taking place for the capture of CO_2 by primary and secondary amines in the abosorber are carbamate and bicarbonate formation. In the stripper CO_2 is regenerated through carbamate reversion. The carbamate formation for the absorption of CO_2 by MEA is given in Equation 1.1.

$$CO_2 + 2NH_2CH_2CH_2OH \rightarrow COO^-NHCH_2CH_2OH + NH_2^+CH2CH2OH \qquad (1.1)$$

2. Literature review

2.1. Degradation of MEA

Three types of amine degradation mechanisms are important in flue gas CO_2-capture; thermal, oxidative and CO_2 induced degradation[15]. Thermal degradation usually occurs in the absence of O_2. The increased rates of thermal degradation in the presence of CO_2 has been explained by aqueous CO_2 acting as a proton donor[16]. Oxidative degradation or autoxidation degradation occurs in the presence of O_2. This is the main reaction type occurring in the absorption column in a CO_2 capture plant. CO_2 induced degradation is a reaction where CO_2 acts irreversibly with amines. This reaction with primary and secondary amines gives both oxazolidinones and diamines[17, 18].

In this thesis the oxidative degradation of monoethanolamine (MEA) loaded with CO_2 has been investigated.

2.1.1. Oxidative degradation mechanisms

Oxidative degradation in a CO_2-capture plant is a result of oxygen in the flue gas reacting with the amine absorbent. It is believed that the oxidative degradation of amines goes through a radical mechanism catalyzed by dissolved metals[19, 20]. This radical mechanism is still not fully understood but there is evidence that it proceeds through an abstraction of hydrogen from nitrogen, α- or β-carbon, or an abstraction of an electron from the nitrogen lone pair, or a combination of both. Which mechanism takes place depends on the structure of the amine, the solvents, the concentration, the acidity and the oxidants[16, 21].

Figure 0.1 describes the different amine autoxidation routes[15, 22]. Route (A) is the direct pathway where a oxidized metal cation [$M^{(n+1)+}$] abstracts one electron from nitrogen R, in RH, as the initial step. This can occurs with both metal and fly ash as a catalyst for the reaction. The metal ion can be reoxidized by hydroxyl radical formation from oxygen, O_2. In route (B) hydrogen is abstracted from the amine, RH, by a hydroxyl radical or an organoperoxy radical. Reaction (C) occurs by hydrogen being abstracted from the organoperoxy radical by an amine RH.

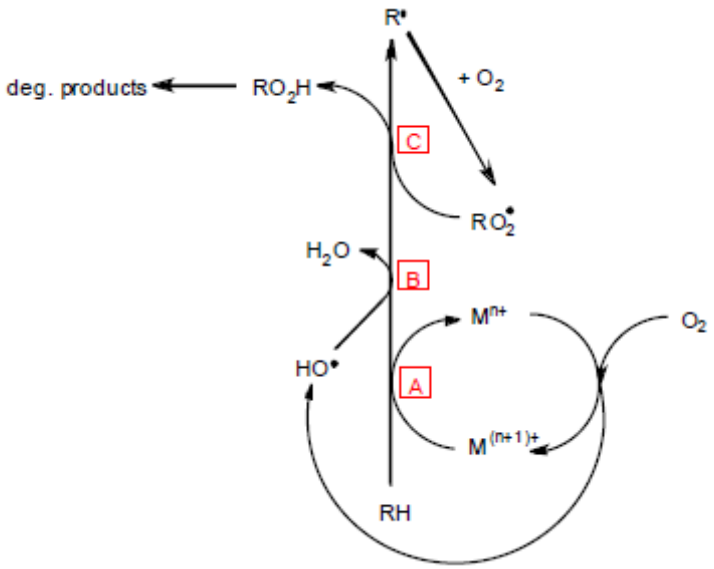

Figure 0.1: Amine autoxidation mechanism as proposed by Bedell[15].

An example of the electron abstraction mechanism (A) for MEA is given in Figure 0.2[19]. Reaction (I) is catalyzed by Fe^{3+}, ClO_2, $R^{\cdot}$, or other one-electron oxidants to give an aminium ion[23-25]. The proton abstraction in (II) can cause reorganization of the molecule giving a carbon-centered radical. Peroxide radical is formed when oxygen reacts with an imine radical (III). This leads to the production of imine and hydrogen peroxide (IV). The imine compound formed by a second reaction with an oxidant (V) hydrolyses to give ammonia and hydroxyacetaldehyde (VI), whereas formaldehyde and ammonia are formed during oxidative fragmentation of the imine (VII)[21].

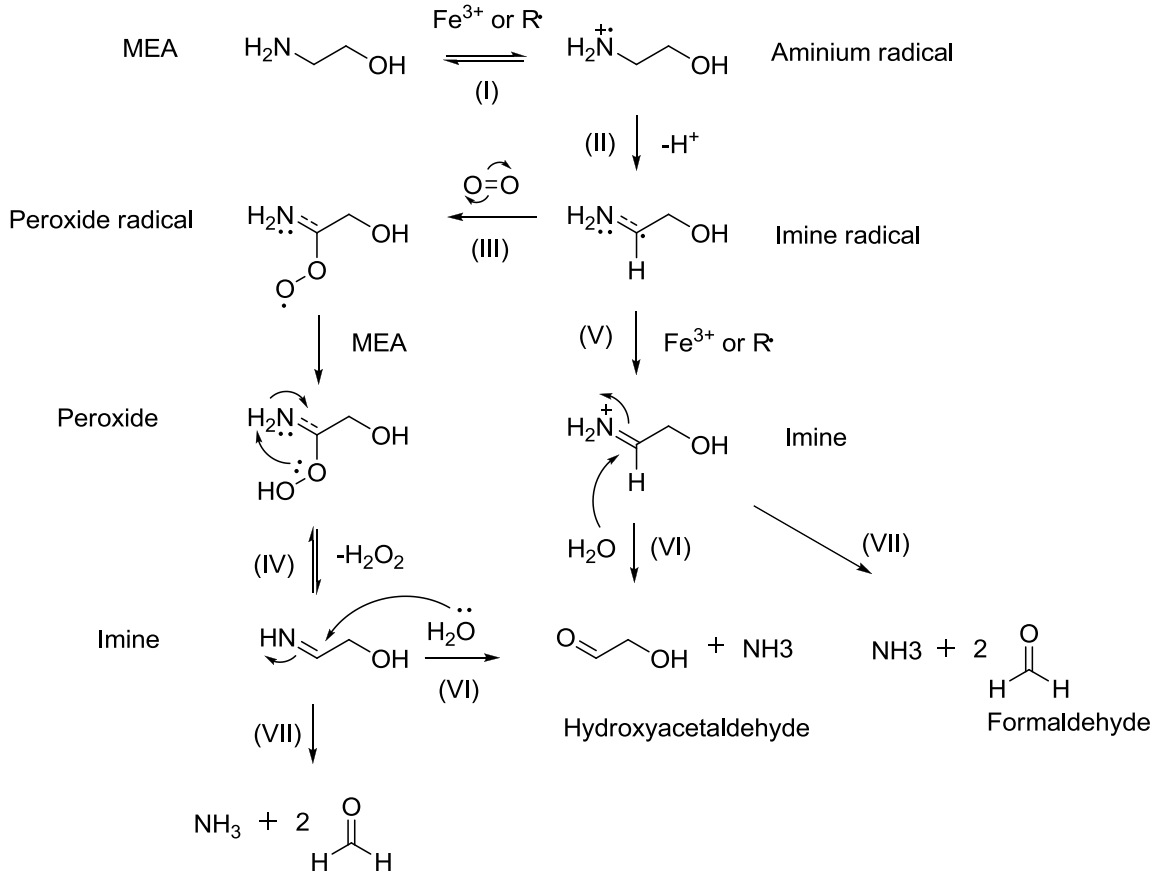

Figure 0.2: Degradation of MEA by single electron transfer by mechanism (A), Figure 1.

The alternative hydrogen abstraction mechanism is initiated by an oxidant such as ClO_2 [26]. The mechanism of MEA is proposed by Petryaev et al [27]. The mechanism proceeds through a five-membered ring transition state, formed by hydrogen bonds between the amine- and alcohol functionality in the alkanolamine. A hydrogen radical is abstracted from the molecule, cleaving the carbon-nitrogen bond by a radical chain. Studies conducted by Alejandre et al., Button et al, and Vorobyov et al. have supported the validity of the cyclic transition state [28-30]. Based on the study by Petryaev et al. the suggested mechanism is shown in Figure 0.3 [31].

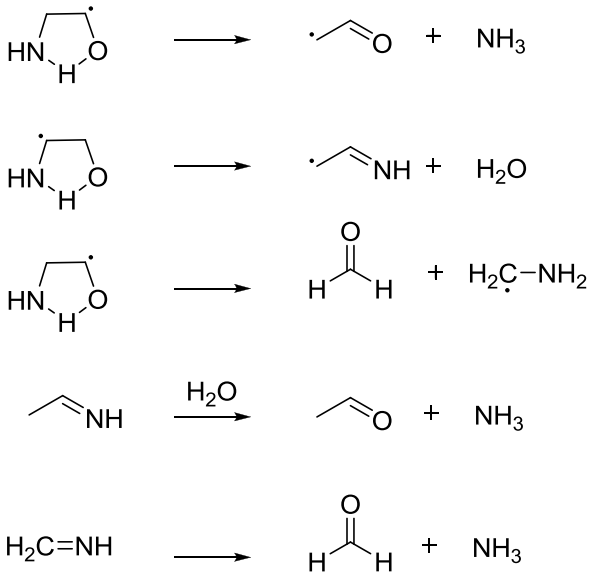

Figure 0.3: Hydrogen abstraction mechanism for MEA degradation by mechanism (B), Figure 2.1.

Both the electron- and hydrogen abstraction mechanisms have been supported by kinetic and experimental studies [21]. Hull and Rosenblatt have also found evidence indicating that electron abstraction is dominant for tertiary amines and hydrogen abstraction is dominant for secondary and primary amines.

The formation of glycine shown in Figure 0.4 is an example of an MEA radical reacting with oxygen via a peroxy radical (C). This type of reaction yields both imines and glycines [15].

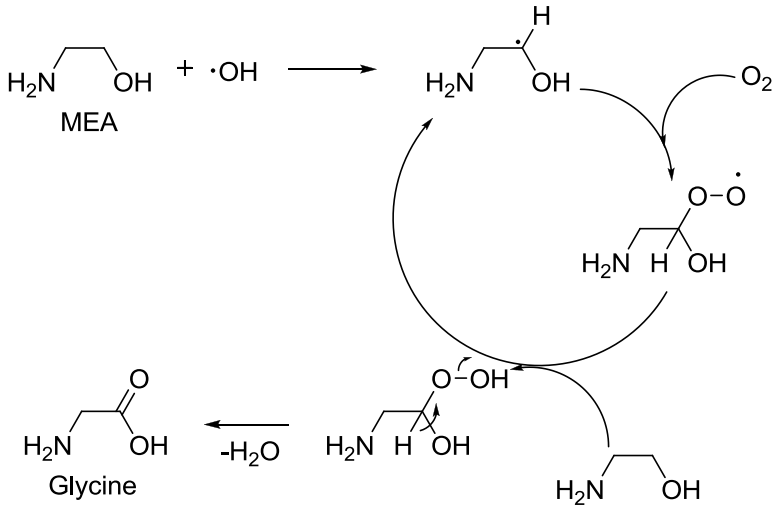

Figure 0.4: Proposed reaction pathway for production of glycine from MEA, by mechanism (C), Figure 1.

2.1.2. Degradation products

Based on the radical mechanisms presented in the previous section, some first order degradation products have been identified as either fragments or oxidized fragments of the MEA molecule [32]. The aldehydes in Figure 0.5 can be regarded as fragments of MEA, whereas the organic acids are oxidized fragments of MEA.

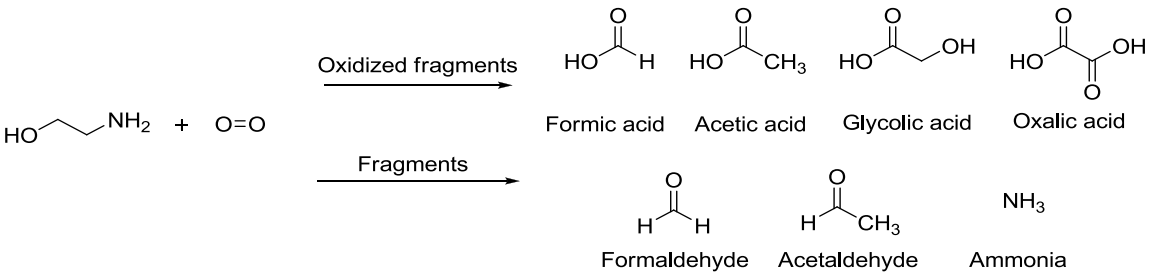

Figure 0.5: First order oxidation products.

In addition to the degradation products shown in Figure 5, other known products of oxidative degradation of MEA that can be detected by the current analysis methods are shown in Table 0.1.

Table 0.1: Secondary MEA degradation products.

Name	Abb.	Structure		M (g/mol)	CAS
2-oxazolidinone	OZD	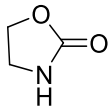	**1**	87.08	497-25-6
N-(2-hydroxyethyl) imidazole	HEI	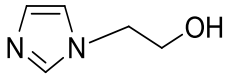	**2**	112.13	1615-14-1
N-(2-hydroxyethyl) formamine	HEF	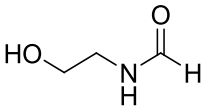	**3**	98.09	693-06-1
N-(2-hydroxyethyl) acetamine	HEA	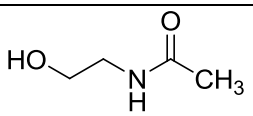	**4**	103.12	142-26-7
4-(2-hydroxyethyl) piperazin-2-one	HEPO	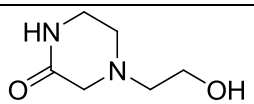	**5**	144.17	23936-04-1
N, N'-bis(2-hydroxyethyl) oxalamide	BHEOX	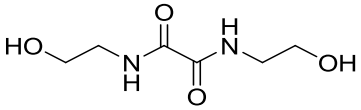	**6**	176.17	1871-89-2
N-(2-hydroxyethyl) glycine	HEGly	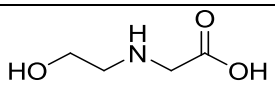	**7**	119.12	5835-28-9

The compounds formed as first stage degradation products are reactive chemicals. Da Silva et al. have proposed that these chemicals can react with solvents or other degradation products. The re-

action of MEA or other primary amines with the organic acids formed in Figure 0.5 is believed to lead to many of the identified secondary oxidative degradation compounds (SDC) [32]. The reaction proceeds through a nucleophilic attack of the carbonyl group by the primary amine of MEA, as shown in Figure 0.6.

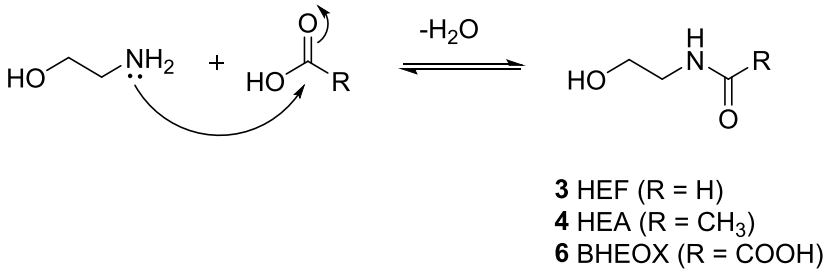

Figure 0.6: Reaction between MEA and first order degradation organic acids.

The proposed mechanism for the formation of OZD, **1**, is shown in Figure 0.7[33]. This reaction is a type of CO_2 induced degradation and is not believed to involve radical intermediates.

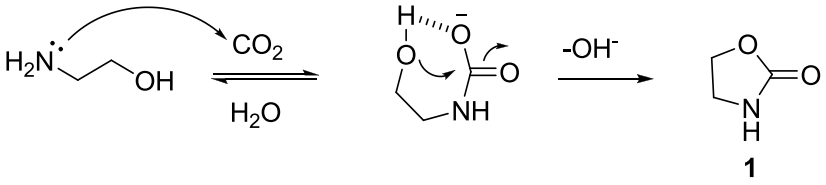

Figure 0.7: The mechanism for formation of OZD 1.

The mechanism for the formation of HEI, **2**, is not yet confirmed, but the compound has previously been obtained by a reaction of ammonia, MEA, formaldehyde and glyoxal. The mechanism shown in Figure 0.8, is proposed by Katsuura et al. and Ben[34-36]. The hetrocyclization mechanism of the two products is uncertain.

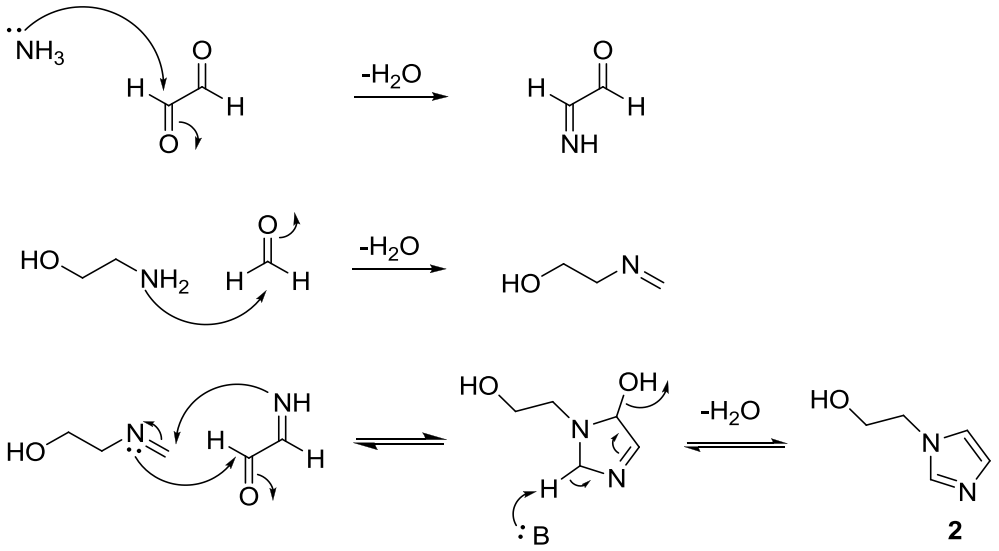

Figure 0.8: Hetrocyclization mechanism for the formation of HEI 2.

In the work done by Vevelstad, a new mechanism for the formation of HEI was suggested [37]. This mechanism is based on the findings of Katsuura, where 2-(methyleneamino)-ethanol and iminoacetaldehyde was reported to produce HEI [34]. These reactants can be formed from MEA, formaldehyde, glyoxal and ammonia, which have all been found in MEA degradation solutions [31, 38]. Vevelstad also proved that HEI could be formed from these four compounds by mixing them at 60 °C. The proposed mechanism is given in Figure 2.9.

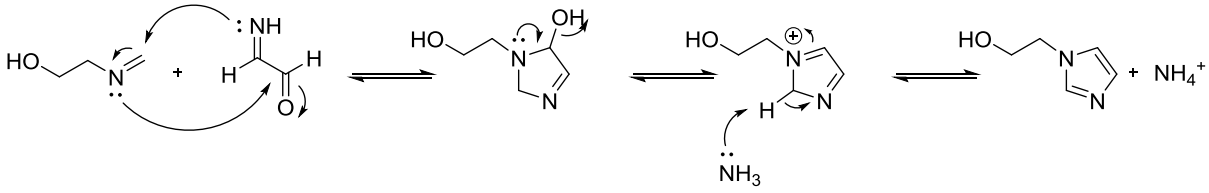

Figure 2.8: New mechanism proposed by Vevelstad for the formation of HEI, 2, in oxidative degradation.

Da Silva et al. have proposed a reaction mechanism for the formation of HEPO, **5**, where HEGly, **7**, reacts with MEA. HEGly is proposed to be formed as a reaction between a first stage oxidative degradation compound and MEA. The precursor of the reaction is however not confirmed [32]. In Section 5.4, a suggested mechanism for the formation of HEGly has been investigated. Figure 0. shows the proposed mechanism for the formation of HEPO. This reaction mechanism also gives an explanation for the formation of *iso*-HEPO. Another proposed reaction mechanism for the formation of HEPO is a reaction where two MEA molecules react to give *N*-(2-hydroxyethyl) ethylenediamine (HEEDA). HEEDA reacts with glycolic acid, and the condensation product cyclizes to give HEPO or *iso*-HEPO.

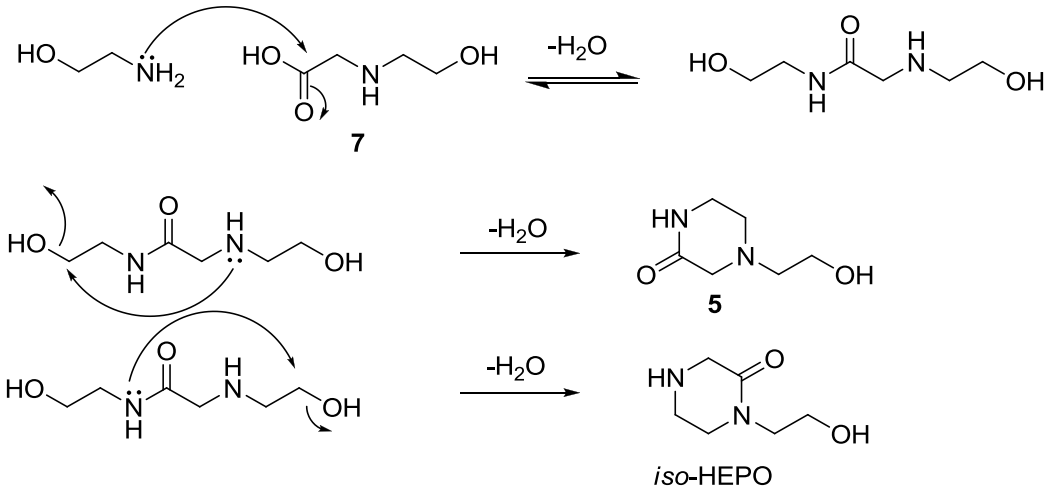

Figure 0.10: Proposed mechanism for the formation of HEPO, *5.*

2.2. Analysis of degradation

To understand the composition of the degradation compounds several analytical techniques have been used[39]. The most common methods for mapping and quantifying degradation compounds are GC-MS (Gas Chromatography-Mass Spectrometry), LC-MS (Liquid Chromatography-Mass Spectrometry) and IC-EC (Ion Chromatography with Electrochemical detection)[40]. The need for multiple analysis methods arise from the different functionalities of the degradation compounds including amines, amides, carboxylic acids, carbonates and carbamates. In this thesis, the use of GC-MS for identification has been investigated. Titration is a typical method for analysis of the total amount of amines and CO_2 in a sample. The Kjeldahl method is another method used for quantitative determination of nitrogen in chemical substances.

2.2.1. GC-MS

GC-MS is an analytical method used to investigate multiple compounds in one sample[41]. It is a combination of two common analytical methods, gas chromatography and mass spectrometry, Figure 0.9. GC-MS is used for the separation of amines because it was found to be a sensitive technique, which was able to separate and detect a great number of degradation products within a short period of time[33].

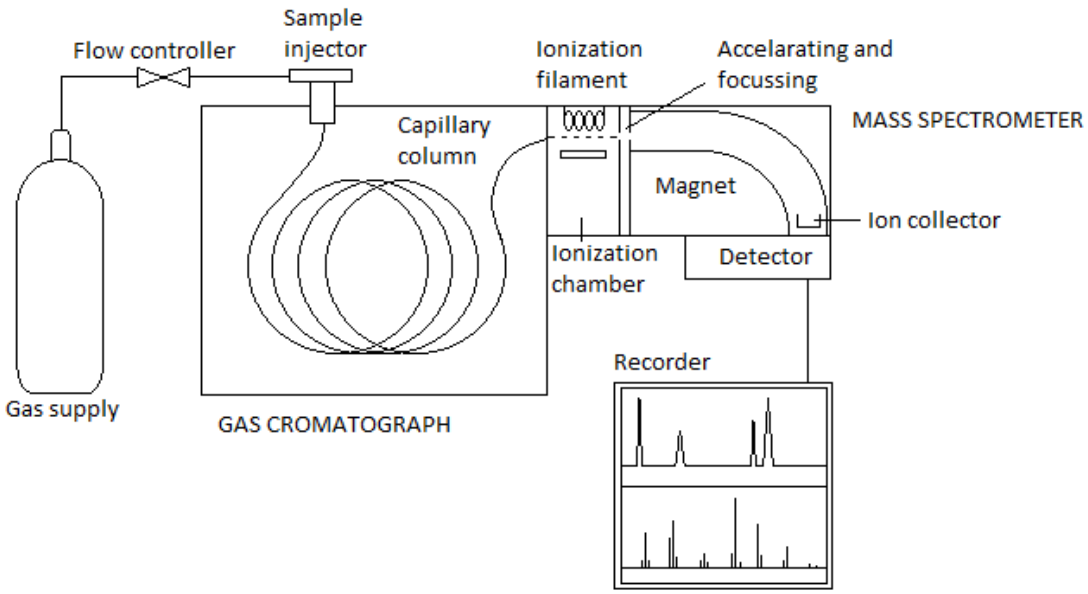

Figure 0.9: A schematic illustration of the GC-MS instrument.

Separation of amines by gas chromatography [33]

In gas chromatography the material under analysis (the analyte) is vaporized before it is transported through a capillary column by a carrier gas, the mobile phase[42]. The analytes need to be stable at the temperatures and volatile[43]. The inside of the capillary column is coated with a microscopic layer of liquid or polymer being the stationary phase. The stationary phase interacts with the compounds in the analyte to different degrees. This makes the compounds elute with different speeds through the column. The time one compound use to travel through the column is known as the retention time. Polarity and molecular weight affects the retention time of a compound. In a specific column, the retention time of a specific molecule can be used to identify the molecule when the conditions are the same.

To get a good separation of amines, the system of parameters shown in Table 2.2, has been proposed [44].

Table 0.2: Important parameters to consider for GC-MS analysis of MEA degradation products.

Considered	Type selected	Reason for choice
Solvent selection	Water	The amine solution is already aquous. Other solvents like methanol may react with the degradation products.
Column	Capillary, medium polar, water-resistant.	Capillary columns have a higher analysis speed compared to a packed column.
Injection mode	Split-injection	Some compounds are in low concentration. This is preferred over split and on-column injection because it gives a higher resolution.
Gas carrier	Helium	Hydrogen gas cannot be used with a mass spectrometer and nitrogen gas gives a lower detection

The GC-Columns available is either packed columns or capillary columns. Capillary columns are more favorable because they have shorter retention times and give narrower peaks. The advantage of a packed column is that they can tolerate a larger amount of sample. Capillary columns are the most common columns found today [45]. The wall capillary columns are a fused silica matrix. Fused silica is preferred because of its inertness.

There are two types of capillary columns. The Wall Coated Open Tubular (WCOT) column is a Gas-Liquid Chromatography (GLC) column whose walls are coated with a liquid stationary phase. Porous Layer Open Tubular (PLOT) columns coated with a solid stationary phase are Gas-Solid Chromatography (GSC) columns. PLOT columns are not used expect for in special cases, for example for separation of isomers and fixed gases [46].

The usual detectors for gas chromatography are Thermal Conductivity Detector (TCD), Flame Ionization Detector (FID), or Nitrogen-Phosphorous Detector (NPD). These detectors have different sensi-

tivity, and information. In GC-MS the mass spectrometer acts as the detector, giving both quantitative and qualitative information.

Identification by mass spectrometry [47, 48]

When compounds have been separated through the gas chromatography column, they can be analyzed in a mass spectrometer. Figure 0.10 shows a schematic figure of how the mass spectrometer works. The compounds are first ionized before they are accelerated through a magnetic field that separate the ions based on their mass/charge ratio (m/z).

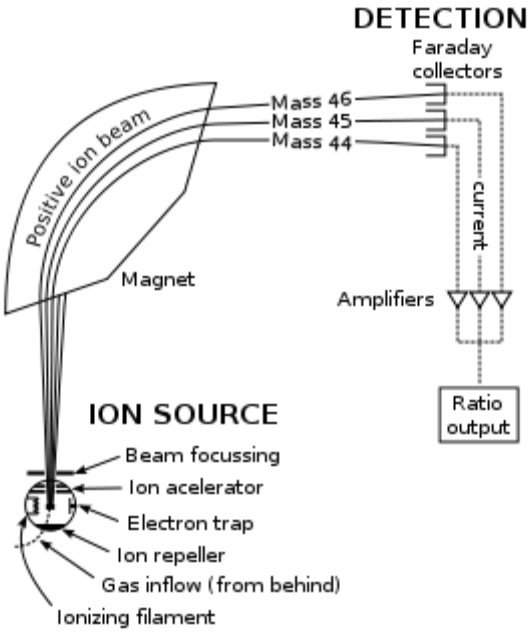

Figure 0.10: Schematic illustration of mass spectrometer[49].

The ionization method is chosen on behalf of the compounds which are analyzed. The common methods for gas-phase ionization are Electron Impact Ionization (EI) and Chemical Ionization (CI).

Electron Impact Ionization (EI) is the most common and usually the standard form of ionization used for GC-MS. When the molecules have entered the MS source, they are bombarded with free electrons emitted from a filament, see Figure 10. When the molecules are attacked by electrons, they produce radical cations, known as molecular ions. A molecular ion can fragment in a characteristic and predictable way. The recorded fragment mass specters can be compared with a library which contains specters of millions of compounds. One of the most common libraries is the National Institute of Standard (NIST) library. EI Mode is an aggressive ionization method that causes the molecules to fragment extensively, making it sometimes difficult to find the original molecular mass (the molecular ion peak).

Chemical Ionization (CI) is the most important type of “soft ionization” techniques used when a molecular ion peak is desired. Instead of bombarding the molecules with high energy electrons, a rea-

gent gas (methane, isobutene or ammonia) is ionized. The sample molecules collide with the reagent gas ions at a relatively high gas pressure, and are ionized by proton transfer $[M+1]^+$, electrophilic addition, $[M+18]^+$, or charge exchange $[M]^+$.

The mass spectrometer can be used in two different modes, Full Scan and Selective Ion Mode (SIM). These modes can be run separately or combined.

The Full Scan mode gives a complete Mass Spectrometry specter showing all molecular ion peaks. This is useful for determining unknown compounds in a sample. The Full Scan mode is often used to identify the specific mass fragments for a molecule before using the SIM method. The target range usually shown in Full Scan is typically between 50 m/z to 400 m/z.

In Selective Ion Mode (SIM), specific mass fragments of compounds, usually determined from full scan, are preselected before analysis. When the sequence is run only the chosen mass fragments are detected in the machine. This makes it easier to detect small fragments since the Mass Spectrometer only is focusing on a small number of fragments. In SIM mode it is possible to identify all the compound peaks or only focus on one. Quantification of peaks is usually done in SIM mode.

3. Experimental

3.1. The oxidative degradation setup

3.1.1. The oxidative degradation apparatus

For this thesis six oxidative degradation experiments were run in three parallels. These experiments will be named M1 to M6 according to when they were run. Two similar apparatuses were used for the degradation experiments. An illustration of the oxidative degradation experimental apparatus is shown in Figure 3.1. Oxygen gas, or an air and oxygen gas mix **1**, and CO_2 gas **2**, entered the apparatus through mass flow controllers (MFC) **3**. The flow of the different gases was set by the MFC's, giving a specific volume percentage of oxygen in the gas stream. This will later be referred to as oxygen percentage or oxygen concentration. The gas streams were later combined to give the reaction gas stream.

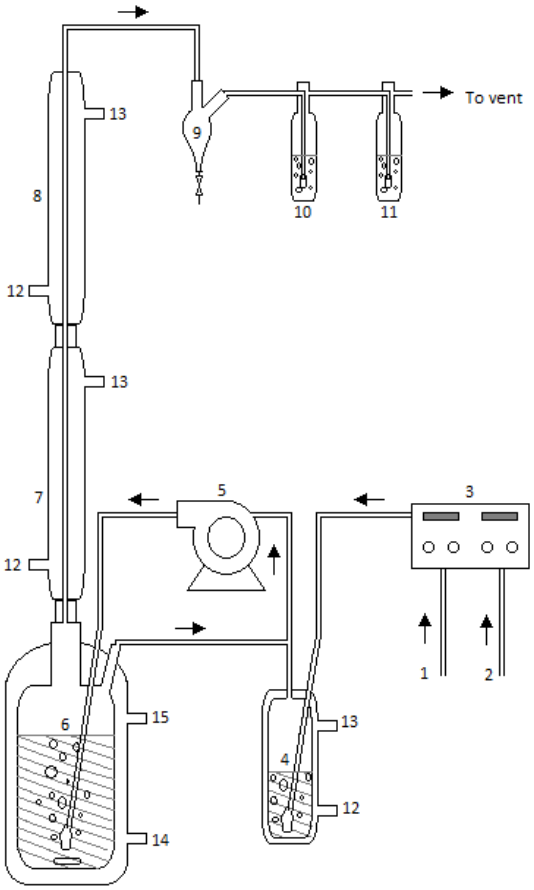

Figure 3.1: Oxidative degradation apparatus.

The reaction gas was bubbled through a reaction vessel **4**, which was filled with water to pre-saturate the gas. This was to maintain the water balance in the main reactor **6**.The reaction vessel was cooled with tap water. The pre-saturated gas and recirculation gas was led into a gas pump (ATB, 50L/min) **5**, which pumps the gas into the main reaction vessel **6**. The reaction gas was bubbled through the

prepared MEA solution during stirring. The main reaction vessel was heated with water from a heating circulator at a set temperature, 55 or 65°C, entering through **14** and exiting through **15**. The gas was then led though two connected condensers cooled with tap water entering through **12** and exiting through **13**. The condensers were connected to a two-necked separatory funnel **9**. After the separatory funnel the gas was led through two gas-washing bottles **10** and **11**, filled with H_2SO_4 (1 M). The washed gas was led to a vented fume hood.

The set up of the mass flow controllers are given in Figure 3.2. The two apparatuses were run in three parallels, giving a total of six experiments. Setup 1 was used for the first two experiments, while the setup 2 was used the last four experiments. For a more detailed description of each experiment see section 3.3.2. MFC 1 and MFC 3 adjusted the mass flow of CO_2, and MFC 2 and MFC 4 adjusted the mass flow of the premixed oxygen/nitrogen gas into the reactors. The mass flow through MFC 5 was combined with the mass flow through MFC 6 or MFC 7 and the flows were adjusted to give the right oxygen percentage for the experiments. In setup 2 the gas mixture controlled by MFC 5 and MFC 7 was used for both reactors.

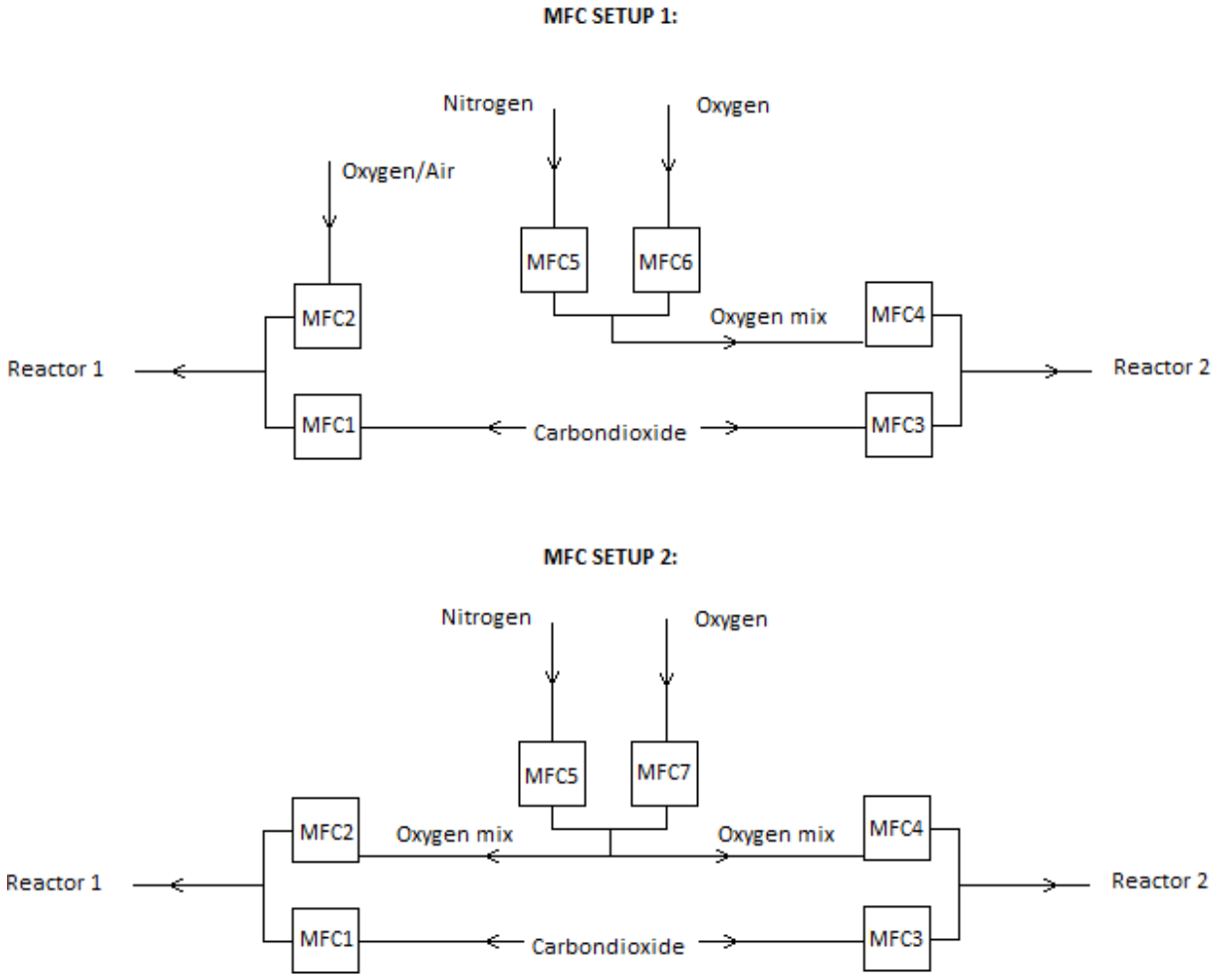

Figure 3.2: The different mass flow controller setups used for the conducted experiments.

3.1.2. Calibration of the mass flow controllers

MFC 6 and 7 were calibrated before experiment M1 and M2. All the mass flow controllers except MFC 7 were calibrated before experiment M3 and M4 was started. This was done by measuring the amount of nitrogen gas let though the controllers at various opening percentages. Soap solution was put in a rubber container at the bottom of a glass cylinder of known volume. When the gas was led into the bottom side of the cylinder, the rubber container was squeezed so that the soap solution covered the gas inlet for a short time, and a soap film started moving up the cylinder. The time was taken for the film to move a specific distance corresponding to a known volume.

The openings required for the wanted oxygen mass flow concentrations were calculated using the obtained calibration curves. The values used for the calibration of each of the mass flow controllers are given in Appendix B. The openings of the mass flow controllers are given in Table 3.1. The oxygen and carbon dioxide percentages and volumetric gas velocities for the experiments are given in Table 3.2. For the first two experiments the oxygen percentages were recalculated according to the newest calibration.

Table 3.1: Percentage openings for mass flow controllers for each parallel of experiments.

Experiment	Opening (%)					
	MFC 1	MFC 2	MFC 3	MFC 4	MFC 5	MFC 7 (6)
M1 and M2	3.4	6.8	3.4	6.3	13.3	8
M3 and M4	2.8	6.1	3.5	6.6	16	12.6
M5 and M6	2.8	6.1	3.5	6.6	29.9	1.7

**MFC 6 was used for experiment M2.*

Table 3.2: Flow of CO_2 through MFC 1 and 3, and O2 mix through MFC 2 and 4. Total gas flow and total O2 and CO2 volume percentage for all experiments.

Experiment	Flow O2 Mix (NL/min)	Flow CO_2 (NL/min)	Total gas flow (NL/min)	O_2 (%)	CO_2 (%)
M1	0.39	0.009	0.4	98	2.3
M2	0.33	0.0073	0.34	5.6	2.1
M3	0.35	0.0075	0.36	49	2.1
M4	0.35	0.0075	0.36	49	2.1
M5	0.35	0.0075	0.36	5.9	2.1
M6	0.35	0.0075	0.36	5.9	2.1

3.2. The oxidative degradation experiment

3.2.1. Preparation of MEA solution

Water (1400 g, 77.71 mol) was added quickly to a solution of MEA (600 g, 9.82 mol) and stirred at room temperature for 15 minutes to give MEA (30wt%). CO_2 (0.4 equiv.) was loaded to the 30wt% MEA solution (1 equiv.) by bubbling the gas into a given amount of MEA solution. Na_2SO_4 (2-1 g) was added to some of the batches. The specific amounts for each batch are given in Table 3.3.

Table 3.3: Amounts of reagents in each batch.

Experiment	MEA 30wt% [g]	MEA [moles]	CO_2 [g]	CO_2 [moles]	Loading, α	Na_2SO_4 [g]
M1	961.09	4.72	83.12	1.889	0.400	1.65
M2	959.85	4.714	83.03	1.887	0.400	1.83
M3	946.23	4.647	81.71	1.857	0.399	-
M4	945.97	4.646	81.68	1.856	0.399	-
M5	952.25	4.677	81.41	1.850	0.396	0.99
M6	961.10	4.721	82.78	1.881	0.398	1.02

3.2.2. Experiment startup

The MEA solution (30wt%, α=0.4) was added to the main reaction vessel. H_2SO_4 [0.5 M] was added to the gas-washing bottles. The relevant temperature was set for the heating circulator. The cooling water was turned on slowly. The gas bottles were opened and the mass flow controllers were turned on to obtain the chosen conditions. The circulation pump and the magnetic stirring were turned on. The specific parameters for each experiment are given in Table 3.4.

Table 3.4: Parameters for start-up of the oxidative degradation experiment.

Experiment	M1	M2	M3	M4	M5	M6
MEA solution [g]	1044.21	1042.88	1027.94	1027.65	1033.66	1043.88
Temperature [^oC]	75	75	65	75	55	65
Oxygen [%]	98	6	50	50	6	6

3.2.3. Sampling

Samples were taken from the reactor and the gas-washing bottles. Sampling time and the sample mass for the main reaction vessel are given in

***Table 3.5*.**

Table 3.5: Amount of solution taken from the reaction vessel for each sample.

Exp.	**M1**		**M2**		**M3**		**M4**		**M5**		**M6**	
Sample No.	Time [days]	Sample mass [g]	Time [days]	Sample mass [g]	Time [days]	Sample mass [g]	Time [days]	Sample mass [g]	Time [days]	Sample mass [g]	Time [days]	Sample mass [g]
1	0	54.44	0	53.7	0	27.11	0	26.96	0	29.51	0	29.37
2	0.9	4.82	0.9	4.7	1.1	4.9	1.1	4.87	1	4.94	1	5.19
3	3	4.89	3	4.81	3.2	4.97	3.2	4.93	3	4.93	3	5.08
4	6.3	4.89	6.4	4.85	7.1	4.85	7.1	5.08	7	5.03	7	5.03
5	8.1	4.91	8.1	4.81	10	5.09	10	5.21	13.9	4.93	13.9	4.98
6	10.1	4.81	10.1	4.84	14	4.79	14	4.82	20.9	5.29	20.9	5.34
7	13	5.04	13	5.07	21.2	5.07	21.2	4.86	28	5.02	28	4.94
8	17.2	4.71	17.2	4.95	28.1	56.85	28.1	54.95	34.8	4.86	34.8	5.03
9	21.2	4.57	21.2	52.13					41.8	53.85	41.8	55.82
10	24	4.77										
11	29.9	4.78										
12	35.9	58.78										

The gas-washing bottles were refilled with H_2SO_4 [0.5 M] when samples were taken from the reaction vessel. The first bottle, **10**, was filled with about twice as much H_2SO_4 as the second bottle, **11**. The sampling time and the mass of H_2SO_4 added to each bottle in the six experiments are found in Appendix C.

3.2.4. Finishing the experiment

After 3-6 weeks the experiment was completed. The last samples were taken and the pump and heating were turned off. The gas bottles for nitrogen, CO_2 and O_2 were closed. The gas-washing bottles were removed and replaced with a gas-washing bottle with distilled water. The solution in the main reaction vessel was cooled to room temperature and the solution was removed from the reaction vessel. The reaction vessel was filled with distilled water, stirred for an hour and emptied twice. The reaction vessel was filled with distilled water, heated to the reaction temperature and stirred overnight. The reaction vessel was cooled to room temperature, emptied and filled with distilled water. The cooling water was turned off.

3.3. Mixing experiments

Two different tests were performed to investigate the formation mechanism of *N*-(2-hydroxyethyl)-glycine (HEGly) by preparing mixtures of intermediate compounds assumed to participate in the suggested mechanism.

3.3.1. Low pH experiment

MEA (1.51 g, 0.025 mol) was added slowly to a mixture of formic acid (23.59 g, 0.51 mol) and glyoxylic acid (50 wt% in water, 7.05 g, 0.048 mol). The reaction mixture was stirred for 72 hours at 40-55 °C. Samples were taken during the experiment, and at the end of the experiment.

3.3.2. High pH experiment

MEA (28.55 g, 0.48 mol) was added slowly to a mixture of water (38.02 g, 2.11 mol) and glyoxylic acid (50 wt% in water, 2.97 g, 0.02 mol). Formic acid (4.60 g, 0.10 mol) was added, and the mixture was stirred for 44 hours at 45-55 °C. Samples were taken at the beginning, during and at the end of the experiment.

3.4. Analytical methods

Different analytical methods were used in order to identify and quantify degradation compounds in the experiments. The chromatographic procedures for GC-MS, LC-MS/MS and IC-EC will be described first. The amine concentration and the total amount of CO_2 were analyzed by the titration methods described in the middle of this chapter. Total nitrogen concentration (Kjeldahl), Heat-Stable Salts (HSS) and density was analyzed by an external contractor.

3.4.1. GC-MS

GC-MS was used to compare the results for HEF and HEPO given by LC-MS.

The MEA solution samples were analyzed on a GC-MS in both Full Scan and SIM mode. The samples and the standards were diluted with distilled water. The samples were diluted to 100 mg/g. The standards were diluted to the following concentrations: 2000, 1428, 1000, 750, 500, 200, 100, 70, 50 and 10 µg/g. The carrier gas was Helium.

The analytes were injected into the column by an Agilent 7693 Autosampler. The Varian Woot Fused Silica, CP-Sil 8CB for Amines, P/N: CP7596, was used to separate the different analytes for SIM analysis of the samples. The column was 30 m with a diameter of 0.32 mm, and was run on a 7890A GC-system. Quantification was done using the standards listed in Appendix A.

The mass spectrometer was an Agilent 5975C inert XL EI/CI MSD with a Triple-Axis Detector. The method described by Lepaumier[50] was used for quantification in the beginning. The samples were then diluted in methanol, see section 4.3.

3.4.2. IC-EC

Gøril Flatberg at IKP, NTNU performed the IC-EC analyses.

The MEA solution samples were analyzed for anions on a Dionex ICS-5000 IC-EC system. The samples and standards were diluted with deionized water (18.2 MΩ). The unknown samples were diluted from 1:50 to 1:10 000 based on mass. The external standards were diluted to 10, 5, 2.5, 1 and 0.5 mg/ml.

The eluent was potassium hydroxide diluted in deionized water (18.2 MΩ) purified by an ICW-3000 water purifier. The system includes an Autosampler (AS-50), a Gradient pump (GP50), a Column Oven (TCC- 3000), a CD conductivity detector, a CRD200 carbonate removal device, an eluent generator system, a ASR300 suppressor, and an Ion Pac AS11-HC column (2mm*250mm) with an Ion Pac AG11-HC guard column (2mm*50mm). Quantification was done using the standards listed in Appendix A.

This method was used to find the concentration of formate, oxalate, nitrate, nitrite, and sulphate (PPM).

3.4.3. LC-MS

Kai Vernstad and Astrid Hyldbakk at SINTEF biotechnology performed the analyses of the samples on LC-MS/MS.

The MEA solution samples and the samples from the gas-washing bottles were analyzed on a LC-MS/MS system. The eluent was formic acid in water (25 mM), with a flow rate of 0.6 ml/min. The analyte was injected to a Supelco Analytical Ascentis® Express RP-Amide HPLC Column, 2.7 µm, Cat. No.:53931-U, by an Agilent Infinity Autosampler 1200 Series G4226A. The column was 15 cm with an inner diameter of 4.6 mm. The molecules were converted to ions by electrospray ionization (ESI). An Agilent 6460 Triple Quadrupole Mass Spectrometer coupled with an Agilent 1290 Infinity LC Chromatograph was used to obtain the mass spectrum.

This method was used to determine the MEA concentration (mol/L) and the concentration of the degradation products (µg/ml) listed in Table X, section X.X. Some of the samples were also analyzed for: DEA (mmol/L), nitrosodiethanolamine (NDELA), nitroso-HeGly, NH3 and the alkylamines: methylamine, ethylamine, dimethylamine and diethylamine.

For more details around the method used see study by de Silva et al[32].

3.4.4. Amine titration

The MEA solution samples were analyzed for total amine concentration by titration. The sample (0.2 g) were diluted with distilled water (50 ml). The solution was titrated with sulfuric acid (0.2 N) on a Mettler Toledo G20 Compact titrator equipped with a Mettler Toledo Rondolino carousel and a Mettler Toledo DGi115-SC pH probe.

3.4.5. CO2 titration

The amount of CO_2 in the first and last sample of the MEA solution for each experiment was analyzed by titration. The sample (1g) was added to a solution of barium chloride (0.1 N, 25 ml) and sodium hydroxide (0.1 N, 50 ml). An identical solution without sample was made as a blank sample. The mixtures were boiled for 4 minutes, and the precipitate was filtrated. The filtrate was added distilled water (~40 ml) and HCl (0.1 N, 60 g). This solution was titrated with sodium hydroxide (0.1 N) on a

Metrohm 809 Titrando. The system includes a Metrohm 814 Sample processer, a Metrohm 800 Dosino dosing unit and a Metrohm 6.0262.100 pH probe. This method is also described by Ma'mun[51].

3.4.6. Density, Heat-Stable Salts and Kjeldahl

The density was analyzed on a Mettler Toledo DM 40 Density Meter, at 22°C. This was done for the start and end samples.

The amount of heat-stable salts was analyzed by Merete Wiig at SINTEF using an ion-exchange based wet chemistry method and titration with NaOH.

The Kjeldahl method was used to analyze the samples for total nitrogen. This was done by an external contractor by the standard method[52].

4. Evaluation of uncertainty in analytical results

4.1. IC-EC

4.1.1. Instrumentation and methods

For the Ion Chromatography analyses, the Instrumentation had been out of order until one month before the delivery date of this thesis. The method used for analysis of the samples from the reaction vessel was therefore not optimized.

Because of the short time most of the results for the compound concentrations were generated using an automated computer method which is less accurate than a more time consuming manual method. The program had multiple ways of integrating the peaks, and did not respond well to negative peaks, Figure 4.1. The retention time of the formate peak varied between 8.1 -9.9 min and the peak were sometimes as broad as 3 min. This led the program to have difficulties recognizing the peak, and splitting it into multiple integration areas.

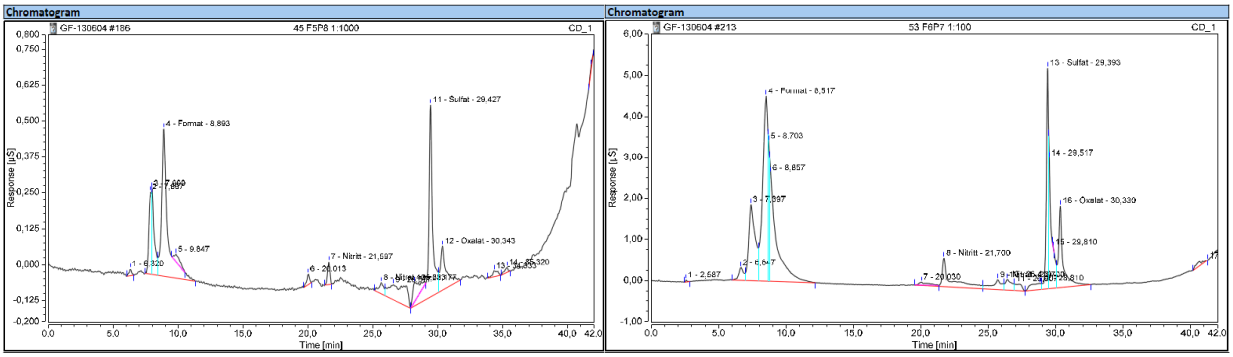

Figure 4.1: Figures of IC-EC specters for samples at different dilutions. The colored lines show the automatically generated areas used to quantify each peak.

Each sample was analyzed using three different dilutions. The automatic program showed higher concentrations of anions for the most diluted samples. The generated results for experiment M1 are given in Appendix D1. As an example: The dilutions 1:10 000, 1:1 000 and 1:500 for nitrite in sample 9, gives respectively these results for nitrite: 3689.2, 769.9 and 646.6 PPM. The effect the dilution has on the computer calculated results seems to mainly influence the anions found in low concentrations. The values that were used in Section 5.2, are mostly the automatically generated results from the least diluted samples, but some values are from higher dilutions. Therefore, the IC-EC results can only be used to identify very distinct trends in the anion concentrations by comparing the different experiments.

For the manual method the integrations were done by hand, but it was not possible to address the problems concerning broad peaks and an uneven baseline. To do this the samples needs to be reanalyzed using a new method of chromatography.

At the end of the work for this thesis most of the samples had been analyzed manually, and these are the results that will be presented in Section 5.3.1.

4.1.2. Comparison of sulphate concentrations

In experiment P1-P4, M1, M2, M5 and M6 known amounts of sodium sulphate (Na_2SO_4) was added. This was compared with the IC-EC results for the first sample of each experiment. The values are given in Table 4.1.

Table 4.1: The sulphate concentration of the first samples calculated from the added amount of sodium sulphate, and the values given by IC-EC analysis.

Experiment	Added sulphate (mg/kg)	Measured sulphate (mg/kg)	Diff (%)
M1	1068.74	1067.02	0
M2*	1186.84	1270.96	7
M5*	647.79	767.08	18
M6*	660.89	775.83	17
P1	1969.30	1820.68	-8
P2	1930.44	1858.77	-4
P3	1926.22	1608.41	-16
P4	2003.39	1716.24	-14

**Results are calculated from computer program described in section 4.1.1.*

These results show that the results given by the computer method described in Section 4.2 give a higher concentration of sulphate than the actual values. The method used to find the concentrations for the project specialization gives lower concentration.

For experiment M1 the standard deviation was calculated for the analyzed concentration. Table 4.2 shows the results and standard deviation with the maximum and minimum values for the sulphate concentration. The sodium sulphate was added to monitor the water balance throughout the experiment. Since the values between minimum and maximum overlaps for all the samples except sample 6 and 8, these results cannot be used to monitor the water balance, and a more precise method of analysis is needed.

Table 4.2: Sulphate concentrations results with standard deviation from IC-EC.

Sample #	Time (Days)	Mean PPM)	STD (PPM)	Min (PPM)	Max (PPM)
1	0.0	1067.022	#N/A	#N/A	#N/A
2	0.9	1096.369	#N/A	#N/A	#N/A
3	3.0	1294.824	382.600	912.223	1677.424
4	6.4	1263.601	158.101	1105.500	1421.702
5	8.1	1211.233	72.387	1138.847	1283.620
6	10.1	1111.646	40.025	1071.621	1151.672
7	13.0	1135.226	46.948	1088.279	1182.174
8	17.2	1187.511	31.854	1155.657	1219.365
9	21.2	1152.115	23.386	1128.730	1175.501

4.2. LC-MS

The MEA concentrations (mol/L) for experiment M5 and M6 were analyzed in parallel (run 1; M5 and M6 versus run 2; M5 and M6) by LC-MS twice. In the first run the dilutions were done by SINTEF Biolab, and in the second run the first dilution was done by the author. The results from the first and second run are compared for both experiments in Table 4.3.

Table 4.3: Results for the first and second analysis of MEA concentrations in M5 and M6.

Experiment	M5			M6		
Time (days)	MEA, run 1 (mol/L)	MEA, run 2 (mol/L)	Difference (%)	MEA, run 1 (mol/L)	MEA, run 2 (mol/L)	Difference (%)
0.0	6.08	5.35	14	5.87	5.20	11
1.0	6.24	5.12	22	5.36	4.91	8
3.0	5.97	5.18	15	5.31	4.95	7
7.0	5.82	5.09	14	5.14	4.69	9
13.9	5.50	4.64	18	5.41	4.53	16
20.9	5.39	4.55	18	5.10	4.96	3
28.0	5.02	4.35	15	4.83	4.63	4
34.8	5.10	4.25	20	4.87	4.17	14
41.8	4.92	4.12	19	4.42	4.49	-2

As can be seen from table 4.3, the maximum-minimum difference between the values for run 1 vs run 2, V_{max}, given for the MEA concentration is 24%. It seems like it is a systematic deviation between the first and second run. These results can therefore not be used to say anything specific about the reduction of MEA in the samples. The reaction rate for MEA in the experiments will be shown in section 5.X. For experiment M5 the V_{max} is 7%, this means that the reaction rate for this experiment is more likely to be close to the actual value compared to experiment M6 which has a V_{max} of 18%.

In Table 4.4, the concentrations of MEA (mol/kg) prepared in the initial solutions, before and after loading with CO_2, are compared to the results given for the first sample by LC-MS analysis. The values for the unloaded solution were used because the CO_2 in the samples are released at temperatures above 121 $^{\circ}$C [53]. The measuring method for MEA seems to give higher values than expected. If the values for each particular experiment are subsequently higher for each sample this will not greatly affect the calculated reaction rates. The nitrogen balance presented in section 5.2.1 might however show a higher recovery rate (R_N) since this is calculated from the measured MEA values.

Table 4.4: Difference in percent between calculated and measured concentration of MEA in start samples.

Experiment	Concentration of MEA in loaded solution (mol/kg)	Concentration of MEA in unloaded solution (mol/kg)	MEA measured by LC-MS (mol/kg)	Difference Unloaded/Measured MEA (%)
M1	4.52	4.91	5.06	3
M2	4.52	4.91	5.77	15
M3	4.52	4.91	5.75	15
M4	4.52	4.91	5.93	17
M5, run 1	4.52	4.91	6.08	19
M5, run 2	4.52	4.91	5.35	8
M6, run 1	4.52	4.91	5.87	16
M6, run 2	4.52	4.91	5.2	6
P2	4.53	4.91	5.22	6
P3	4.55	4.91	5.25	6
P4	4.53	4.91	5.22	6

4.3. GC-MS

The method described by Lepaumier [50] was used to separate the analytes for GC-MS. This method separated the peaks of the standards, but the signal response for the different dilutions did not correspond well, see Figure 4.2. As can be seen from the figure, the signal for 750 µg/ml was a lot higher than the signal for 1 000 µg/ml.

This method has been used previously by Vevelstad and Lepaumier without troubles. The instrumentation was then expected to have caused the problem. The old column was replaced without any results. The pumps were later replaced without improving the signals.

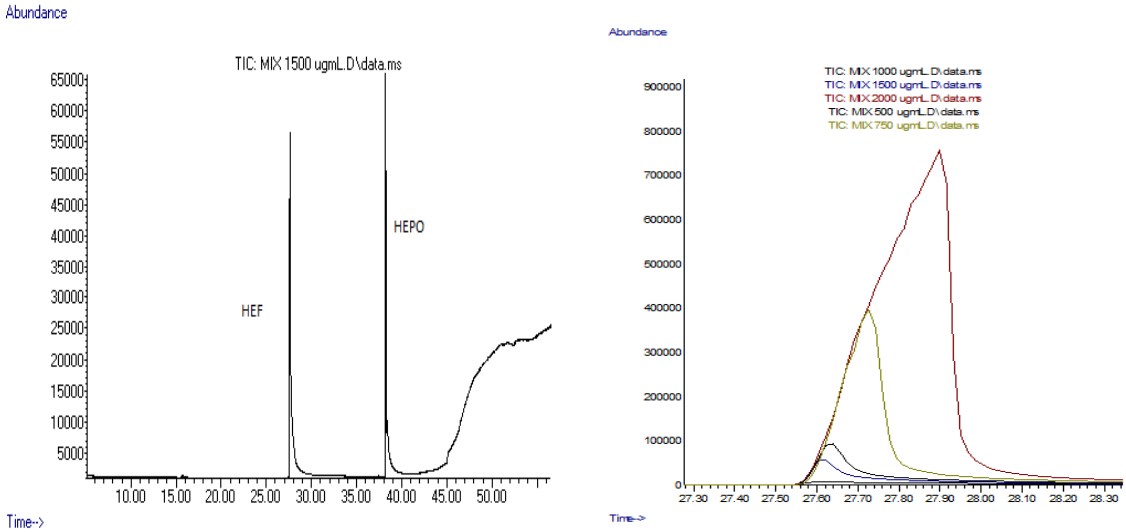

(a) (b)

Figure 4.2: Figure (a) shows the peaks of the standards in a 1500 µg/ml dilution. Figure (b) is a diagram of the HEF peaks for all the dilutions overlayed.

The dilutions had been done with distilled water as described in the method, but since water is known to be difficult to use in GC columns[54], the standards were diluted in methanol. When the results for the different methanol dilutions of the standards were compared, the peak areas gave a better match with the dilution concentrations. This is presented in Figure 4.3 with the calibration curve for HEF.

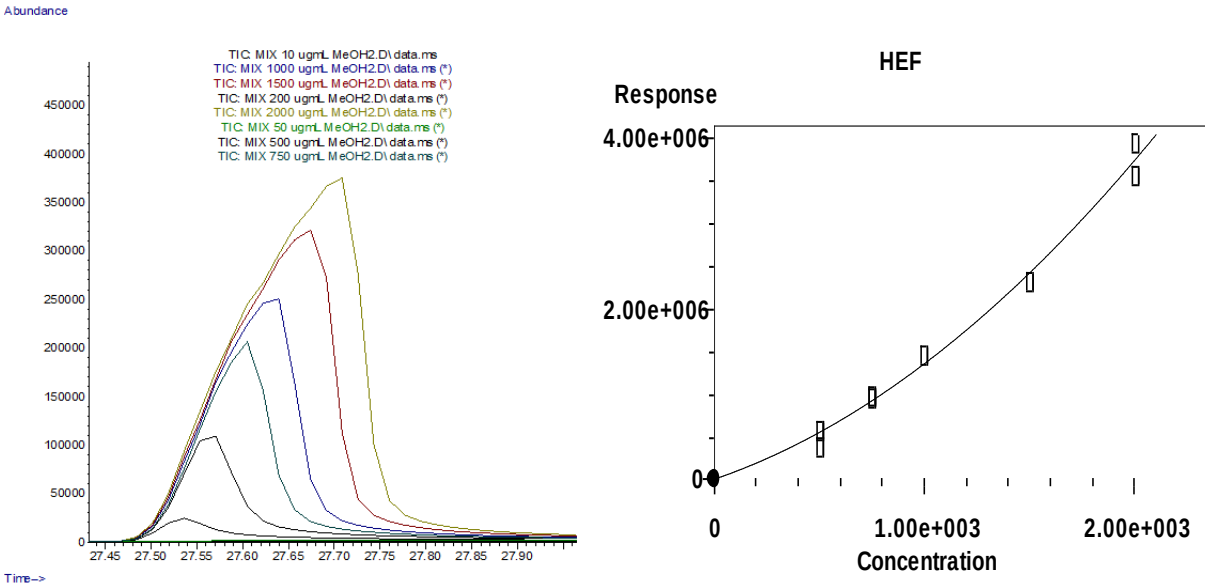

(a) (b)

Figure 4.3: Figure (a) shows the HEF peaks of all the methanol dilutions overlaid. Figure (b) shows the calibration curve obtained from the results.

The product samples for experiment M1 were diluted in methanol, with dilutions 1:20 and 1:50. Sample 9 was analyzed four times for both dilutions to compare the responses. The other samples were run twice. The overlaid specters for sample 9 in both dilutions are shown in Figure 4.4.

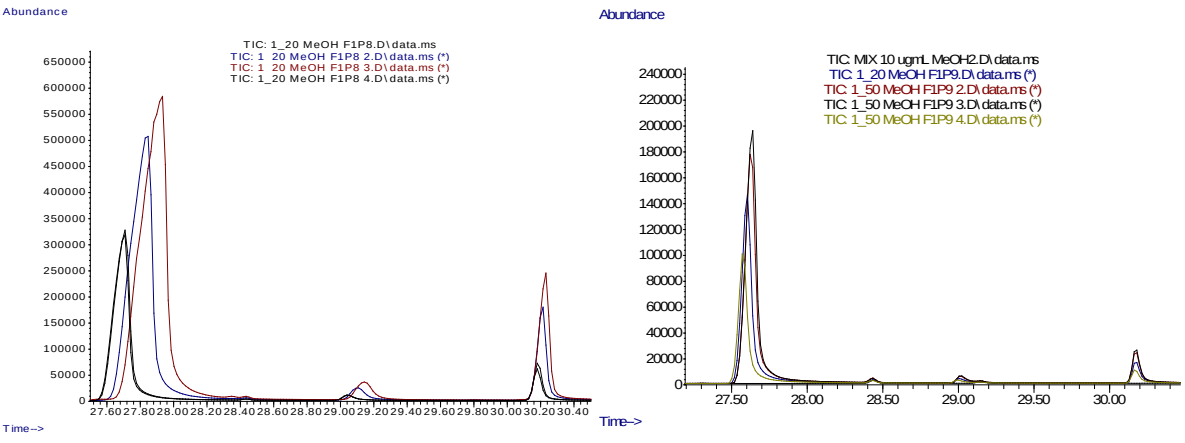

(a) (b)

Figure 4.4: Overlaid specters of four analyses of the same sample. In (a) the peaks for the 1:20 dilution is showed, and the 1:50 dilution in (b).

For the 1:50 dilution both the shape of the compound peaks and the similarity of the responses was improved. The standard deviation was calculated for the results from the 1:50 dilution, and the values with standard deviation are shown in Appendix D1.

The results were compared with the results obtained from LC-MS, and the obtained concentrations for both methods of analysis are shown in Figure 4.5, for HEF and HEPO.

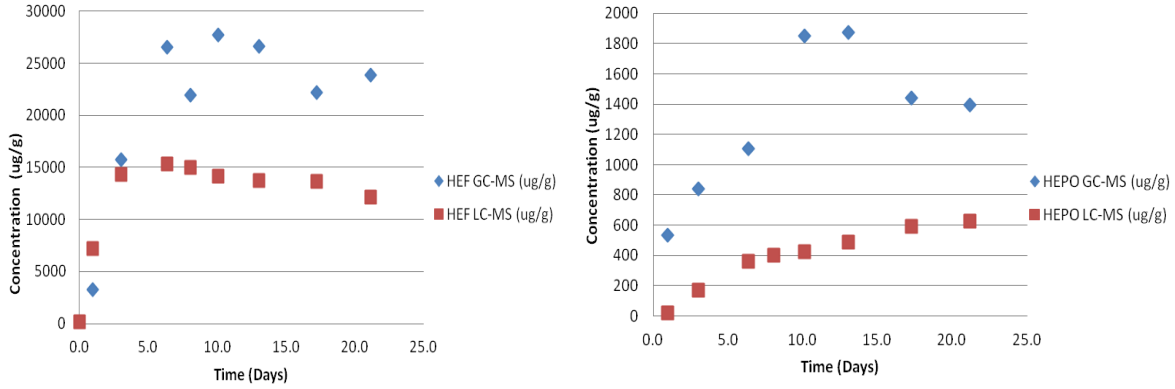

(a) (b)

Figure 4.5: Concentrations for HEF (a) and HEPO (b) analyzed by GC-MS and LC-MS for the samples in M1.

The concentrations found for HEF by GC-MS was up to twice of what LC-MS showed, while for HEPO the values were up to four times as high. The standard deviation for the GC-MS samples was calculated to reach 50% of the mean value. The values given by LC-MS fall significantly below the confidence interval calculated for GC-MS, and the values for GC-MS and LC-MS is not comparable. Because of the discussed problems with GC-MS, the LC-MS results will be deemed the most valid. The degradation pattern shown for HEF in GC-MS is although similar to the results given by LC-MS, and maybe GC-MS will give useable results for the samples if they were more diluted.

5. Results and discussion

In this chapter the results obtained from the oxidative degradation experiments will be presented and discussed. The analytical results for the six experiments performed for this thesis is presented in Appendix D. The results of this thesis will also be compared with the results given in the project specialization report (project) [55], and the doctoral thesis of Vevelstad [37]. The combined results give a matrix of different temperatures and oxygen flow percentages, see Table 5.1. The experiments performed for the project and master thesis, are marked *P* and *M* respectively. The experiments performed by Vevelstad are marked *V*.

Table 5.1: Matrix of oxidative degradation experiments performed at NTNU.

Temperature	Volume percentage of oxygen in gas flow			
	6 %	21 %	50 %	98 %
55 C	M5	P2, V1, V2	V3	V4
65 C	M6	P4	M3	P3
75 C	M1	V5	M4	M2

The results describing the validity of the results for each experiment are presented first. Then the different experimental results will be compared. The trends shown for the degradation compounds will be discussed compared to the suggested reaction mechanisms. At the end of this chapter the results from the mixing experiments will be discussed.

5.1. Validation of experiments

5.1.1. Water balance

The water balance was calculated from the mass of solution added to the reactor at the start of the experiments minus the total mass of the samples, and the total mass of solution taken out of the reactor at the end of the experiments. The water balance for each of the experiments is given in

Table 5.***2***.

The experimental results are considered valid when the change in water mass is less than 7% in either direction. Experiment **P1** has a water loss of 18% and will therefore not be discussed further in this thesis.

The increase in water in some of the experiments is due to the wetting of the CO_2 gas let into the reactor. The mass of water absorbed by the CO_2 was adjusted by the height of water over the sinter in the wetting chamber. For experiment **M5** and **M6**, the water was 1 cm above the sinter, giving the best results for the water balance.

The experiments that show a decrease in water mass has either not had enough water over the sinter in the wetting chamber, or had a leakage in the system somewhere.

Table 5.2: Water balance for all oxidative degradation experiments.

Experiment	T (°C)	O_2 (%)	Water balance (%)
M5	55	6	1.5
P2	55	21	-3.8
V1	55	21	7.5
V2	55	21	6.1
V3	55	50	7.5
V4	55	98	6.1
M6	65	6	1.0
P1	65	21	-18.2
P4	65	21	-3.8
M3	65	50	-2.2
P3	65	98	-5.5
M1	75	6	7.1
V5	75	21	6.0
M4	75	50	-1.1
M2	75	98	-2.2

5.1.2. pH in washing bottles

The exit gas was bubbled through two flasks containing H_2SO_4 (0.05 M) to capture ammonia and MEA. The flasks were changed every 2-7 days, depending on the assumed amount of degradation. To investigate if the maximum capture capacity was reached for any of the experiments, the pH in the washing bottles were measured. The results are given in Table 5.3. Only the results for the experiments showing a pH higher than 2, in any of the bottles, are shown in the table.

Table 5.3: pH measured in the samples from the gas washing bottles, flask 2 is in parentheses.

	M1	M2	M3	M4
T (°C)	75	75	65	75
O_2 (%)	98	6	50	50
Sample 1	9-10 (0)	0-1 (0)	9 (0)	9 (0)
Sample 2	9-10 (8-9)	1-2 (0)	8-9 (0)	1-2 (0)
Sample 3	1 (0)	0-1 (0)	2 (0)	8-9 (0)
Sample 4	9-10 (0)	1 (0)	1 (0)	3-4 (0)
Sample 5	9-10 (0)	0-1 (0)		
Sample 6		1 (0)		
Sample 7		0-1 (0)		

The results show that only sample two of experiment M1 consumed all the amount of acid in both bottles. This means that all the ammonia in the gas phase was not captured for this experiment. The results for ammonia in the gas washing bottles of M1 are therefore assumed to show less ammonia than what was released as gas.

5.2. Overall degradation in experiments

5.2.1. Nitrogen balance

The total weight percent of nitrogen in the end samples analyzed by the Kjeldahl method [52], was compared to the weight percent of nitrogen containing compounds accounted for from LC-MS and NH3 analyses. The results for the project and master thesis are presented in Table 5.4.

Table 5.4: Nitrogen recovery from end samples.

Experiment	T (°C)	O_2 (%)	Time (Days)	Kjeldahl (wt%)	MEA (%)	N in known compounds (wt%)	Nitrogen recovery (RN, %)
M5	55	6	42	5.93	4.82	0.08	83
P2	55	21	21	6.70	5.44	0.18	84
V1	55	21	21	6.00	5.34	0.24	93
V2	55	21	21	5.70	5.36	0.11	96
V3	55	50	21	5.80	5.16	0.17	92
V4	55	98	21	5.60	4.59	0.22	86
M6	65	6	42	5.76	5.28	0.12	94
P4	65	21	21	5.93	4.76	0.18	83
M3	65	50	28	5.38	3.05	0.38	64
P3	65	98	21	5.37	2.99	0.43	64
M2	75	6	36	4.63	4.52	0.21	102
V5	75	21	21	4.60	2.59	0.28	62
M4	75	50	28	4.77	2.07	0.35	51
M1	75	98	21	5.17	1.99	0.43	47

The MEA results for experiment M5 and M6 have an uncertainty of up to ±10%, see Section 4.1. The experiments performed by Vevelstad have an uncertainty of up to ±5%. The trends in the results indicate that the oxygen concentration does not influence the amount of nitrogen containing compounds for the low temperature experiments. For the experiments at 65 and 75 °C, the nitrogen recovery is low when the oxygen concentration is more than 6%. The temperature does not seem to influence the amount of unknown degradation compounds, when the oxygen concentration is low. This indicates that the unknown degradation compounds formed are both temperature and oxygen dependent.

In

Table 5.***5***, the molar balance for nitrogen in MEA, Equation 5.1, is shown. The formation of each of the degradation compounds were calculated as shown by Lepaumier [50], by the Equation 5.2. $\tau_{f,i}$ is the formation percentage for each degradation compound and ν_i is the number of nitrogen atoms in each compound. C^{o}_{MEA}, C^{end}_{MEA} and C^{end}_{i} is the molar concentration of MEA in the start and end sample, and of a degradation compound *i* in the end sample, respectively. N unidentified is the formation percentage of unidentified compounds from the initial concentration of MEA.

$$C^{o}_{MEA} = C^{end}_{MEA} + \sum_{i} C^{end}_{i} \quad (5.1)$$

$$\tau_{f,i} = \nu_i \cdot \frac{C^{end}_{i}}{C^{o}_{MEA}} \cdot 100 \quad (5.2)$$

Table 5.5: Molar balance for nitrogen in MEA, and formation percentage of all degradation compounds.

	M5	P2	M6	P4	M3	P3	M2	M4	M1
T (°C)	55	55	65	65	65	65	75	75	75
O_2 (%)	6	21	6	21	50	98	6	50	98
Time (Days)	42	21	42	21	28	21	21	28	36
MEA start (mol/L)	5.71	5.22	5.53	5.22	5.26	5.25	4.62	5.43	5.27
MEA end (mol/L)	4.52	4.28	4.46	3.72	2.36	2.31	3.47	1.58	1.52
MEA loss (%)	21	18	19	29	55	56	25	71	71
% formation									
DEA	0.0053	0.0084	0.0061	0.0075	0.0070	0.0055	0.012	0.004	0.010
NH_3	0.16	0.50	0.25	0.87	2.1	2.3	0.49	1.6	1.6
HeGly	0.27	0.50	0.62	0.34	0.21	0.14	1.3	0.20	0.30
HEF	0.52	1.28	0.53	0.89	1.98	2.15	0.87	1.66	2.19
BHEOX	0.046	0.056	0.035	0.079	0.15	0.18	0.036	0.093	0.091
HEA	0.030	0.060	0.059	0.047	0.15	0.094	0.10	0.27	0.22
HEPO	0.046	0.078	0.086	0.067	0.08	0.059	0.12	0.079	0.15
OZD	0.082	0.079	0.050	0.093	0.42	0.30	0.041	0.54	0.26
HEI	0.10	0.49	0.28	0.68	1.29	2.33	0.99	1.34	3.20
Total organic	1.25	3.05	1.92	3.08	6.35	7.58	3.99	5.74	8.00
NO2	0.024*	0.192	0.033*	0.162	0.90	0.78	0.02*	0.14*	1.39
NO3	0.068*	0.043	0.055*	0.056	0.30	0.37	0.03*	0.64*	0.57
Total inorganic	0.092*	0.235	0.088*	0.218	1.201	1.152	0.05*	0.78*	1.967
NH_3 from flasks	2.68	-	4.37	-	9.54	10.42	7.61	12.87	12.14
Total MEA loss from degradation compounds (%)	4	3	6	3	17	19	12	19	22
N unidentified (%)	17	15	13	25	38	37	13	52	49

*Results were automatically generated from IC-EC, and are very uncertain.

The formation of NH3, HEF and HEI seems to be the main contributors to the degradation of MEA. This is in accordance with the results found by Vevelstad [37]. The NH3 values from the flasks are recalculated from the concentrations in the gas washing bottle, and due to the loss of acidity for both washing bottles in experiment M1, the NH3 value for the flasks in M1 is uncertain. For experiment M2, NH3 is accounting for about a third of the degradation of MEA and is by far the main degradation compound.

5.2.2. Kinetics

The reaction rate of the experiments was investigated by calculating the rate constant for all the experiments with regards to MEA.

The rate expression for oxidative degradation of MEA as described by Supap et al, is shown in Equation 5.3, where *r* is the reaction rate, *k* is the rate constant and [MEA] is the MEA concentration.

$$r = \frac{dC}{dt} = k[MEA] \tag{5.3}$$

The reaction of MEA to the various degradation compounds is assumed to be first order with regards to MEA. Integrating the rate expression over the time *t* and rearranging the expression gives Equation 5.4.

$$\ln \frac{[MEA]^o}{[MEA]} = k \cdot t \tag{5.4}$$

Plotting ln([MEA]°/[MEA]) against *t* gives a slope of k. The rate constants for the experiments were also calculated for second order reactions by plotting 1/[MEA] versus *t*. The plots for experiment M3 are shown in Figure 5.1.

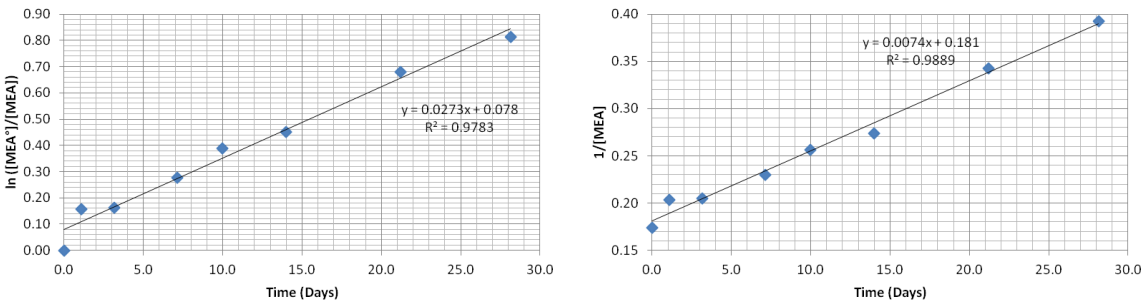

Figure 5.1: Plot for first (a) and second (b) order reaction for experiment M3. The rate constant k is the value found in front of x in the equation.

The coefficients of determination, R^2, were very similar for both the first order and second order plots. This can indicate that MEA goes through a second order reaction rather than a first order reaction. This is although quite unlikely as this would mean that MEA polymerizes in the reaction vessel. Therefore the rate constants for a first order reaction with regards to MEA are compared.

The rate constants *k,* were found for all experiments by plotting. The values obtained are shown in Figure 5.2.

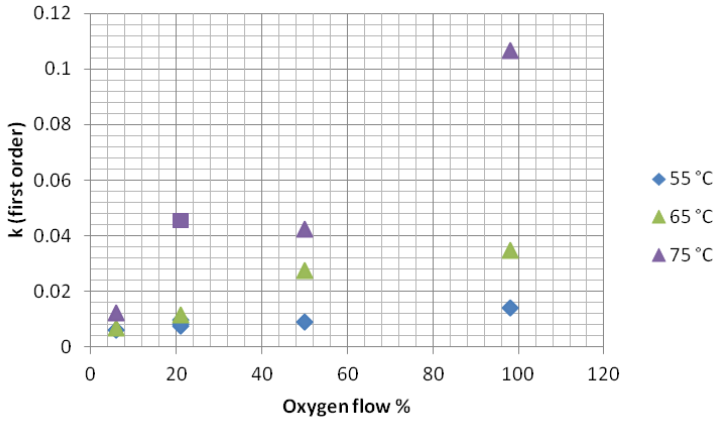

Figure 5.2: Rate constants at different oxygen concentrations and temperatures for all experiments. Square markers are the experiments performed by Vevelstad[37].

The plot shows that the reaction rate for the experiments is not greatly affected by the oxygen flow when the temperature is low. The reaction rate increases however by a factor 3 going from 65°C to 75°C at 98% oxygen. This indicates that some of the degradation reactions take place at a temperature above 65°C.The first order reaction rates found for the experiments are listed in Table 5.6.

Table 5.6: Rate constant k for all experiments

Experiment	O_2 (%)	T (C)	k
M5	6	55 °C	0.0061
P2	21	55 °C	0.0096
V1	21	55 °C	0.0083
V2	21	55 °C	0.0074
V3	50	55 °C	0.0088
V4	98	55 °C	0.014
M6	6	65 °C	0.0069
P4	21	65 °C	0.0115
M3	50	65 °C	0.0273
P3	98	65 °C	0.0349
M2	6	75 °C	0.0121
V5	21	75 °C	0.0454
M4	50	75 °C	0.0424
M1	98	75 °C	0.1067

5.2.3. Amine loss

The amine concentration is calculated from the titration results for the different experiments discussed. The amine loss in percent, α, is calculated by Equation 5.5. C_m^o and C_m^i are the molar concentrations of amines in the start sample and in sample *I*, respectively. For these calculations sample *I* is the end sample. The amine loss for the experiments is shown in

Figure 5.***3***.

$$a = \frac{C_m^o - C_m^i}{C_m^o} \cdot 100 \qquad (5.5)$$

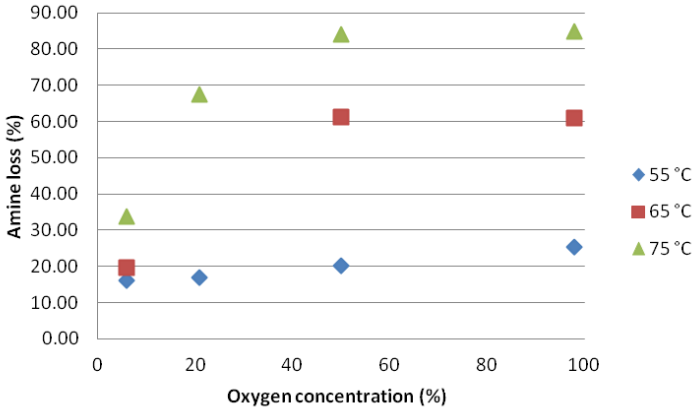

Figure 5.3: Amine loss (%) for experiments performed with different oxygen concentrations and temperatures.

As can be seen from the figure, the amine loss is significantly higher for the experiments at 65 and 75 °C compared to the 55 °C experiments. An increase in the oxygen concentration of the volumetric gas flow does not seem to increase the amine loss after it has reached 50%.

The development of the amine concentration for the experiments performed at 75 °C, and the experiments with an oxygen concentration of 6% are shown in Figure 5.. The normalized amine concentration is found using Equation 5.6.

$$C_N = \frac{C_m^i}{C_m^o} \qquad (5.6)$$

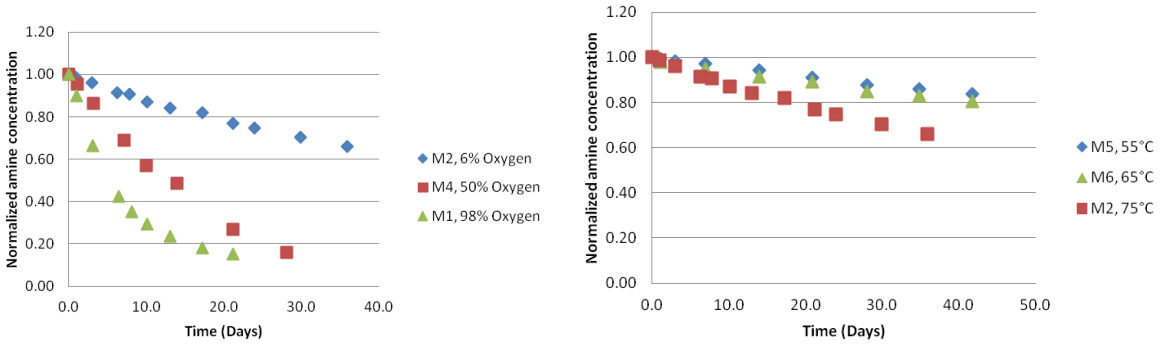

(a) (b)

Figure 5.4: Reduction in amine concentration over time for experiments at 75 °C (a), and experiments at 6% oxygen concentration.

5.2.4. Loading of CO_2 in end samples

The loading of CO_2 in MEA (α) was calculated by dividing the molar concentration of CO_2 with the amine concentration for all the end samples of the experiments. The measured values for the CO_2 concentrations can be found in Appendix D. The results are illustrated in Figure 5.5.

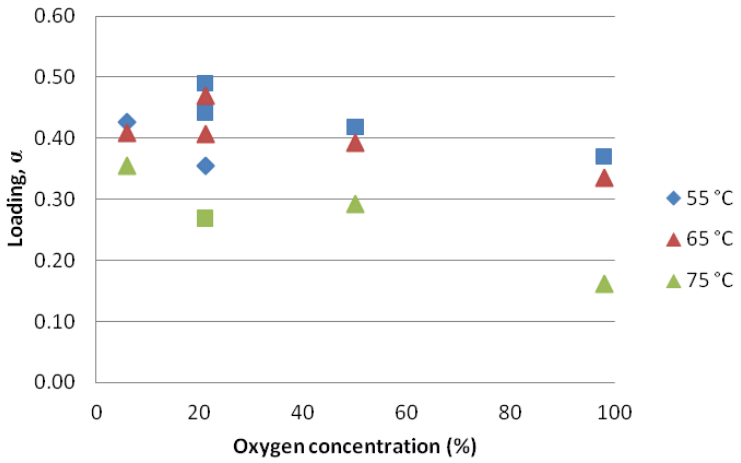

Figure 5.5: Loading of end samples for experiments at different temperatures and oxygen concentrations. The square points are the experiments performed by Vevelstad [37].

The initial loading α, of the samples was 0.4 and for some of the experiments the loading increased. This might be due to differences in the calibration of the gas flow as discussed in chapter 4. The loading does not change significantly for the 55 and 65 °C experiments. For the 75 °C experiments the loading decreases with increasing oxygen concentration. Some of the decrease in loading might be caused by desorption of CO_2 which happens when the temperature rises, but this is generally for temperatures over 121 °C [53]. A decrease in loading might suggest the formation of thermal degradation compounds. Thermal degradation compounds are found to be formed when CO_2 is present, suggesting that the formation mechanism involves CO_2[56]. It has been shown [57] that the loading has a first order effect on the degradation rate of MEA, and therefore this is believed to have an impact on the speed of degradation. Assuming that the loading has decreased linearly, the greatest effect will be on the last samples of the experiments.

5.2.5. Anion balance

The total concentration of anions in the end samples were compared with the results for heat-stable salts (HSS). The results are given in

Table 5.*7*. From the anions formate contributes to 75% of the anions analyzed in all the samples. Oxalate and nitrite have about the same degradation contributing to around 10% each, and nitrate had a contribution of 4%.

Table 5.7: Concentration of HSS compared to analyzed anions in end samples.

	T (°C)	O_2 (%)	Time (Days)	HSS (eq/kg)	Total identified anions (mol/kg)	Identified (%)
M5	55	6	42	0.089	0.05	59
P2	55	21	21	0.264	0.07	26
M6	65	6	42	0.138	0.09	62
P4	65	21	21	0.248	0.13	54
M3	65	50	28	0.595	0.32	53
P3	65	98	21	0.650	0.37	57
M2	75	6	36	0.230	0.18	80
M4	75	50	28	0.835	0.61	73
M1	75	98	21	1.009	0.75	74

The trend show that HSS, as the other degradation compounds, are formed at higher temperatures and oxygen concentrations. The unidentified HSS might be due to the presence of amides, as shown by Vevelstad[37]. It does not seem to be a distinct trend between the amount of HSS formed in an experiment and the amount of HSS accounted for by anion analysis.

5.3. Degradation compounds

In this section the results for the first and second order degradation compounds will be presented and discussed with regards to the proposed mechanisms given in Section 2.2.

5.3.1. First order degradation compounds

The first order degradation compounds were analyzed by the IC-EC method. As discussed in chapter 4, this method showed some inconsistency in the quantification, and will therefore give some uncertainties in the results. The concentrations (PPM) found for all the analyzed anions are given in Appendix D.

Formate

The formate was the first order degradation compound that was found to have the highest concentration of anions in the degradation solution. A graph showing the concentration of formate in mmol/kg after 21 days for all experiments is shown in Figure 5.6.

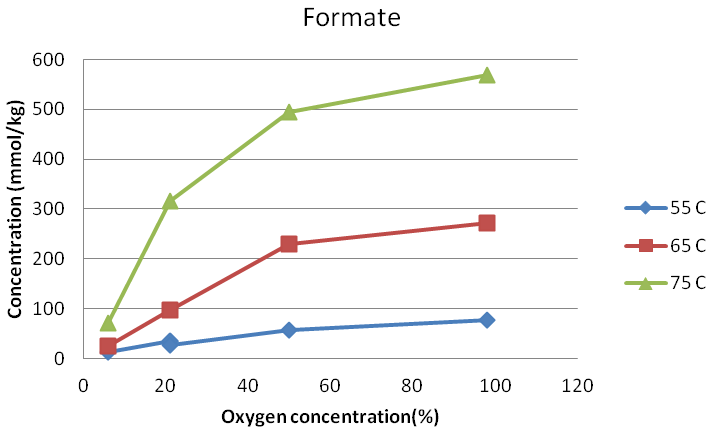

Figure 5.6: Concentration of formate for samples at 21 days at different reaction temperatures and oxygen percentages.

The trends in the figure seem to indicate that the development of formate is influenced highly by the temperature of the reactor. For the experiments performed at 98% oxygen the formate concentration after 21 days is about 7 times as high for the experiment performed at 75 °C compared to the experiment at 55 °C. The concentration of oxygen in the gas stream seems to influence the formation of formate in a linear way until the oxygen concentration reaches 50%. This supports the literature stating that formation of formate involves oxygen. From 50 to 98% the oxygen does not influence the formation of formate in a significant way.

The development of formate throughout the experiment is shown for some experiments in Figure 5.7.

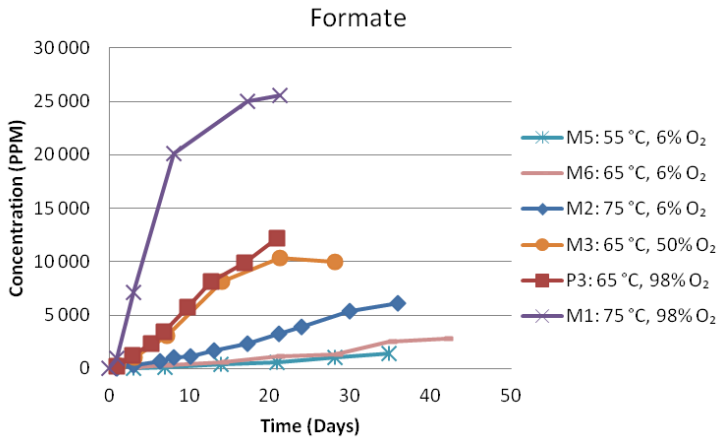

Figure 5.7: The development of the formate concentration as a function of time for some of the performed experiments.

The figure shows a trend where the formation of formate gradually slows down for experiment M1 and M3. This might be due to the high degradation of the reactant MEA, but it can also indicate that formate is consumed to produce secondary degradation compounds (SDC). Formate is as stated in Section 2.2 believed to participate in the formation of HEF.

Oxalate

The concentration of the oxalate anion was found to be at about a tenth of the concentration of formate for the experiments combined. The oxalate concentrations found in mmol/kg for the experiments after 21 days is shown in Figure 5.8.

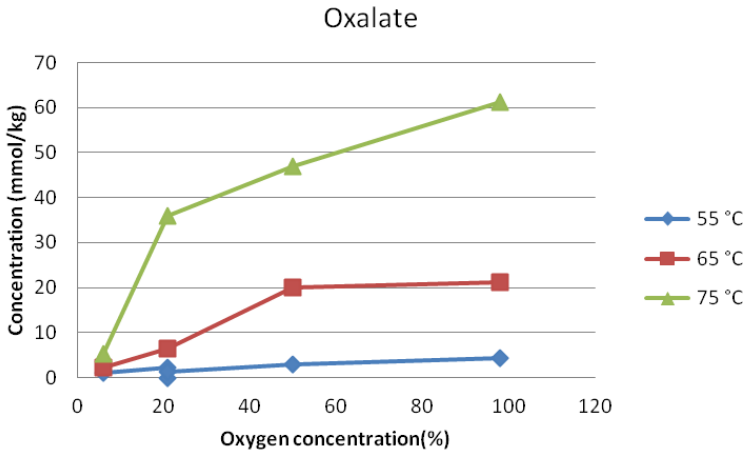

Figure 5.8: Concentration of oxalate for samples at 21 days at different reaction temperatures and oxygen percentages.

The trends seen in the accumulated concentrations of oxalate under different conditions seem to be similar to the trends seen for formate. This also supports the statement that both anions are formed through a similar mechanism involving oxygen.

Looking at the development of oxalate over time for some of the experiments, the anion seems to growth proportionally over time for the experiments performed at high oxygen percentages and temperatures. This is shown in Figure 5.9.

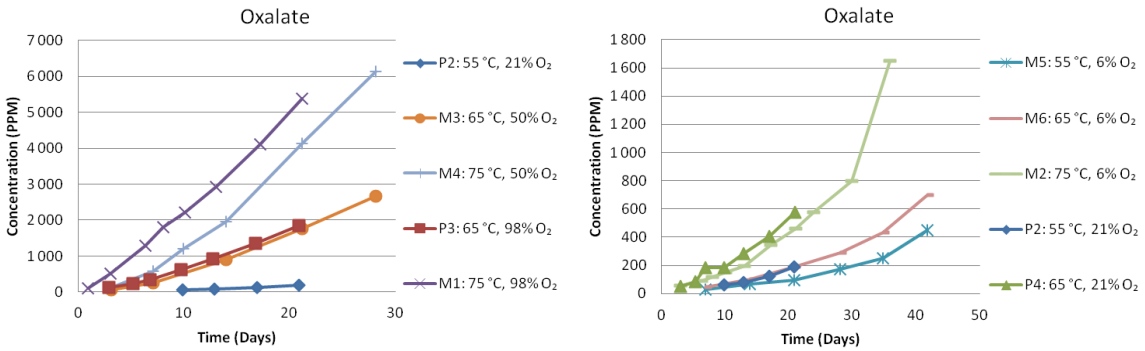

Figure 5.9: The development of the oxalate concentration as a function of time for some of the performed experiments.

For the experiments performed with a low oxygen concentration the oxalate seems to have a more exponential growth. This might be due to oxalate forming from some of the other degradation compounds.

Nitrate

Nitrate was found in the smallest concentration of the anions analyzed for. It was at about half the concentration of oxalate and 20 times smaller than formate. The concentration of nitrate found in the solution after 21 days is shown in Figure 5.10.

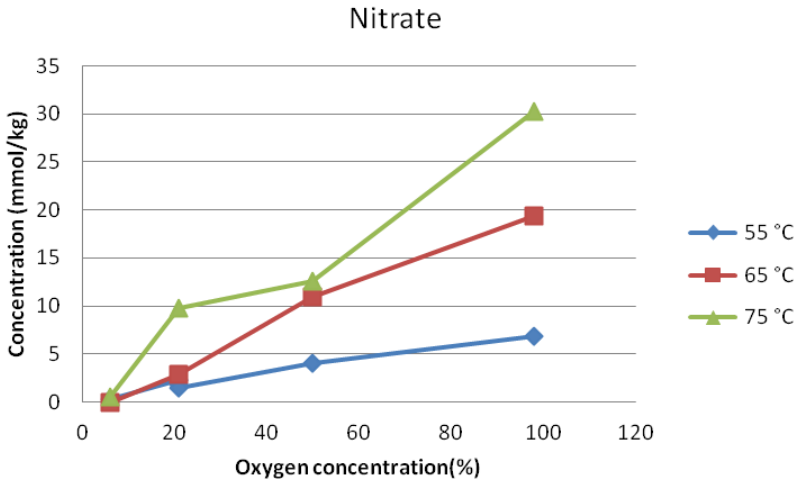

Figure 5.10: Concentration of nitrate for samples at 21 days at different reaction temperatures and oxygen percentages. Point at 21% O_2 and 75 °C is from experiment by Vevelstad.

The concentration of nitrate found in the solution seems to increase when it comes to the oxygen concentration in the gas stream. This is also the case for the temperatures at the highest oxygen con-

centration. At the lower oxygen concentrations the trend also indicates that nitrate increases with the temperature, but this is difficult to say anything certain about due to the variation in the data.

How nitrate has evolved in the reactors for some of the experiments is shown in Figure 5.11. The uncertainty in the values is up to 35%. This might be due to difficulties in quantifying compounds of low concentration.

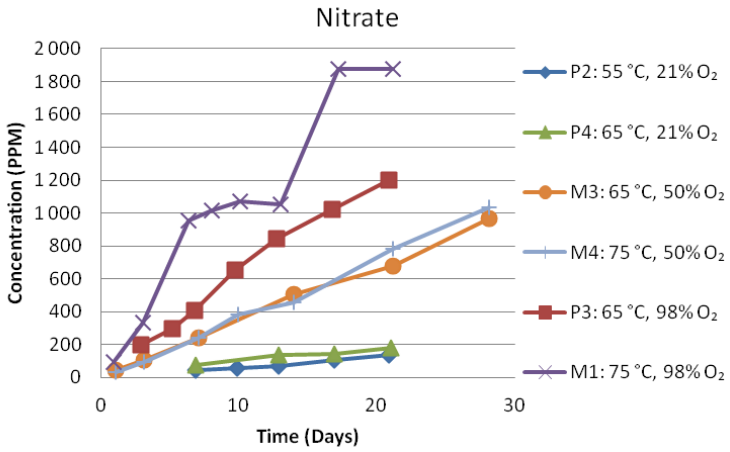

Figure 5.11: The development of the nitrate concentration as a function of time for some of the performed experiments.

From the graph it seems like nitrate also has a linear development over time. The concentration of nitrate in the samples seems to double when the oxygen concentration doubles. If a better method is found for analyzing anions by IC-EC it would be possible to see if the formation of nitrate gradually slows down for M1.

Nitrite

The concentration of nitrite found in the experiments is at about the same level as the oxalate concentration. The nitrite sample concentration in the experiments after 21 days is shown in Figure 5.12.

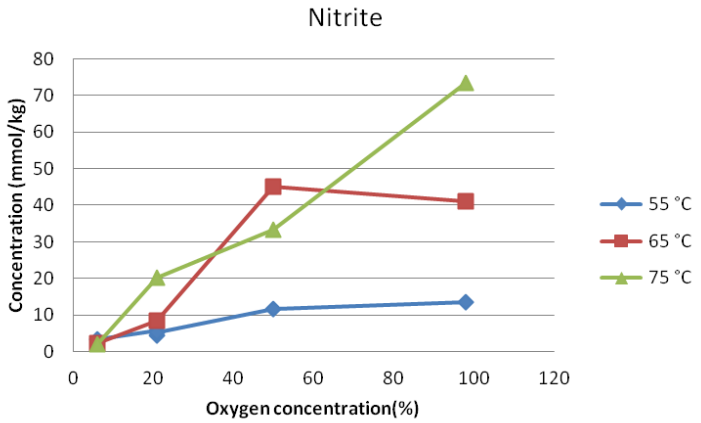

Figure 5.12: Concentration of nitrate for samples at 21 days at different reaction temperatures and oxygen percentages.

Nitrite also seems to show a linear trend of increase in concentration relative to the oxygen flow. The high concentration of nitrite for 50% O_2, 65 °C, is most likely due to uncertainties in the analytical method. The development of nitrite shows a similar degradation pattern as nitrate

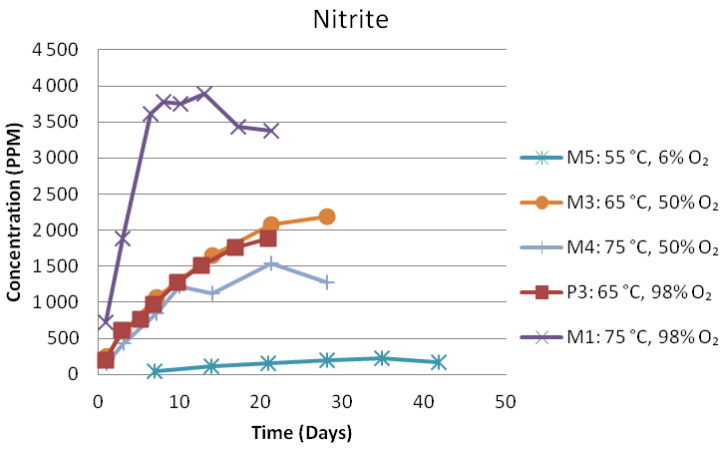

Figure 5.13: The development of the nitrite concentration as a function of time for some of the performed experiments.

In Figure 5.13 the development of nitrite over time for some of the experiments is shown. In almost all the experiments the growth of nitrite slows down after about 21 days. For experiment M1 the amount of nitrite in the reactor decreases after a peak at about 10 days. Nitrate and nitrite is believed to be formed though oxidation of NO_x formed from oxidized nitrogen [38]. The decrease in nitrate for M1 can either be caused by the nitrite reacting on to other degradation compounds, or by the anions being reduced back to nitrogen oxides.

5.3.2. Secondary degradation compounds (SDC)

HEF

HEF is the SDC analyzed for by LC-MS found in the highest concentration in total for the experiments. The amount of HEF found in the samples taken after 21 days for all the experiments are shown in Figure 5.14.

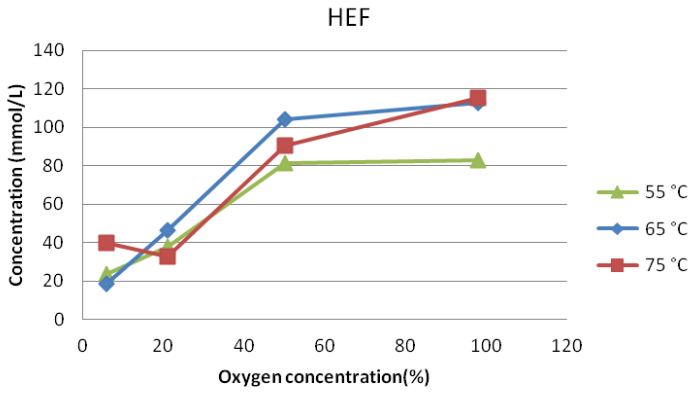

Figure 5.14: Concentration of HEF in samples at 21 days at different reaction temperatures and oxygen percentages.

Figure 5.14 show that the development rate of HEF does not change significantly when the oxygen concentration goes from 50% to 98%. HEF is believed to be formed through the mechanism shown in Figure 2.6, where formate is believed to participate in the formation. When comparing the results with the trends seen for formate, the formation of HEF does not increase in the same rate as formate with regards to the oxygen concentration. This can be due to HEF being involved in reactions that take place at a higher oxygen concentration, and therefore is consumed. This also explains why the HEF concentration for 75 °C is larger at 6% oxygen compared to 21% oxygen. The temperature does not seem to affect the development of HEF in any significant way.

In Figure 5.15 the development of HEF over time is compared for some of the experiments.

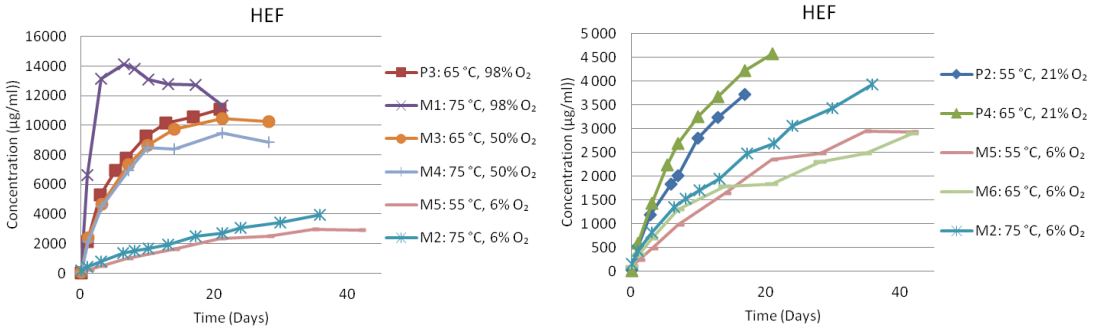

Figure 5.15: The development of the HEF concentration as a function of time for some of the performed experiments.

The results show that for M1 the HEF concentration has a peak at about 10 days. This is the same trends as is seen for nitrite. This can be caused by HEF and nitrite needing similar conditions for formation, but it can also be a result of the two compounds being involved in the formation of another degradation compound. To investigate if this is the case, a mixture experiment of HEF and nitrite can be performed, and analyzing the solution for new products. The formation of HEF seems to be depending on the oxygen flow when the oxygen concentration and temperature is low. For high oxygen concentrations the formation seems however more temperature dependent.

HEA

HEA is the third smallest degradation compound analyzed for in the degradation mix, and has a formation of about a tenth of HEF. The formation of HEA after 21 days is shown for the experiments in Figure 5.16.

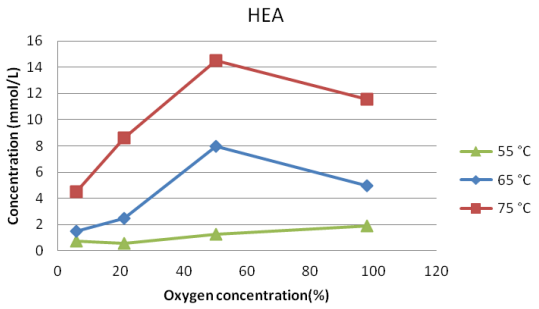

Figure 5.16: Concentration of HEA for samples at 21 days at different reaction temperatures and oxygen percentages.

The trend shows that HEA is formed at a higher rate with increasing temperatures. HEA is assumed to be formed from acetic acid, which had not been analyzed because of low detection limits, and the trends shown in the graph cannot be compared to see if the development is similar. As can be seen from the graph the formation of HEA has a peak at an oxygen concentration of 50%. This can be due to either less acetic acid in the high temperature experiments, or as a result of acetic acid reacting to other compound at these conditions. It can also be explained by HEA being an intermediate in the formation of other degradation compounds at high temperatures. As seen in Figure 5.17, HEA seems to increase about linearly over time, but for experiment M1, the concentration decreases slightly over the last week.

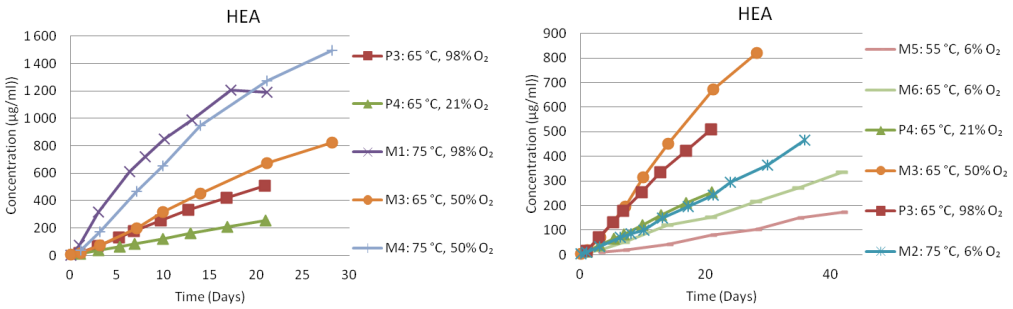

Figure 5.17: The development of the HEF concentration as a function of time for some of the performed experiments.

BHEOX

BHEOX accounts for 2% of the combined results found for SDCs in the experiments after 21 days. The concentration of BHEOX found in the solution after 21 days is shown in Figure 5.18.

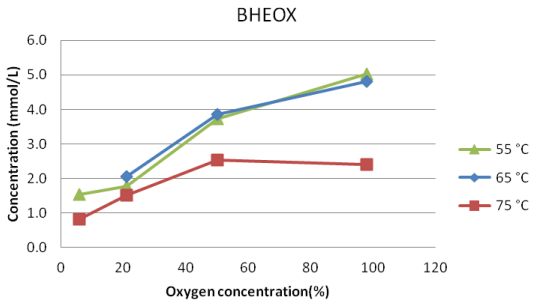

Figure 5.18: Concentration of BHEOX for samples at 21 days at different reaction temperatures and oxygen percentages.

The trends seen for the concentration of BHEOX at 21 days show that the experiments performed at the highest temperature has the smallest concentration. The experiments at 55 and 65 °C seem to be formed at about the same rate. As for HEF the oxygen concentration has the most pronounced effect between 6 and 50%.

Comparing the results of the experiments over time gives the graphs shown in Figure 5.19. It seems like the amount of BHEOX decreases at the end for almost all the experiments. The mechanism of formation of BHEOX is known to be a reversible mechanism with oxalate. As seen in Section 5.3.1 the formation of oxalate increases at high temperatures. It seems that the formation of oxalate is favored over time, which is also supported by its formation rate over time seen for the experiments with low oxygen concentration. The decrease in concentration for BHEOX over time, especially for the high temperature experiments, might also be caused by other degradation compounds formed at high temperatures with BHEOX as an intermediate.

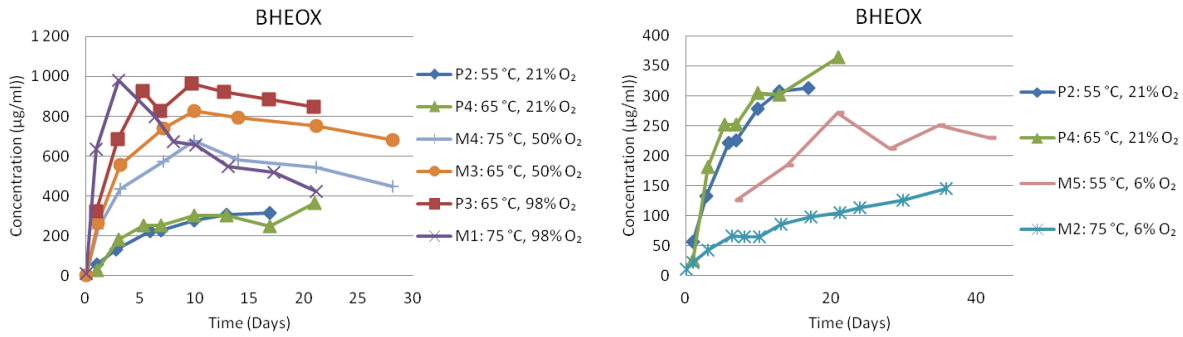

Figure 5.19: The development of the BHEOX concentration as a function of time for some of the performed experiments.

OZD

The OZD concentrations contributed to about 10% of the SDCs found by analysis. The formation of OZD relative to the oxygen concentration seems to be pronouncedly favored for a 50% concentration of oxygen in the gas stream, as shown in Figure 5.20. This is seen especially for the experiments performed at 65 and 75 °C.

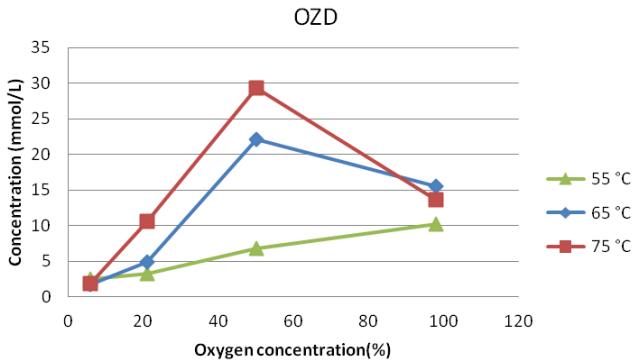

Figure 5.20: Concentration of OZD for samples at 21 days at different reaction temperatures and oxygen percentages.

The mechanism for formation of OZD is suggested to be induced by CO_2. The concentration of CO_2 in the solution is significantly reduced at the experiments with high oxygen concentration and temperature, and may be the cause of the low formation of OZD at these points. The increase in the formation of OZD at 50% oxygen might also be explained by further reactions of OZD at higher oxygen percentages. If this is the case the mechanism for formation most likely involves oxygen.

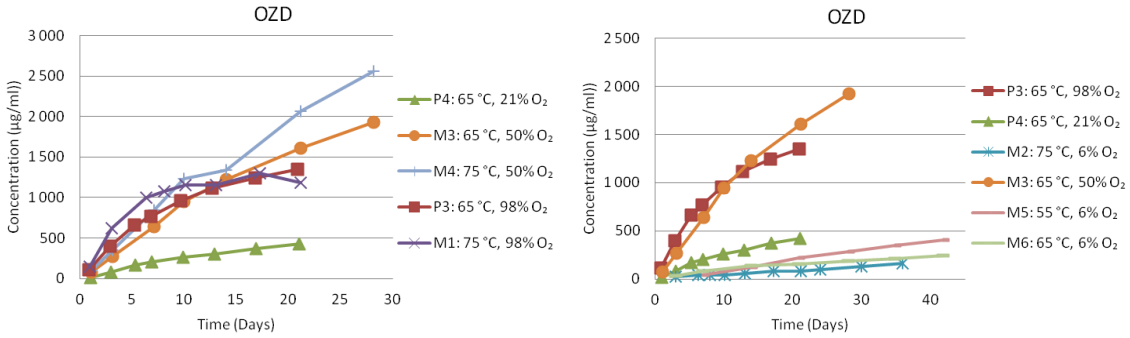

Figure 5.21: The development of the OZD concentration as a function of time for some of the performed experiments.

Figure 5.21 shows the development of the OZD concentration in the experiments over time. From the graphs it seems like the formation rate is similar for the experiments with oxygen concentration over 50% at a temperature of 65 degrees or higher. Experiment M1 shows a slight reduction in OZD at the end of the experiment.

HEI

The concentration of HEI found for the experiments after 21 days corresponds to about 20% of the total amount of SDCs analyzed for. The formation of HEI seems to increase linearly with regards to the oxygen concentration. The exception is the experiment at 75 °C and 6% oxygen (M2), as seen in Figure 5.22, which shows the same trend as seen for HEF. This can indicate a relation between the mechanisms for HEI and HEF. If this is due to HEI being an intermediate for further reaction, the reaction that takes place is both depending on temperature and oxygen concentration.

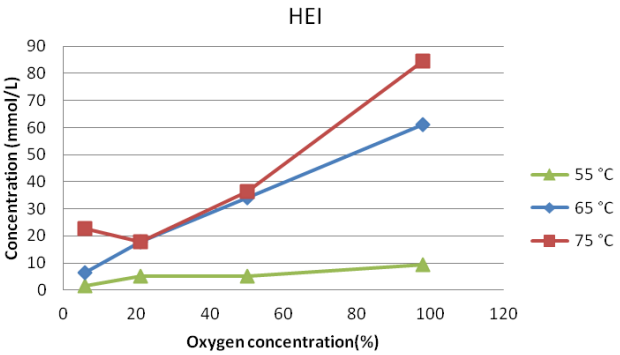

Figure 5.22: Concentration of HEI for samples at 21 days at different reaction temperatures and oxygen percentages.

It is difficult to say anything about the formation of HEI from the assumed intermediated, since the samples were not analyzed for the aldehydes believed to be involved. It is although likely the HEI is formed from through multiple reactions, since the formation is both depending on oxygen and temperature. The concentration of HEI at 55 °C seems to increase linearly with time, but for the experiments performed at higher temperatures the formation slows down over time. In experiment M1, HEI decreases at the end of the experiment, indicating further degradation.

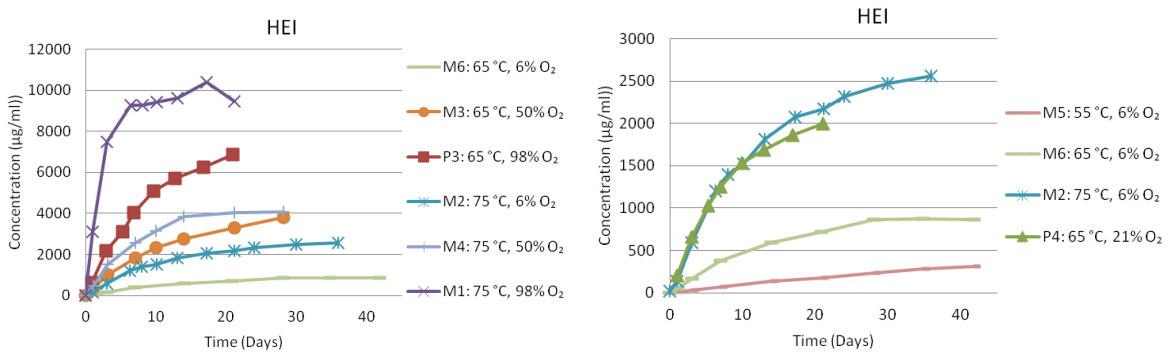

Figure 5.23: The development of the HEI concentration as a function of time for some of the performed experiments.

HEPO

HEPO is the SDC that has been found in the smallest concentration for the total group of experiments. In contrast to the other SDCs HEPO has a decrease of formation at 50% oxygen for the 75°C experiments, as shown in figure 5.24. In figure 5.25 the development of HEPO for this experiment is shown. It seems like the values given for the sample concentrations of this experiment do not follow a smooth curve, and it might therefore be some uncertainty in the value given. The values will also be more uncertain because of difficulties analyzing for very small concentrations.

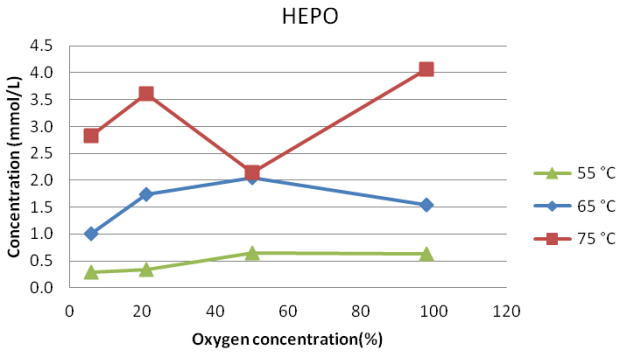

Figure 5.24: Concentration of HEPO for samples at 21 days at different reaction temperatures and oxygen percentages.

If the discussed point is ignored, the concentration of HEPO seems to not depend on the oxygen concentration. The concentration does however seem to have a linear relationship with the temperature for most of the experiments. The curves for the concentration over time show that, for the experiments with high degradation, the rate of formation decreases towards the end of the experiments. For the low degradation experiments, the formation rate seems to grow over time.

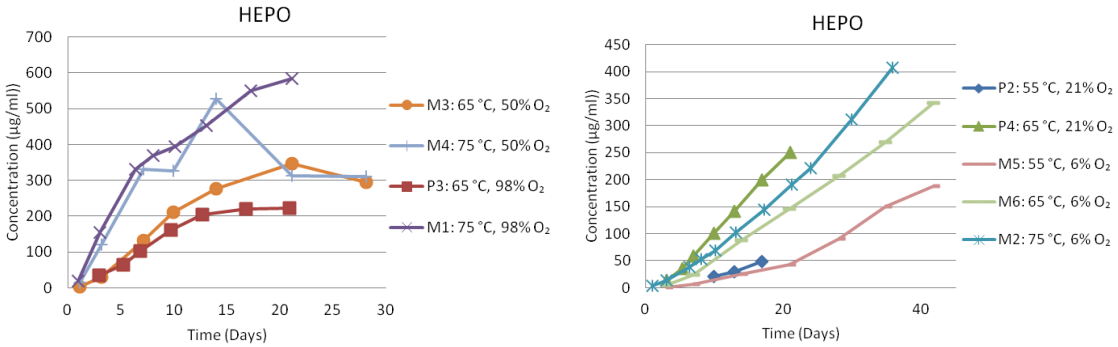

Figure 5.25: The development of the HEPO concentration as a function of time for some of the performed experiments.

HEGly

HEGly is a secondary degradation product that is contributes to about 12% of the total concentration of the analyzed SDCs. The formation of HEGly in the performed experiments after 21 days is shown in Figure 5.26.

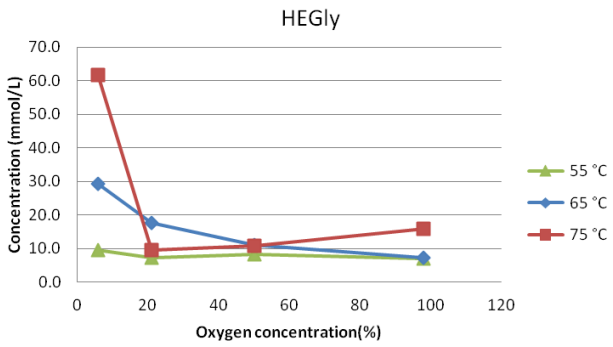

Figure 5.26: Concentration of HEGLy for samples at 21 days at different reaction temperatures and oxygen percentages.

From the figure it is evident that HEGly is formed at a much higher rate when the oxygen concentration is low (6%). For the 6% experiments the formation also seems to have a linear relationship with temperature, whereas the experiments at 21% and higher does not seem to show a very distinct temperature dependency.

The trends seen in the development of HEGly over time is that the formation rate of HEGly decreases over time. This is shown in Figure 5.27. For experiment M4(75 °C, 50% O_2), the concentration of HEGly decreases after about 7 days. This can indicate that HEGly is part of an unknown reaction leading to other unknown degradation compounds. This might also mean the formation of HEGly is in a relationship with OZD or HEA, which show a favored formation at 50% oxygen.

The formation mechanism of HEGly has been important to understand as HEGly was found to be among the dominant degradation compounds in MEA pilot plant samples [32]. A new mechanism for HEGly has been suggested, and mixing experiments have been performed to investigate its validity. This is discussed in Section 5.4.

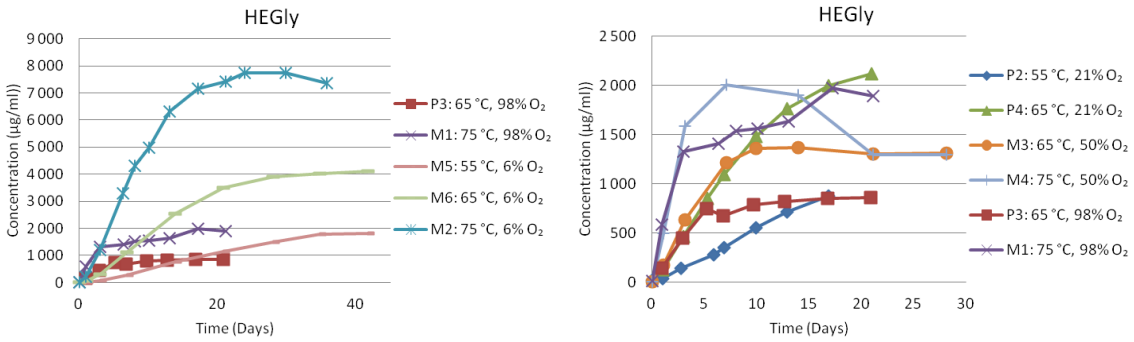

Figure 5.27: The development of the HEGLy concentration as a function of time for some of the performed experiments.

5.4. Mixing experiments for HEGly

A credible formation mechanism for HEGly has not yet been verified. Previously assumed precursor such as DEA and glycine, which both show a similar structure to HEGly, had not seemed to produce significant amounts of HEGly when mixed [58]. A new mechanism of formation has therefore been proposed where glycol aldehyde or glyoxylic acid has been assumed to be the precursors, see Figure 5.28.

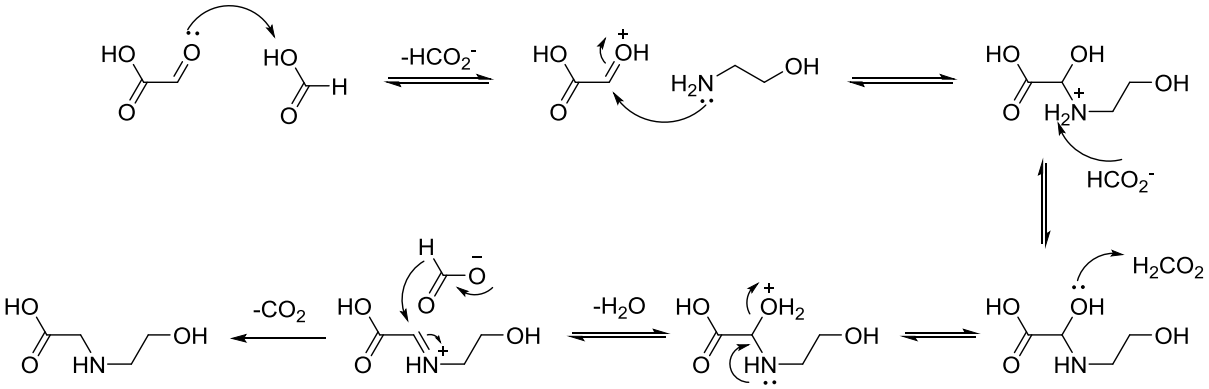

Figure 5.28: Proposed mechanism for the formation of HEGly

The proton transfer steps are however uncertain, and may be affected by pH, components in the solution and reaction conditions. Molecular modelling can be used to suggest which proton transfer mechanisms are more likely to occur. Eide-Haugmo has shown how to do quantum mechanical calculations to find the reaction energy for various reactions[56]. This can show which mechanical step is more favorable for reaction.

To investigate if the suggested mechanism is plausible two mixing experiments were performed by mixing glyoxylic acid, formic acid and MEA. The first reaction solution was acidic and prepared by having an excess amount of formic acid, and MEA as the limiting component. The second experiment was run with glycolic acid as the limiting component and an excess of MEA, making the solution basic and more similar to the actual conditions of the CO_2 absorption column. The concentration of the degradation compound HEGly found for the experiments are shown in Figure 5.8. The values used for the valculation is given in Appendix E.

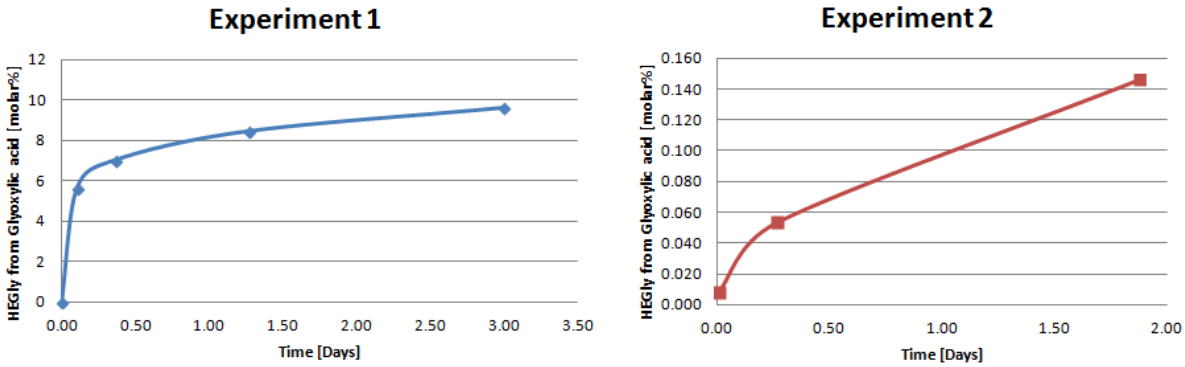

Figure 5.8: Formation of HEGly from glyoxylic acid (molar%) for mixing experiments over time.

The results show that HEGly was formed at a high rate for experiment 1. The formation of HEGly reached 10% of the original molar concentration of glyoxylic acid after 3 days. This result seems to support the suggested mechanism. For experiment 2 the formation of HEGly was only 0.14% of the original concentration of glyoxylic acid. HEF was however formed from 17% of the glyoxylic acid concentration. This might be a result of HEF forming from formic acid and MEA, but HEF was also found in the solution when only glyoxylic acid had been added.

The results found from the second mixing experiment seem to contradict the suggested mechanism, but this may also be because the formation of HEGly is slower in basic conditions. Because the experiment only was run for 2 days, more experiments are needed to fully understand if the mechanism is plausible or not.

6. Conclusion

For more comparable results of the experimental values, the mass flow controllers should be calibrated regularly and the water balance should be monitored by the amount of water in the wetting chambers.

The nitrogen balance shows that changing the temperature does not seem to influence the amount of nitrogen containing degradation compounds with low oxygen concentration (6%) in the gas stream. For experiments performed at 65 degrees or higher, the formation of unknown degradation compounds increases when the oxygen concentration goes from low (6%) to medium (50%), but does not seem to be affected significantly when the oxygen concentration is increased beyond that.

The reaction rate of the degradation of MEA show the same trends that are seen in the nitrogen balance. The development seen of the MEA concentrations is in accordance with the degradation reaction being first order with regards to MEA. The degradation would also fit the curve for a second order reaction of MEA, but this is highly unlikely. The amine loss for the experiments show the same trends for degradation as seen in the nitrogen balance.

The loading of CO_2 to the amine concentration seems not to be close to constant for the experiments performed at 55 and 65 °C. At 75°C the loading decreases when the oxygen flow is increased. This suggests that there is some formation of thermal degradation compounds at 75 °C.

First order degradation compounds found in the solution as anions are found to be present in the solutions in the order: formate > oxalate/nitrite > nitrate. The dependency on oxygen concentration and temperature for the anions are given in Table 6.1.

Table 6.1: Trends seen for anions relative to oxygen concentration and temperature. Yes means the trend is seen in all experiments

Anion	Oxygen dependent	Temperature dependent
Formate	Up to 50% O_2	Yes
Oxalate	55-65 °C: Up to 50% O_2, 75°C:Yes	Yes
Nitrate	Yes	98% O_2:Yes, other exp: Unknown
Nitrite	Yes	98% O_2:Yes, other exp: Unknown

The formation of compounds seen in the total mass of experiments, give the following order for secondary degradation products: HEF > HEI > HEGly > OZD > HEA > BHEOX > HEPO. The trends for these degradation compounds regarding oxygen concentration and temperature is given in Table 6.2.

Table 6.2: Trends seen for degradation compounds relative to oxygen concentration and temperature. Yes means the trend is seen in all experiments

Secondary degradation compound	Oxygen dependent	Temperature dependent
HEF	From 6 to 50%	In early stages for high O_2(%)
HEI	Yes	Yes, mainly 55-65 °C
HEGly	Favored at 6%	Mainly for 6% O_2
OZD	Peak at 50%	6% to 50% O_2: Yes
HEA	Peak at 50%	Yes
BHEOX	Mainly from 6 to 50%	Less formed at 75 °C
HEPO	No	Yes

The mechanism for the formation of HEGly suggested by Vevelstad seems to be unlikely, but further experiments are needed to conclude.

7. Suggestions for further work

There is still more work needed to be done to improve the understanding of the degradation of MEA. For the oxidative degradation setup, running experiments over a longer period of time would increase the understanding of the development of some of the degradation compounds. It would be of interest to rerun some of the experiments to see if the results are reproducible. This is mainly for the experiments run at high temperatures and oxygen percentages as these experiments often show more variation in the curves of formation.

For the experiments that has been performed during this work, more accurate methods for quantification is needed to be developed for both LC-MS, GS-MS and IC-EC. The MEA quantification by LC-MS should be altered since the given concentrations does not seem to be in accordance with the calculated values. The quantification by GC-MS seemed to work better using methanol as a solvent, and higher dilutions of the samples may give better results. Finding ways to analyze and quantify the development of more of the suggested degradation compounds will give a better picture of which compounds are formed from what precursors.

To investigate which unidentified degradation compounds are formed, synthesis experiments mixing known degradation compounds can be conducted. It would be interesting to analyse the reaction mixture after separating the solution using column chromatography and analyzing the different compounds by NMR. Mixing nitrite and BHEOX would be interesting in order to investigate if they form any known or unidentified degradation compounds, as described in Section 5.3.2. If unidentified degradation compounds are found, mechanisms of formation should be suggested.

To find more evidence for the formation mechanism of HEGly or to dismiss it, more experiments similar to the mixing experiments performed are needed. Some suggested reactions are mixing glycol aldehyde with formic acid and MEA. These experiments should also be performed over a larger time interval, compared to the mixing experiments performed for this thesis, to get a more detailed understanding of the reaction.

References

1. Pachauri, R.K., *Climate change 2007. Synthesis report. Contribution of Working Groups I, II and III to the fourth assessment report.* 2008.
2. Meinshausen, M., et al., *Greenhouse-gas emission targets for limiting global warming to 2[thinsp][deg]C.* Nature, 2009. **458**(7242): p. 1158-1162.
3. Van Aalst, M.K., *The impacts of climate change on the risk of natural disasters.* Disasters, 2006. **30**(1): p. 5-18.
4. Rodhe, H., *A comparison of the contribution of various gases to the greenhouse effect.* Science, 1990. **248**(4960): p. 1217-1219.
5. Keeling, C.D., *Rewards and penalties of monitoring the Earth.* Annual Review of Energy and the Environment, 1998. **23**(1): p. 25-82.
6. Metz, B., et al., *Carbon dioxide capture and storage.* 2005.
7. Metz, B., et al., *IPCC special report on carbon dioxide capture and storage: Prepared by working group III of the intergovernmental panel on climate change.* IPCC, Cambridge University Press: Cambridge, United Kingdom and New York, USA, 2005. **2**.
8. Buhre, B.J.P., et al., *Oxy-fuel combustion technology for coal-fired power generation.* Progress in Energy and Combustion Science, 2005. **31**(4): p. 283-307.
9. Lyngfelt, A., B. Leckner, and T. Mattisson, *A fluidized-bed combustion process with inherent CO2 separation; application of chemical-looping combustion.* Chemical Engineering Science, 2001. **56**(10): p. 3101-3113.
10. Gibbins, J. and H. Chalmers, *Carbon capture and storage.* Energy Policy, 2008. **36**(12): p. 4317-4322.
11. Rochelle, G.T., *Amine scrubbing for CO2 capture.* Science, 2009. **325**(5948): p. 1652-1654.
12. Notz, R., et al., *Selection and Pilot Plant Tests of New Absorbents for Post-Combustion Carbon Dioxide Capture.* Chemical Engineering Research and Design, 2007. **85**(4): p. 510-515.
13. Rao, A.B. and E.S. Rubin, *A Technical, Economic, and Environmental Assessment of Amine-Based CO2 Capture Technology for Power Plant Greenhouse Gas Control.* Environmental Science & Technology, 2002. **36**(20): p. 4467-4475.
14. Abu-Zahra, M.R.M., et al., *CO2 capture from power plants. Part I. A parametric study of the technical performance based on monoethanolamine.* International Journal of Greenhouse Gas Control, 2007. **1**(1): p. 37-46.
15. Bedell, S.A., *Amine autoxidation in flue gas CO2 capture—Mechanistic lessons learned from other gas treating processes.* International Journal of Greenhouse Gas Control, 2011. **5**(1): p. 1-6.
16. Bedell, S.A., *Oxidative degradation mechanisms for amines in flue gas capture.* Energy Procedia, 2009. **1**(1): p. 771-778.
17. Kennard, M.L. and A. Meisen, *Mechanisms and kinetics of diethanolamine degradation.* Industrial & engineering chemistry fundamentals, 1985. **24**(2): p. 129-140.
18. Kim, C., *Degradation of alkanolamines in gas-treating solutions: kinetics of di-2-propanolamine degradation in aqueous solutions containing carbon dioxide.* Industrial & engineering chemistry research, 1988. **27**(1): p. 1-3.
19. Chi, S. and G.T. Rochelle, *Oxidative degradation of monoethanolamine.* Industrial & engineering chemistry research, 2002. **41**(17): p. 4178-4186.
20. Dennis Jr, W.H., L.A. Hull, and D.H. Rosenblatt, *Oxidations of amines. IV. Oxidative fragmentation.* The Journal of Organic Chemistry, 1967. **32**(12): p. 3783-3787.
21. Rosenblatt, D., et al., *Oxidations of amines. II. Substituent effects in chlorine dioxide oxidations.* Journal of the American Chemical Society, 1967. **89**(5): p. 1158-1163.

22. Beckwith, A.L., et al., *Amine autoxidation in aqueous solution.* Australian Journal of Chemistry, 1983. **36**(4): p. 719-739.
23. Audeh, C. and J.L. Smith, *Amine oxidation. Part II. The oxidation of some trialkylamines with alkaline potassium hexacyanoferrate (III).* J. Chem. Soc. B, 1970: p. 1280-1285.
24. Smith, J.L. and L. Mead, *Amine oxidation. Part VII. The effect of structure on the reactivity of alkyl tertiary amines towards alkaline potassium hexacyanoferrate (III).* J. Chem. Soc., Perkin Trans. 2, 1973(2): p. 206-210.
25. Smith, J.L. and L. Mead, *Amine Oxidation. Part IX. Oxidation of Some Substituted Tertiary Alkylamines and Some N, N-dimethylphenethylamine with Potassium Hexacyanoferrate (III).* J. Chem. Soc. Perkin II, 1976: p. 1172-1176.
26. Rosenblatt, D.H., et al., *Oxidations of amines. V. Duality of mechanism in the reactions of aliphatic amines with permanganate.* The Journal of Organic Chemistry, 1968. **33**(4): p. 1649-1650.
27. Petryaev, E., A. Pavlov, and O. Shadyro, *Homolytic deamination of amino alcohols.* Zh. Org. Khim, 1984. **20**(1): p. 29-34.
28. Alejandre, J., et al., *Force field of monoethanolamine.* The Journal of Physical Chemistry B, 2000. **104**(6): p. 1332-1337.
29. Button, J., et al., *Molecular dynamics simulation of hydrogen bonding in monoethanolamine.* Fluid phase equilibria, 1996. **116**(1): p. 320-325.
30. Yazvikova, N., L. Zelenskaya, and L. Balyasnikova, *Mechanism of side reactions during removal of carbon dioxide from gases by treatment with monoethanolamine.* Zhurnal Prikladnoi Khimii, 1975. **48**(3): p. 674-676.
31. Gouedard, C., et al., *Amine degradation in CO2 capture. I. A review.* International Journal of Greenhouse Gas Control, 2012. **10**: p. 244-270.
32. da Silva, E.F., et al., *Understanding 2-Ethanolamine Degradation in Postcombustion CO2 Capture.* Industrial & Engineering Chemistry Research, 2012. **51**(41): p. 13329-13338.
33. Lepaumier, H., et al., *Comparison of MEA degradation in pilot-scale with lab-scale experiments.* Energy Procedia, 2011. **4**: p. 1652-1659.
34. Katsuura, A. and N. Washio, *Preparation of imidazoles from imines and iminoacetaldehydes*. 2005, Nippon Synthetic Chemical Industry Co., Ltd., Japan . p. 6 pp.
35. Kawasaki, N., et al., *Preparation of 1-substituted imidazoles*. 1991, Mitsui Toatsu Chemicals, Inc., Japan . p. 7 pp.
36. Ben, D.S.P., *Process for the preparation of -1-(2-hydroxyethyl) imidazole*. 2005, India . p. 6pp.
37. Vevelstad, S., *CO2 absorbent degradation*, in *Department of Chemical Engineering*. 2013, Norwegian University of Science and Technology: Trondheim.
38. Sexton, A.J. and G.T. Rochelle, *Reaction products from the oxidative degradation of monoethanolamine.* Industrial & Engineering Chemistry Research, 2010. **50**(2): p. 667-673.
39. Supap, T., et al., *Analysis of monoethanolamine and its oxidative degradation products during CO2 absorption from flue gases: A comparative study of GC-MS, HPLC-RID, and CE-DAD analytical techniques and possible optimum combinations.* Industrial & engineering chemistry research, 2006. **45**(8): p. 2437-2451.
40. Kadnar, R. and J. Rieder, *Determination of anions in amine solutions for sour gas treatment.* Journal of Chromatography A, 1995. **706**(1): p. 339-343.
41. Christie, W.W., *Gas chromatography and lipids.* 1989.
42. Poppe, H., *Some reflections on speed and efficiency of modern chromatographic methods.* Journal of Chromatography A, 1997. **778**(1): p. 3-21.
43. Greibrokk, T. and T. Andersen, *High-temperature liquid chromatography.* Journal of Chromatography A, 2003. **1000**(1): p. 743-755.
44. Strazisar, B.R., R.R. Anderson, and C.M. White, *Degradation pathways for monoethanolamine in a CO2 capture facility.* Energy & Fuels, 2003. **17**(4): p. 1034-1039.
45. Dandeneau, R.D. and E. Zerenner, *An investigation of glasses for capillary chromatography.* Journal of High Resolution Chromatography, 1979. **2**(6): p. 351-356.

46. Zechmeister, L., et al., *Principles and Practice of Chromatography.* Principles and Practice of Chromatography., 1943(2nd Edit).
47. Silverstein, R. and F. Webster, *Spectrometric Identification of Organic Compounds6*. 2006: John Wiley & Sons.
48. Hoffmann, E., *Mass spectrometry*. 1996: Wiley Online Library.
49. Revesz, K.M., J.M. Landwehr, and J. Keybl, *Measurement of delta13C and delta18O Isotopic Ratios of CaCO3 Using a Thermoquest Finnigan GasBench II Delta Plus XL Continuous Flow Isotope Ratio Mass Spectrometer With Application to Devils Hole Core DH-11 Calcite*. 2001, DTIC Document.
50. Lepaumier, H., et al., *Degradation of MMEA at absorber and stripper conditions.* Chemical Engineering Science, 2011. **66**(15): p. 3491-3498.
51. Ma'mun, S., et al., *Selection of new absorbents for carbon dioxide capture.* Energy Conversion and Management, 2007. **48**(1): p. 251-258.
52. Kjeldahl, J., *A new method for the determination of nitrogen in organic matter.* Z. Anal. Chem, 1883. **22**: p. 366.
53. Yeh, J.T., H.W. Pennline, and K.P. Resnik, *Study of CO2 absorption and desorption in a packed column.* Energy & fuels, 2001. **15**(2): p. 274-278.
54. Poole, C.F. and S.K. Poole, *Chromatography today*. 1991: Elsevier Science Publishers.
55. Johansen, M.T., *Degradation of absorbent systems*, in *Department of Chemistry*. 2012, Norwegian University of Science and Technology: Trondheim.
56. Eide-Haugmo, I., *Environmental impacts and aspects of absorbents used for CO2 capture*. 2011, Norwegian University of Science and Technology.
57. Davis, J. and G. Rochelle, *Thermal degradation of monoethanolamine at stripper conditions.* Energy Procedia, 2009. **1**(1): p. 327-333.
58. Knuutila, H., et al., *Formation and destruction of NDELA in 30wt% MEA (monoethanolamine) and 50wt% DEA (diethanolamine) solutions.* Oil and Gas Science and Technology Journal, 2013.

Appendix A: External standards used for quantification of degradation products by GS-MS and IC-EC

Table A.1: Standards used for quantification on a GC-MS apparatus.

Standard	Abb.	Purity [%]	CAS No.	Lot No.	Supplier
N-(2-hydroxyethyl) formamine	HEF	97	693-06-1	G28W033	Alfa Aesar
N, N'-bis(2-hydroxyethyl) oxalamide	BHEOX	99	1871-89-2	E4544B	Alfa Aesar
N-(2-hydroxyethyl) imidazolidinone	HEIA	97	3699-54-5	J26U041	Alfa Aesar
2-oxazolidinone	OZD	98	497-25-6	MKBJ2536V	Aldrich
N-(2-hydroxyethyl) imidazole	HEI	97	1615-14-1	1420DH	Aldrich
4-(2-hydroxyethyl) piperazin-2-one	HEPO	97	23936-04-1	H30070	Tyger
N-(2-hydroxyethyl) acetamine	HEA	99	142-26-7	100455	Aldrich

Table A.2: Standards used for quantification by IC-EC apparatus.

Standard	Purity [%]	CAS No.	Lot No.	Supplier
Oxalic acid	99	144-62-7	BCBO6467V	Sigma-Aldrich
Formic acid	98	64-18-6	1434094	Fluka analytical
Sodium nitrite	97	7632-00-0	1451880	Sigma-Aldrich
Potassium nitrite	99	7757-79-1	06228CJ	Sigma-Aldrich
Glycolic acid	99	79-14-1	2.84E+08	Fluka analytical
Sodium sulfite	99	7757-82-6	A019196201	Sigma-Aldrich

Appendix B1: Calibration of mass flow controllers

Calibration of MFC 1

Innstilt gassflow (%) av max	Målt mengde gass (L)	Tid (s)	(L/min)	Middel (L/min)	(NL/min) omregnet
30	0.027	14.10	0.115		
	0.027	14.10	0.115		
	0.027	14.09	0.115		
	0.027	14.15	0.114	0.115	0.107
20	0.027	21.03	0.077		
	0.027	21.00	0.077		
	0.027	21.03	0.077		
	0.027	21.09	0.077	0.077	0.072
10	0.027	41.75	0.039		
	0.027	41.72	0.039		
	0.027	41.78	0.039		
	0.027	41.72	0.039	0.039	0.036
2	0.004	24.94	0.008		
	0.004	24.66	0.009		
	0.004	24.79	0.008		
	0.004	24.62	0.009	0.008	0.008

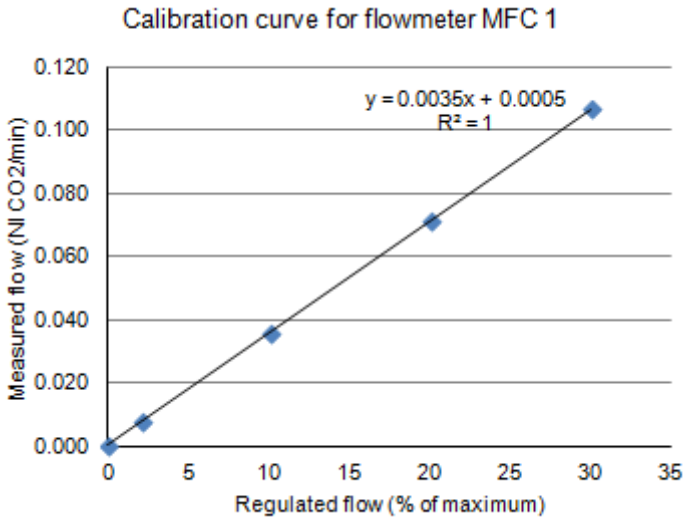

Figure B1-1: MFC 1: Values found for calibration

Calibration of MFC 2

Figure B1-2: MFC 2: Values found for calibration

Innstilt gassflow (%) av max	**Målt mengde gass (L)**	**Tid (s)**	**(L/min)**	**Middel (L/min)**	**(NL/min)** omregnet
60	1.000	17.06	3.517		
	1.000	16.97	3.536		
	1.000	17.00	3.529		
	1.000	16.97	3.536	3.529	3.278
30	0.500	16.26	1.845		
	0.500	16.25	1.846		
	0.500	16.28	1.843		
	0.500	16.25	1.846	1.845	1.714
10	0.200	16.50	0.727		
	0.200	16.47	0.729		
	0.200	16.59	0.723		
	0.200	16.50	0.727	0.727	0.675

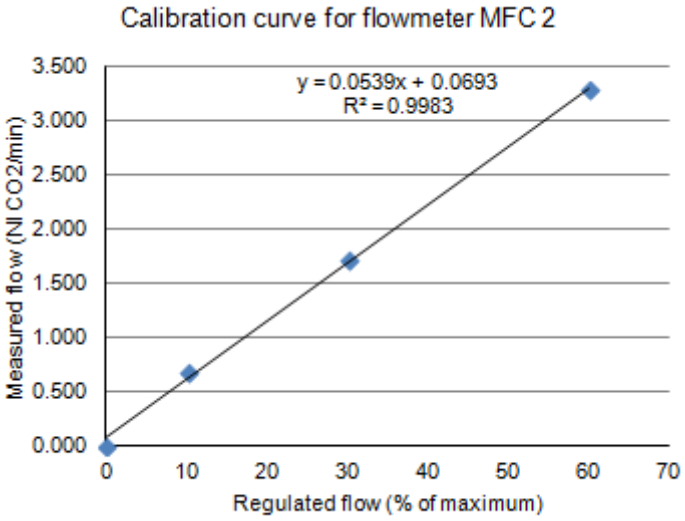

Calibration of MFC 3

MFC 3: Values found for calibration

Innstilt gassflow (%) av max	Målt mengde gass (L)	Tid (s)	(L/min)	Middel (L/min)	(NL/min) omregnet
30	0.027	13.38	0.121		
	0.027	13.31	0.122		
	0.027	13.31	0.122		
	0.027	13.41	0.121	0.121	0.113
10	0.027	35.54	0.046		
	0.027	35.56	0.046		
	0.027	35.54	0.046		
	0.027	35.56	0.046	0.046	0.042
2	0.004	13.69	0.015		
	0.004	13.69	0.015		
	0.004	13.66	0.015		
	0.004	13.71	0.015	0.015	0.014

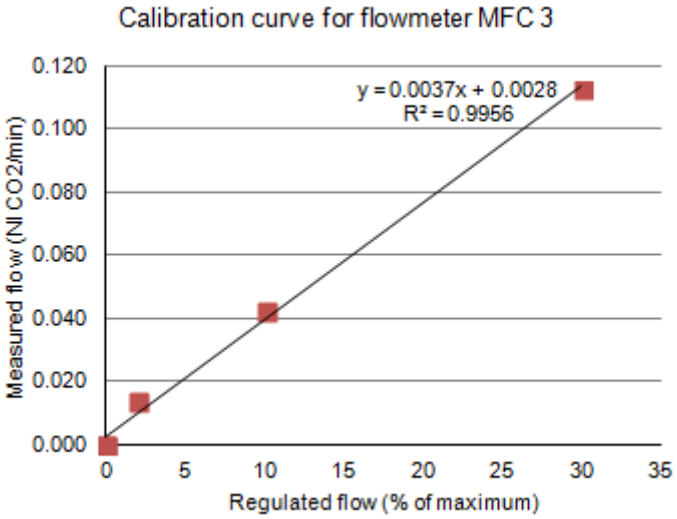

Calibration of MFC 4

MFC 4: Values found for calibration

Innstilt gassflow (%) av max	Målt mengde gass (L)	Tid (s)	(L/min)	Middel (L/min)	(NL/min) omregnet
60	1.000	17.75	3.380		
	1.000	17.69	3.392		
	1.000	17.78	3.375		
	1.000	17.72	3.386	3.383	3.143
30	0.500	17.59	1.706		
	0.500	17.54	1.710		
	0.500	17.50	1.714		
	0.500	17.47	1.717	1.712	1.590
10	0.200	19.88	0.604		
	0.200	19.88	0.604		
	0.200	20.04	0.599		
	0.200	19.91	0.603	0.602	0.559

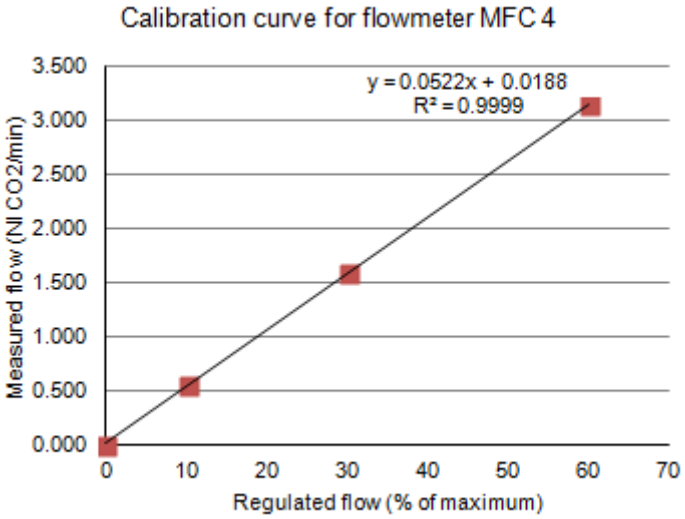

Calibration of MFC : First calibration

MFC 5: Values found for calibration; Calibration 1

Innstilt gassflow (%) av max	**Målt mengde gass (L)**	**Tid (s)**	**(L/min)**	**Middel (L/min)**	**(NL/min)** omregnet
50	0.50	23.59	1.27		
	0.50	23.50	1.28		
	0.50	23.44	1.28		
				1.28	1.14
30	0.50	39.50	0.76		
	0.50	39.54	0.76		
	0.50	39.56	0.76		
				0.76	0.68
10	0.20	47.22	0.25		
	0.20	47.35	0.25		
	0.20	47.13	0.25		
	0.20	47.31	0.25	0.25	0.23
5	0.10	48.00	0.13		
	0.10	48.03	0.12		
	0.10	48.50	0.12		
	0.10			0.12	0.11

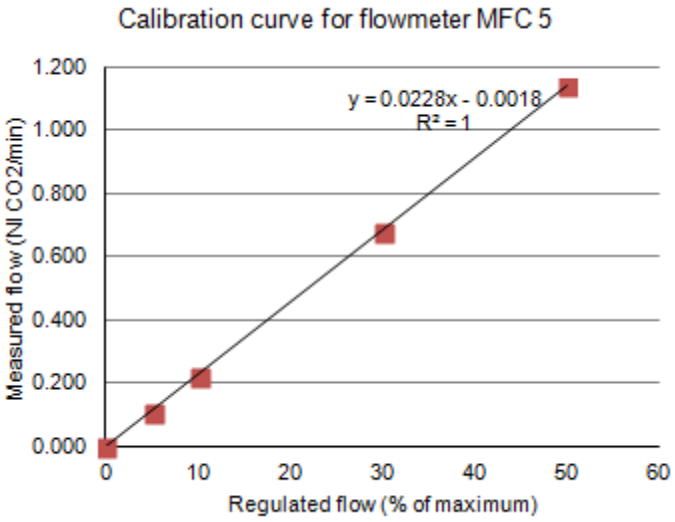

Calibration of MFC : Second calibration

MFC 5: Values found for calibration; Calibration 2

Innstilt gassflow (%) av max	Målt mengde gass (L)	Tid (s)	(L/min)	Middel (L/min)	(NL/min) omregnet
50	0.50	23.03	1.30		
	0.50	23.06	1.30		
	0.50	23.08	1.30		
	0.50	23.10	1.30	1.30	1.19
30	0.20	15.44	0.78		
	0.20	15.62	0.77		
	0.20	15.52	0.77		
	0.20	15.56	0.77	0.77	0.71
10	0.10	23.25	0.26		
	0.10	23.44	0.26		
	0.10	23.62	0.25		
	0.10	23.44	0.26	0.26	0.23

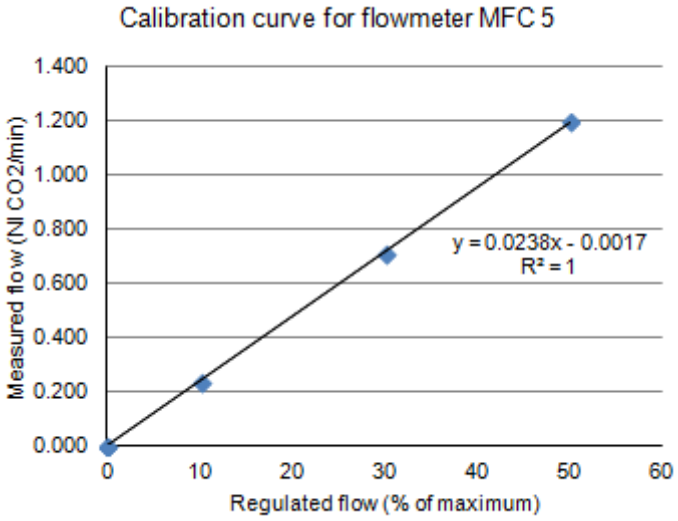

Calibration of MFC 6

MFC 6: Values found for calibration

Innstilt gassflow (%) av max	**Målt mengde gass (L)**	**Tid (s)**	**(L/min)**	**Middel (L/min)**	**(NL/min)** omregnet
30	0.03	20.47	0.08		
	0.03	20.50	0.08		
	0.03	20.34	0.08	0.08	0.07
20	0.03	29.91	0.05		
	0.03	29.69	0.05		
	0.03	29.85	0.05	0.05	0.05
10	0.03	62.63	0.03		
	0.03	62.56	0.03		
	0.03	62.53	0.03	0.03	0.02

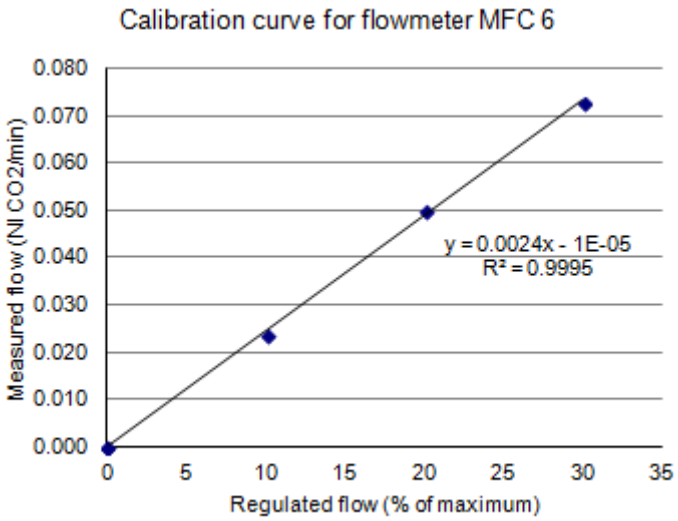

Calibration of MFC 7

MFC 7: Values found for calibration

Innstilt gassflow (%) av max	Målt mengde gass (L)	Tid (s)	(L/min)	Middel (L/min)	(NL/min) omregnet
60	0.800	24.24	1.980		
	0.800	24.28	1.977		
	0.800	24.28	1.977		
	0.800	24.29	1.976	1.978	1.837
40	0.500	22.91	1.309		
	0.500	22.94	1.308		
	0.500	22.92	1.309		
	0.500	22.93	1.308	1.309	1.216
20	0.200	15.60	0.769		
	0.200	15.50	0.774		
	0.200	15.40	0.779		
	0.200	15.50	0.774	0.774	0.719
10	0.100	19.19	0.313		
	0.100	19.16	0.313		
	0.100	19.10	0.314		
	0.100	19.10	0.314	0.314	0.291

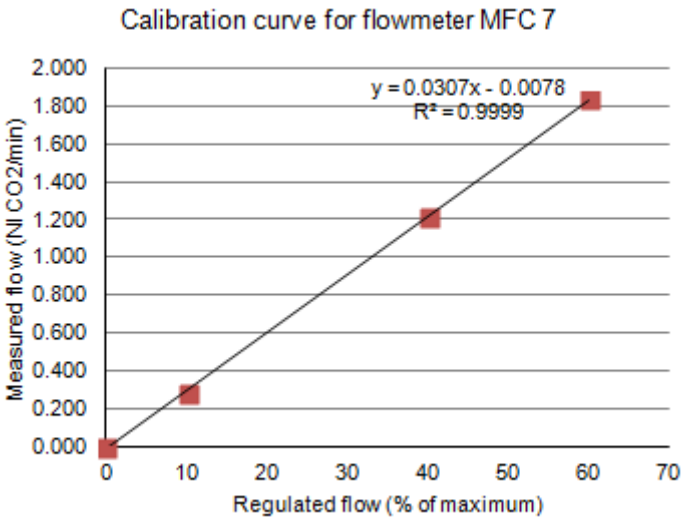

Appendix B2: Mass flow controller parameters for experiments

Table B1: Openings and flows through MFCs for experiment M1 and M2

MFC's for CO2 stream	Composition vol%	Flow NL/min	Opening of flow controller %
Reaktor 1 (MFC 1)	100	0.009	3.40
Reaktor 2 (MFC 2)	100	0.0073	3.40

MFC's for N2/O2 stream	Composition vol%	Flow NL/min	Opening of flow controller %
Reactor 1 (MFC 2)	100	0.387	6.80
Reactor 2 (MFC 4)	100	0.334	6.31

MFC's for mixing gas	Composition vol%	Flow NL/min	Opening of flow controller %
O2 (MFC 6)	6.00	0.38	19.99
N2 (MFC 5)	94.00	0.38	30.15
Total	100	0.76	

Table B2: Openings and flows through MFCs for experiment M3 and M4

MFC's for CO2 stream	Composition vol%	Flow NL/min	Opening of flow controller %
Reaktor 1 (MFC 1)	100	0.0075	2.81
Reaktor 2 (MFC 2)	100	0.0075	3.50

MFC's for mixed stream	Composition vol%	Flow NL/min	Opening of flow controller %
O2 + N2 (MFC 2)	100	0.35	6.13
O2 + N2 (MFC 4)	100	0.35	6.61

MFC's for mixing gas	Composition vol%	Flow NL/min	Opening of flow controller %
O2 (MFC 7)	50.00	0.38	12.63
N2 (MFC 5)	50.00	0.38	16.04
	100	0.76	

Table B3: Openings and flows through MFCs for experiment M5 and M6

MFC's for CO2 stream	Composition vol%	Flow NL/min	Opening of flow controller %
Reaktor 1 (MFC 1)	100	0.0075	2.81
Reaktor 2 (MFC 2)	100	0.0075	3.50

MFC's for mixed stream	Composition vol%	Flow NL/min	Opening of flow controller %
O2 + N2 (MFC 2)	100	0.35	6.13
O2 + N2 (MFC 4)	100	0.35	6.61

MFC's for mixing gas	Composition vol%	Flow NL/min	Opening of flow controller %
O2 (MFC 7)	6.01	0.0454	1.73
N2 (MFC 5)	93.99	0.7106	29.93
	100	0.756	

Appendix C : Measured parameters for gas-washing bottles

Tables C1: Experiment M1: 75 °C, 98% O_2, Measured H_2SO_4 and NH_3 in samples

Gas-washing bottle 1						
Sample nr.	**P.nr**	**Date**	**Time**	**Day**	**0.5 M H2SO4 (g) added**	**Mass of H2SO4 before sampling [g]**
1	P13599	07.02.13	13:45	3.0	94.2	79.31
2	P13600	12.02.13	14:40	8.0	75.8	45.41
3	P13601	17.02.13	14:10	13.0	143.2	126.95
4	P13602	21.02.13	18:50	17.2	120.6	105.81
5	P13603	25.02.13	17:20	21.1	150.5	132.76

Gas-washing bottle 2						
Sample nr.	**P.nr**	**Date**	**Time**	**Day**	**0.5 M H2SO4 (g) added**	**Mass of H2SO4 before sampling [g]**
1	P13604	07.02.13	13:45	3.0	46.4	46.32
2	P13605	12.02.13	14:40	8.0	43.1	42.86
3	P13606	17.02.13	14:10	13.0	68.2	68.12
4	P13607	21.02.13	18:50	17.2	65.1	65.01
5	P13608	25.02.13	17:20	21.1	85.5	85.00

Gas-washing bottle 1						
Sample nr.	**P.nr**	**Date**	**Time**	**Day**	**NH3 (ug/mL)**	**NH3 ug**
1	P13599	07.02.13	13:45	3.0	28736	2279084.677
2	P13600	12.02.13	14:40	8.0	46414	2107678.358
3	P13601	17.02.13	14:10	13.0	11044	1402020.566
4	P13602	21.02.13	18:50	17.2	22883	2421249.172
5	P13603	25.02.13	17:20	21.1	5082	674626.578

Gas-washing bottle 2						
Sample nr.	**P.nr**	**Date**	**Time**	**Day**	**NH3 (ug/mL)**	**NH3 ug**
1	P13604	07.02.13	13:45	3.0	86	3966.597451
2	P13605	12.02.13	14:40	8.0	33956	1455348.417
3	P13606	17.02.13	14:10	13.0	3	210.3552412
4	P13607	21.02.13	18:50	17.2	1986	129127.7378
5	P13608	25.02.13	17:20	21.1	1	92.6058

Tables C2: Experiment M2: 75 °C, 6% O_2, Measured H_2SO_4 and NH_3 in samples

Gas-washing bottle 1						
Sample nr.	**P.nr**	**Date**	**Time**	**Day**	**0.5 M H2SO4 (g) added**	**Mass of H2SO4 before sampling [g]**
1	P13621	07.02.13	13:55	3.0	98.1	83.22
2	P13622	12.02.13	14:50	8.0	79.9	50.94
3	P13623	17.02.13	14:30	13.0	147.1	118.16
4	P13624	21.02.13	19:00	17.2	115.0	91.53
5	P13625	25.02.13	17:40	21.2	147.4	126.87
6	P13626	06.03.13	12:25	29.9	123.8	75.29
7	P13627	12.03.13	13:00	36.0	150.9	115.44

Gas-washing bottle 2						
Sample nr.	**P.nr**	**Date**	**Time**	**Day**	**0.5 M H2SO4 (g) added**	**Mass of H2SO4 before sampling [g]**
1	P13628	07.02.13	13:55	3.0	55.5	54.47
2	P13629	12.02.13	14:50	8.0	51.2	49.26
3	P13630	17.02.13	14:30	13.0	79.2	76.92
4	P13631	21.02.13	19:00	17.2	73.7	71.77
5	P13632	25.02.13	17:40	21.2	80.2	78.73
6	P13633	06.03.13	12:25	29.9	75.6	71.74
7	P13634	12.03.13	13:00	36.0	84.6	82.15

Gas-washing bottle 1						
Sample nr.	**P.nr**	**Date**	**Time**	**Day**	**NH3 (ug/mL)**	**NH3 ug**
1	P13621	07.02.13	13:55	3.0	4481	372914.9533
2	P13622	12.02.13	14:50	8.0	7284	371052.5532
3	P13623	17.02.13	14:30	13.0	5946	702533.7975
4	P13624	21.02.13	19:00	17.2	13195	1207737.435
5	P13625	25.02.13	17:40	21.2	4802	609202.1965
6	P13626	06.03.13	12:25	29.9	24389	1836221.459
7	P13627	12.03.13	13:00	36.0	4635	535012.7175

Gas-washing bottle 2						
Sample nr.	**P.nr**	**Date**	**Time**	**Day**	**NH3 (ug/mL)**	**NH3 ug**
1	P13628	07.02.13	13:55	3.0	< 1	
2	P13629	12.02.13	14:50	8.0	8.0	394.08
3	P13630	17.02.13	14:30	13.0	< 1	
4	P13631	21.02.13	19:00	17.2	4.0	287.08
5	P13632	25.02.13	17:40	21.2	< 1	
6	P13633	06.03.13	12:25	29.9	14.0	1004.36
7	P13634	12.03.13	13:00	36.0	< 1	

Tables C3: Experiment M3: 65 °C, 50% O_2, Measured H_2SO_4 and NH_3 in samples

Gas-washing bottle 1						
Sample nr.	**P.nr**	**Date**	**Time**	**Day**	**0.5 M H2SO4 (g) added**	**Mass of H2SO4 before sampling [g]**
1	P13843	21.03.13	16:00	7.0	138.4	82.74
2	P13844	28.03.13	11:40	13.8	155.6	106.39
3	P13845	04.04.13	16:30	21.0	160.0	106.08
4	P13846	11.04.13	15:40	28.0	157.3	128.86

Gas-washing bottle 2						
Sample nr.	**P.nr**	**Date**	**Time**	**Day**	**0.5 M H2SO4 (g) added**	**Mass of H2SO4 before sampling [g]**
1	P13847	21.03.13	16:00	7.0	71.2	70.15
2	P13848	28.03.13	11:40	13.8	75.9	74.64
3	P13849	04.04.13	16:30	21.0	69.1	67.58
4	P13850	11.04.13	15:40	28.0	78.7	60.00

Gas-washing bottle 1						
Sample nr.	**P.nr**	**Date**	**Time**	**Day**	**NH3 (ug/mL)**	**NH3 ug**
1	P13843	21.03.13	16:00	7.0	32701	2705641.025
2	P13844	28.03.13	11:40	13.8	27663	2943117.637
3	P13845	04.04.13	16:30	21.0	22517	2388564.11
4	P13846	11.04.13	15:40	28.0	187	24146.26358

Gas-washing bottle 2						
Sample nr.	**P.nr**	**Date**	**Time**	**Day**	**NH3 (ug/mL)**	**NH3 ug**
1	P13847	21.03.13	16:00	7.0	2901	203538.1205
2	P13848	28.03.13	11:40	13.8	467	34870.40477
3	P13849	04.04.13	16:30	21.0	8	524.4208
4	P13850	11.04.13	15:40	28.0	< 1	

Tables C4: Experiment M4: 75 °C, 50% O_2, Measured H_2SO_4 and NH_3 in samples

Gas-washing bottle 1						
Sample nr.	**P.nr**	**Date**	**Time**	**Day**	**0.5 M H2SO4 (g) added**	**Mass of H2SO4 before sampling [g]**
1	P13859	21.03.13	16:00	7.0	146.2	101.37
2	P13860	28.03.13	11:40	13.8	157.9	128.85
3	P13861	04.04.13	16:30	21.0	169.9	124.64
4	P13862	11.04.13	15:40	28.0	153.8	107.91

Gas-washing bottle 2						
Sample nr.	**P.nr**	**Date**	**Time**	**Day**	**0.5 M H2SO4 (g) added**	**Mass of H2SO4 before sampling [g]**
1	P13863	21.03.13	16:00	7.0	82.0	78.68
2	P13864	28.03.13	11:40	13.8	84.6	82.49
3	P13865	04.04.13	16:30	21.0	75.9	72.33
4	P13866	11.04.13	15:40	28.0	75.7	72.03

Gas-washing bottle 1						
Sample nr.	**P.nr**	**Date**	**Time**	**Day**	**NH3 (ug/mL)**	**NH3 ug**
1	P13859	21.03.13	16:00	7.0	28907	2930282.316
2	P13860	28.03.13	11:40	13.8	11233	1447411.994
3	P13861	04.04.13	16:30	21.0	24817	3093205.837
4	P13862	11.04.13	15:40	28.0	24201	2611552.571

Gas-washing bottle 2						
Sample nr.	**P.nr**	**Date**	**Time**	**Day**	**NH3 (ug/mL)**	**NH3 ug**
1	P13863	21.03.13	16:00	7.0	2091	164499.2658
2	P13864	28.03.13	11:40	13.8	7	552.8372563
3	P13865	04.04.13	16:30	21.0	958	69261.61674
4	P13866	11.04.13	15:40	28.0	14	977.2540596

Tables C5: Experiment M5: 55 °C, 6% O_2, Measured H_2SO_4 and NH_3 in samples

Gas-washing bottle 1						
Sample nr.	**P.nr**	**Date**	**Time**	**Day**	**0.5 M H2SO4 (g) added**	**Mass of H2SO4 before sampling [g]**
1	P131075	23.04.13	13:20	7.0	137.7	84.37
2	P131076	30.04.13	12:50	14.0	141.8	89.58
3	P131077	07.05.13	11:55	20.9	153.4	117.26
4	P131078	14.05.13	15:40	28.1	146.5	89.87
5	P131079	21.05.13	10:30	34.9	158.9	105.62
6	P131080	28.05.13	09:40	41.8	136.5	82.98

Gas-washing bottle 2						
Sample nr.	**P.nr**	**Date**	**Time**	**Day**	**0.5 M H2SO4 (g) added**	**Mass of H2SO4 before sampling [g]**
1	P131081	23.04.13	13:20	7.0	85.0	84.03
2	P131082	30.04.13	12:50	14.0	74.9	73.89
3	P131083	07.05.13	11:55	20.9	83.1	82.47
4	P131084	14.05.13	15:40	28.1	77.0	75.95
5	P131085	21.05.13	10:30	34.9	80.5	79.30
6	P131086	28.05.13	09:40	41.8	79.8	78.48

Gas-washing bottle 1						
Sample nr.	**P.nr**	**Date**	**Time**	**Day**	**NH3 (ug/mL)**	**NH3 ug**
1	P131075	23.04.13	13:20	7.0	3827	322885.8461
2	P131076	30.04.13	12:50	14.0	5054	452709.6398
3	P131077	07.05.13	11:55	20.9	2451	287363.5708
4	P131078	14.05.13	15:40	28.1	6726	604481.8865
5	P131079	21.05.13	10:30	34.9	4049	427690.3402
6	P131080	28.05.13	09:40	41.8	5229	433877.609

Gas-washing bottle 2						
Sample nr.	**P.nr**	**Date**	**Time**	**Day**	**NH3 (ug/mL)**	**NH3 ug**
1	P131081	23.04.13	13:20	7.0		0
2	P131082	30.04.13	12:50	14.0		0
3	P131083	07.05.13	11:55	20.9		0
4	P131084	14.05.13	15:40	28.1		0
5	P131085	21.05.13	10:30	34.9		0
6	P131086	28.05.13	09:40	41.8		0

Tables C6: Experiment M3: 65 °C, 6% O_2, Measured H_2SO_4 and NH_3 in samples

Gas-washing bottle 1						
Sample nr.	**P.nr**	**Date**	**Time**	**Day**	**0.5 M H2SO4 (g) added**	**Mass of H2SO4 before sampling [g]**
1	P131096	23.04.13	13:20	7.0	130.9	84.82
2	P131097	30.04.13	12:50	14.0	150.1	105.41
3	P131098	07.05.13	11:55	20.9	154.7	124.42
4	P131099	14.05.13	15:40	28.1	147.3	96.25
5	P131100	21.05.13	10:30	34.9	128.8	80.72
6	P131101	28.05.13	09:40	41.8	144.1	93.83

Gas-washing bottle 2						
Sample nr.	**P.nr**	**Date**	**Time**	**Day**	**0.5 M H2SO4 (g) added**	**Mass of H2SO4 before sampling [g]**
1	P131102	23.04.13	13:20	7.0	78.7	75.22
2	P131103	30.04.13	12:50	14.0	74.4	70.84
3	P131104	07.05.13	11:55	20.9	84.2	81.86
4	P131105	14.05.13	15:40	28.1	74.6	70.49
5	P131106	21.05.13	10:30	34.9	75.2	71.58
6	P131107	28.05.13	09:40	41.8	80.1	76.42

Gas-washing bottle 1						
Sample nr.	**P.nr**	**Date**	**Time**	**Day**	**NH3 (ug/mL)**	**NH3 ug**
1	P131096	23.04.13	13:20	7.0	7834	664451.7198
2	P131097	30.04.13	12:50	14.0	8304	875283.2139
3	P131098	07.05.13	11:55	20.9	3685	458451.1205
4	P131099	14.05.13	15:40	28.1	7369	709231.6963
5	P131100	21.05.13	10:30	34.9	7812	630604.4164
6	P131101	28.05.13	09:40	41.8	6639	622977.5292

Gas-washing bottle 2						
Sample nr.	**P.nr**	**Date**	**Time**	**Day**	**NH3 (ug/mL)**	**NH3 ug**
1	P131102	23.04.13	13:20	7.0		
2	P131103	30.04.13	12:50	14.0		
3	P131104	07.05.13	11:55	20.9		
4	P131105	14.05.13	15:40	28.1		
5	P131106	21.05.13	10:30	34.9		
6	P131107	28.05.13	09:40	41.8		

Appendix D: Results for quantification of compounds in solution

D1: Experiment M1: 75 °C, 98% O_2

Table D1: LC-MS results for ammonia and primary/secondary amines for samples from reactor.

Time (Days)	NH_3	Unit
0	97	µg/ml
0.9	1104	µg/ml
3	1546	µg/ml
6.4	1843	µg/ml
8.1	1679	µg/ml
10.1	1949	µg/ml
13	1891	µg/ml
17.2	1626	µg/ml
21.2	1413	µg/ml

Time (Days)	Methyl-amine	Ethyl-amine	Dimethyl-amine	Diethyl-amine	Unit
0	113	< 100	50	449	ng/ml
0.9	348	< 100	40	< 100	ng/ml
3	521	< 100	29	< 100	ng/ml
6.4	660	< 100	19	< 100	ng/ml
8.1	655	< 100	18	< 100	ng/ml
10.1	718	< 100	18	< 100	ng/ml
13	719	< 100	14	< 100	ng/ml
17.2	736	< 100	< 10	< 100	ng/ml
21.2	753	< 100	11	< 100	ng/ml

Table D2: LC-MS results for degradation mix compounds in samples from reactor.

Time (Days)	HeGly	HEF	BHEOX	HEA	HEPO	OZD	HEI	Unit
0	10	159	11	4	< 1	< 10	20	µg/mL
0.9	581	6616	637	75	20	147	3086	µg/mL
3	1324	13117	982	319	155	620	7506	µg/mL
6.4	1404	14108	797	610	330	998	9264	µg/mL
8.1	1534	13838	671	720	369	1076	9286	µg/mL
10.1	1561	13071	655	847	394	1155	9413	µg/mL
13	1637	12772	548	991	452	1154	9625	µg/mL
17.2	1974	12704	518	1204	551	1304	10393	µg/mL
21.2	1892	11319	424	1190	585	1187	9463	µg/mL

Table D3: Concentration of MEA and DEA in samples from reactor found by LC-MS analysis.

Time (Days)	MEA	Unit
0	4.62	mol/L
0.9	4.7	mol/L
3	3.05	mol/L
6.4	2.29	mol/L
8.1	1.91	mol/L
10.1	1.72	mol/L
13	1.62	mol/L
17.2	1.72	mol/L
21.2	1.52	mol/L

Time (Days)	DEA	Unit
0	0.07	mmol/L
0.9	0.29	mmol/L
3	0.41	mmol/L
6.4	0.38	mmol/L
8.1	0.4	mmol/L
10.1	0.42	mmol/L
13	0.45	mmol/L
17.2	0.5	mmol/L
21.2	0.55	mmol/L

Table D5: Concentration of anions in samples from reactor analyzed by IC-EC

Time (Days)	Formate (PPM)	Oxalate (PPM)	Nitrate (PPM)	Sulphate (PPM)	Nitrite (PPM)
0	39	#N/A	#N/A	1 067	#N/A
1	909	101	92	1 096	717
3	7 159	520	334	1 295	1 885
6	#N/A	1 280	953	1 264	3 608
8	20 168	1 797	1 013	1 211	3 779
10	#N/A	2 225	1 072	1 112	3 746
13	#N/A	2 929	1 055	1 135	3 892
17	25 016	4 115	1 879	1 188	3 428
21	25 579	5 388	1 878	1 152	3 379

Table D6: Amine and CO_2 concentration found for samples from the reactor by titration.

Time (days)	Amin (mol/kg)	CO2 (mol/kg)
0.0	0.00	1.78
0.9	0.95	
3.0	3.03	
6.4	6.38	
8.1	8.07	
10.1	10.11	
13.0	13.05	
17.2	17.24	
21.2	21.18	0.11

Table D7: Parameters and concentrations found of HEF and HEI in run in parallels in GC-MS

Sample	F1P1	F1P2	F1P3	F1P4	F1P5	F1P6	F1P7	F1P8	F1P9
Time (Days)	0.0	1.0	3.0	6.4	8.1	10.1	13.0	17.2	21.2
Methanol (g)	0.84	0.80	0.80	0.80	0.79	0.79	0.80	0.79	0.79
Sample (g)	0.02	0.02	0.02	0.02	0.02	0.02	0.02	0.02	0.02
Density (g/mL)	1.09	1.09	1.09	1.09	1.08	1.08	1.08	1.07	1.07
Total (g)	0.86	0.82	0.82	0.82	0.81	0.81	0.82	0.81	0.81
HEF 1 diluted		58.0	396.5	852.5	571.4	680.6	615.0	524.2	564.5
HEF 2 diluted		126.5	446.5	573.1	617.3	757.2	753.0	622.3	728.0
HEF 3 diluted									800.6
HEF 4 diluted									383.6
HEPO 1 diluted		10.0	19.9	36.5	47.2	37.7	39.2	34.8	27.4
HEPO 2 diluted		20.1	25.2	22.8		58.2	57.0	39.7	45.4
HEPO 3 diluted									43.4
HEPO 4 diluted									28.5
Avr. HEF		92.2	421.5	712.8	594.3	718.9	684.0	573.2	619.2
STD (%)		52.6	8.4	27.7	5.5	7.5	14.3	12.1	30.0
Avr. HEPO		15.1	22.6	29.6	47.2	48.0	48.1	37.2	36.2
STD (%)		47.7	16.6	32.8		30.2	26.3	9.3	26.4

D2: Experiment M2: 75 °C, 6% O_2

Table D8: LC-MS results for ammonia and primary/secondary amines for samples from reactor.

Time (days)	NH_3	Unit	Methyl-amine	Ethyl-amine	Dimethyl-amine	Diethyl-amine	Unit
0	97	µg/ml	< 10	358	17	2933	ng/ml
0.9	167	µg/ml	42	244	20	1326	ng/ml
3	213	µg/ml	150	265	24	770	ng/ml
6.3	213	µg/ml	392	284	42	569	ng/ml
7.8	212	µg/ml	466	250	36	402	ng/ml
10.1	207	µg/ml	559	233	42	351	ng/ml
13	218	µg/ml	749	262	50	292	ng/ml
17.2	244	µg/ml	1089	302	61	428	ng/ml
21.2	253	µg/ml	1325	256	65	245	ng/ml
24	283	µg/ml	1527	241	70	208	ng/ml
29.9	331	µg/ml	1845	207	67	170	ng/ml
35.9	383	µg/ml	2126	232	68	186	ng/ml

Table D9: LC-MS results for degradation mix compounds in samples from reactor.

Time (days)	HeGly	HEF	BHEOX	HEA	HEPO	OZD	HEI	Unit
0	5	157	10	3	< 1	< 10	18	µg/mL
0.9	202	418	21	10	3	< 10	140	µg/mL
3	1217	816	43	32	13	24	591	µg/mL
6.3	3294	1348	66	70	39	39	1198	µg/mL
7.8	4307	1523	64	84	53	43	1399	µg/mL
10.1	4989	1697	65	99	69	45	1526	µg/mL
13	6322	1945	85	148	102	59	1818	µg/mL
17.2	7174	2474	98	197	145	78	2071	µg/mL
21.2	7422	2692	105	242	191	82	2172	µg/mL
24	7733	3062	113	295	222	99	2317	µg/mL
29.9	7745	3423	125	365	312	128	2469	µg/mL
35.9	7356	3931	145	465	407	165	2561	µg/mL

Table D10: Concentration of MEA and DEA in samples from reactor found by LC-MS analysis.

Time (days)	MEA	Unit	DEA	Unit
0.0	5.27	**mol/L**	0.07	**mmol/L**
0.9	5.28	**mol/L**	0.11	**mmol/L**
3.0	4.95	**mol/L**	0.15	**mmol/L**
6.3	4.72	**mol/L**	0.2	**mmol/L**
7.8	4.91	**mol/L**	0.22	**mmol/L**
10.1	4.79	**mol/L**	0.24	**mmol/L**
13.0	4.43	**mol/L**	0.29	**mmol/L**
17.2	4.12	**mol/L**	0.36	**mmol/L**
21.2	3.93	**mol/L**	0.37	**mmol/L**
24.0	3.98	**mol/L**	0.44	**mmol/L**
29.9	3.78	**mol/L**	0.5	**mmol/L**
35.9	3.47	**mol/L**	0.54	**mmol/L**

Table D11: Concentration of anions in samples from reactor analyzed by IC-EC

Time (Days)	Formate (PPM)	Oxalate (PPM)	Nitrate (PPM)	Sulphate (PPM)	Nitrite (PPM)
0	#N/A	64	#N/A	1 321	#N/A
1	71	58	#N/A	1 356	#N/A
3	303	60	#N/A	1 266	#N/A
6	702	88	#N/A	1 340	#N/A
8	1 001	119	#N/A	1 360	44
10	1 132	148	#N/A	1 275	45
13	1 649	195	17	1 267	63
17	2 374	346	#N/A	1 258	74
21	3 215	461	34	1 295	90
24	3 939	579	36	1 264	103
30	5 345	798	67	1 257	145
36	6 109	1 650	81	2 414	173

Table D12: Amine and CO_2 concentration found for samples from the reactor by titration.

Time (days)	Amin (mol/kg)	CO2 (mol/kg)
0.0	4.51	1.77
0.9	4.45	
3.0	4.33	
6.3	4.12	
7.8	4.09	
10.1	3.93	
13.0	3.79	
17.2	3.69	
21.2	3.46	
24.0	3.37	
29.9	3.18	
35.9	2.98	1.06

D3: Experiment M3: 65 °C, 50% O_2

Table D13: LC-MS results for ammonia and primary/secondary amines for samples from reactor.

Time (Days)	NH_3	Unit
0	45	µg/ml
1	383	µg/ml
3	498	µg/ml
7	580	µg/ml
10	616	µg/ml
14	745	µg/ml
21	946	µg/ml
28	1854	µg/ml

Methyl-amine	Ethyl-amine	Dimethyl-amine	Diethyl-amine	Unit
< 10	1063	19	8717	ng/ml
55	582	18	3809	ng/ml
140	431	13	3048	ng/ml
221	166	< 10	1451	ng/ml
280	135	< 10	1042	ng/ml
308	< 100	< 10	504	ng/ml
359	< 100	< 10	284	ng/ml
409	< 100	< 10	218	ng/ml

Table D14: LC-MS results for degradation mix compounds in samples from reactor.

Time (days)	HeGly	HEF	BHEOX	HEA	HEPO	OZD	HEI	Unit
0	5	65	3	5	< 1	< 10	5	µg/mL
1	170	2381	263	19	4	75	367	µg/mL
3	630	4694	555	72	31	271	1007	µg/mL
7	1214	7357	740	197	132	639	1819	µg/mL
10	1358	8649	827	315	211	947	2325	µg/mL
14	1369	9745	793	451	277	1227	2775	µg/mL
21	1306	10431	750	673	346	1611	3290	µg/mL
28	1313	10227	679	821	294	1926	3816	µg/mL

Table D15: Concentration of MEA and DEA in samples from reactor found by LC-MS analysis.

Time (Days)	MEA	Unit
0	5.26	mol/L
1	4.51	mol/L
3	4.48	mol/L
7	4.00	mol/L
10	3.58	mol/L
14	3.37	mol/L
21	2.69	mol/L
28	2.36	mol/L

DEA	Unit
0.06	mmol/L
0.13	mmol/L
0.20	mmol/L
0.27	mmol/L
0.28	mmol/L
0.30	mmol/L
0.32	mmol/L
0.37	mmol/L

Table D16: Amine and CO_2 concentration found for samples from the reactor by titration.

Time (days)	Amin (mol/kg)	CO2 (mol/kg)
0.0	4.47	1.78
1.1	4.29	
3.2	3.97	
7.1	3.39	
10.0	3.09	
14.0	2.65	
21.2	2.01	
28.1	1.73	0.68

Table D17: Concentration of anions in samples from reactor analyzed by IC-EC

Time (Days)	Formate (PPM)	Oxalate (PPM)	Nitrate (PPM)	Sulphate (PPM)	Nitrite (PPM)
0	#N/A	#N/A	#N/A	#N/A	#N/A
1	273	#N/A	42	#N/A	249
3	1 083	64	105	#N/A	596
7	3 042	266	243	#N/A	1 073
10	#N/A	#N/A	#N/A	#N/A	#N/A
14	8 096	908	507	#N/A	1 654
21	10 349	1 768	678	#N/A	2 074
28	9 975	2 663	968	#N/A	2 191

D4: Experiment M4: 75 °C, 50% O_2

Table D18: LC-MS results for ammonia and primary/secondary amines for samples from reactor.

Time (days)	NH_3	Unit
0	517	µg/ml
1.1	40	µg/ml
3.2	737	µg/ml
7.1	914	µg/ml
10	1243	µg/ml
14	936	µg/ml
21.2	1540	µg/ml
28.1	1438	µg/ml

Methyl-amine	Ethyl-amine	Dimethyl-amine	Diethyl-amine	Unit
171	< 100	29	817	ng/ml
23	< 100	27	554	ng/ml
382	< 100	25	457	ng/ml
627	< 100	19	218	ng/ml
687	< 100	16	135	ng/ml
1085	< 100	43	1527	ng/ml
740	< 100	15	142	ng/ml
733	< 100	14	115	ng/ml

Table D19: LC-MS results for degradation mix compounds in samples from reactor.

Time (days)	HeGly	HEF	BHEOX	HEA	HEPO	OZD	HEI	Unit
0	2	50	2	< 1	< 1	< 10	3	µg/mL
1	495	2154	236	39	14	93	483	µg/mL
3	1585	4539	434	171	121	353	1514	µg/mL
7	2005	6950	571	469	331	843	2566	µg/mL
10	1550	8517	677	653	327	1236	3150	µg/mL
14	1897	8390	582	947	528	1338	3830	µg/mL
21	1296	9478	542	1273	312	2066	4055	µg/mL

Table D20: Concentration of MEA and DEA in samples from reactor found by LC-MS analysis.

Time (days)	MEA	Unit
0	5.43	mol/L
1	5.06	mol/L
3	4.17	mol/L
7	3.44	mol/L
10	3.14	mol/L
14	3.16	mol/L
21	2.06	mol/L
28	1.58	mol/L

DEA	OZD
0.25	< 10
0.06	< 10
0.4	24
0.38	39
0.29	43
0.36	45
0.21	59
0.21	78

Table D21: Amine and CO_2 concentration found for samples from the reactor by titration.

Time (days)	Amin (mol/kg)	CO2 (mol/kg)
0.0	4.48	1.76
1.1	4.28	
3.2	3.86	
7.1	3.09	
10.0	2.55	
14.0	2.18	
21.2	1.21	
28.1	0.72	0.21

Table D22: Concentration of anions in samples from reactor analyzed by IC-EC

Time (Days)	Formate (PPM)	Oxalate (PPM)	Nitrate (PPM)	Sulphate (PPM)	Nitrite (PPM)
0	#N/A	#N/A	#N/A	#N/A	#N/A
1	389	#N/A	31	#N/A	151
3	1 632	121	92	#N/A	435
7	4 875	582	244	#N/A	850
10	8 770	1 195	385	#N/A	1 224
14	#N/A	1 953	460	#N/A	1 128
21	#N/A	4 132	781	#N/A	1 536
28	22272.29372	6 137	1 034	#N/A	1 271

D5: Experiment M5: 55 °C, 6% O_2

Table D23: Concentration of MEA and DEA in samples from reactor found by LC-MS analysis.

Time (days)	MEA	Unit
0	5.56	mol/L
1	5.71	mol/L
3	5.46	mol/L
7	5.33	mol/L
14	5.03	mol/L
21	4.93	mol/L
28	4.59	mol/L
35	4.66	mol/L
42	4.49	mol/L

DEA	Unit
0.034	mmol/L
0.056	mmol/L
0.081	mmol/L
0.132	mmol/L
0.191	mmol/L
0.213	mmol/L
0.243	mmol/L
0.281	mmol/L
0.302	mmol/L

Table D24: LC-MS results for degradation mix compounds in samples from reactor.

Time (days)	HeGly	HEF	BHEOX	HEA	HEPO	OZD	HEI	Unit
0	8	104	< 100	< 10	< 1	< 10	3	µg/mL
1	14	228	< 100	< 10	< 1	< 10	14	µg/mL
3	72	478	< 100	10	1	< 10	32	µg/mL
7	279	977	126	17	6	44	70	µg/mL
14	772	1632	184	43	26	124	134	µg/mL
21	1135	2347	271	78	43	216	178	µg/mL
28	1484	2475	212	103	91	285	231	µg/mL
35	1797	2947	251	148	150	347	280	µg/mL
42	1806	2929	230	174	189	406	309	µg/mL

Table D25: LC-MS results for ammonia and primary/secondary amines for samples from reactor.

Time (days)	NH_3	Unit
0	30	µg/ml
1	82	µg/ml
3	101	µg/ml
7	124	µg/ml
14	122	µg/ml
21	228	µg/ml
28	121	µg/ml
35	136	µg/ml
42	155	µg/ml

Methyl-amine	Ethyl-amine	Dimethyl-amine	Diethyl-amine	Unit
< 10	353	23	1991	ng/ml
< 10	213	24	1270	ng/ml
< 10	209	19	768	ng/ml
27	218	24	552	ng/ml
46	164	15	339	ng/ml
65	129	18	343	ng/ml
84	< 100	15	368	ng/ml
104	< 100	12	264	ng/ml
125	< 100	12	195	ng/ml

Table D26: Amine and CO_2 concentration found for samples from the reactor by titration.

Time (days)	Amin (mol/kg)	CO2 (mol/kg)
0.0	0.00	1.78
1.0	1.05	
3.0	2.96	
7.0	6.95	
13.9	13.92	
20.9	20.87	
28.0	28.05	
34.8	34.83	
41.8	41.77	0.11

Table D27: Concentration of anions in samples from reactor analyzed by IC-EC

Time (Days)	Formate (PPM)	Oxalate (PPM)	Nitrate (PPM)	Sulphate (PPM)	Nitrite (PPM)
0	#N/A	#N/A	#N/A	889	#N/A
1	#N/A	#N/A	#N/A	794	#N/A
3	28	#N/A	#N/A	795	#N/A
7	129	#N/A	#N/A	793	51
14	394	66	#N/A	773	115
21	607	96	22	831	156
28	1 041	172	#N/A	752	197
35	1 433	251	#N/A	742	231
42	1 485	448	100	890	164

D6: Experiment M6: 65 °C, 6% O_2

Table D28: LC-MS results for ammonia and primary/secondary amines for samples from reactor.

Time (Days)	NH_3	Unit
0	32	µg/ml
1	156	µg/ml
3	235	µg/ml
7	247	µg/ml
14	187	µg/ml
21	255	µg/ml
28	216	µg/ml
35	220	µg/ml
42	236	µg/ml

Methyl-amine	Ethyl-amine	Dimethyl-amine	Diethyl-amine	Unit
< 10	413	24	1845	ng/ml
28	284	27	997	ng/ml
68	217	24	673	ng/ml
153	204	25	602	ng/ml
259	159	28	354	ng/ml
380	186	31	320	ng/ml
480	220	32	266	ng/ml
553	175	39	145	ng/ml
613	185	31	163	ng/ml

Table D29: LC-MS results for degradation mix compounds in samples from reactor.

Time (Days)	HeGly	HEF	BHEOX	HEA	HEPO	OZD	HEI	Unit
0	5	88	< 100	< 10	< 1	< 10	3	µg/mL
1	61	353	< 100	11	< 1	< 10	48	µg/mL
3	300	677	< 100	20	4	33	166	µg/mL
7	1105	1305	< 100	52	24	82	376	µg/mL
14	2527	1789	< 100	121	87	139	596	µg/mL
21	3496	1835	< 100	153	146	151	716	µg/mL
28	3913	2299	< 100	216	207	188	863	µg/mL
35	4016	2483	108	272	270	210	872	µg/mL
42	4105	2890	169	335	343	242	865	µg/mL

Table D30: Concentration of MEA and DEA in samples from reactor found by LC-MS analysis.

Time (Days)	MEA	Unit
0	5.37	mol/L
1	4.91	mol/L
3	4.86	mol/L
7	4.71	mol/L
14	4.96	mol/L
21	4.67	mol/L
28	4.42	mol/L
35	4.46	mol/L
42	4.05	mol/L

DEA	Unit
0.046	mmol/L
0.068	mmol/L
0.113	mmol/L
0.186	mmol/L
0.245	mmol/L
0.306	mmol/L
0.3	mmol/L
0.359	mmol/L
0.337	mmol/L

Table D31: Amine and CO_2 concentration found for samples from the reactor by titration.

Time (Days)	Amin (mol/kg)	CO2 (mol/kg)
0	4.53	1.76
1	4.44	
3	4.39	
7	4.30	
14	4.13	
21	4.03	
28	3.85	
35	3.76	
42	3.65	1.49

Table D32: Concentration of anions in samples from reactor analyzed by IC-EC

Time (Days)	Formate (PPM)	Oxalate (PPM)	Nitrate (PPM)	Sulphate (PPM)	Nitrite (PPM)
0	#N/A	#N/A	#N/A	801	#N/A
1	#N/A	#N/A	#N/A	784	#N/A
3	82	#N/A	#N/A	764	35
7	291	46	#N/A	778	65
14	582	100	#N/A	753	98
21	1 091	189	#N/A	776	108
28	1 319	290	#N/A	707	118
35	2 563	431	74	867	173
42	2 802	697	65	1 017	165

Appendix E: LC-MS degradation mix results for mixing experiments.

Table E1: Acidic conditions

Time (Days)	HeGly	HEF	BHEOX	HEA	HEPO	OZD	HEI	Unit
0.10	9938	< 100	< 1	< 1	< 1	< 10	< 1	**µg/mL**
0.37	12379	< 100	< 1	< 1	< 1	< 10	< 1	**µg/mL**
1.26	14873	< 100	< 1	< 1	< 1	< 10	< 1	**µg/mL**
3.00	16909	< 100	< 1	< 1	< 1	< 10	< 1	**µg/mL**

Table E2: Basic conditions

Time (Days)	HeGly	HEF	BHEOX	HEA	HEPO	OZD	HEI	Unit
0	8	223	< 100	< 10	< 1	< 10	33	**µg/mL**
0.01	5	928	< 100	< 10	< 1	< 10	77	**µg/mL**
0.26	34	3757	< 100	< 10	< 1	< 10	146	**µg/mL**
1.88	94	11175	< 100	< 10	< 1	< 10	202	**µg/mL**